JUSTUS-LIEBIG-UNIVERSITÄT GIESSEN

MONASH University

The hormonal regulation of the prostate

Influence of the natriuretic peptides

INAUGURAL DISSERTATION

submitted in partial fulfilment of the requirements for the award

of the degree of

Dr. rer. nat. / Ph.D.

As part of the joint award Ph.D. program of the

Justus-Liebig-University, Giessen, Germany and

Monash University, Melbourne, Australia

Submitted by

Magdalena Anastazja Kuchta

From Gliwice

M.Sc. Biochemistry, Halle (Saale)

Nauheim, 02.07.2024

From the Institute of Anatomy and Cell Biology
Signalling Transduction
Faculty of Medicine
Justus-Liebig University, Giessen, Germany
Supervisor: **Prof. Dr. Ralf Middendorff**

(External) Supervisor and Committee Member/Reviewer: **Prof. Dr. Ralf Middendorff**
(Internal) Supervisor and Committee Member/Reviewer: **Prof. Dr. Nikola-Michael Prpic-Schäper**
Committee Member/Reviewer: **Prof. Dr. Florian Wagenlehner**
Committee Member/Reviewer: **PD Dr. Ellen Kauschke**

Date of Disputation: **25.01.2024**

Mit Genehmigung des Fachbereiches 08 – Biologie und Chemie
Der Justus-Liebig Universität Giessen
Dekan/Dean: Prof. Dr. Thomas Wilke

and

Faculty of Monash Institute of Pharmaceutical Sciences
Faculty of Medicine, Nursing and Health Sciences – Molecular and Translational Sciences
Monash University, Melbourne, Australia
Main Supervisor: **Dr. Betty Exintaris**
Supervisors: **Dr. Michael Whittaker** and **Prof. Dr. Kate Loveland**

MONASH University

The hormonal regulation of the prostate

Influence of the natriuretic peptides

Magdalena Anastazja Kuchta

Master of Science in Biochemistry

INAUGURAL DISSERTATION

As part of the joint award Ph.D. program of the

Justus-Liebig-University, Giessen, Germany and

Monash University, Melbourne, Australia

A thesis submitted for the degree of Doctor of Philosophy at

Monash University in 2023

Faculty of Monash Institute of Pharmaceutical Sciences

Faculty of Medicine, Nursing and Health Sciences – Molecular and Translational Sciences

Table of Content

Declaration / Selbstständigkeitserklärung

I hereby declare, that I have completed this dissertation single-handily without unauthorized help of a second party and only with the assistance acknowledged therein. I have appropriately acknowledged and cited all text passages that are derived verbatim from or are based on the content of published work of others, and all information relating to verbal communications. I have abided by the principles of good scientific conduct laid down in the charter of the Justus-Liebig-University Giessen 'Satzung der Justus-Liebig-Universität zur Sicherung guter wissenschaftlicher Praxis' in carrying out the investigations described in the dissertation. I consent to the use of anti-plagiarism software to check my thesis according to § 25 Abs. 6 of the "Allgemeine Bestimmungen für modularisierte Studiengänge".

Hiermit versichere ich, die vorgelegte Thesis selbstständig und ohne unerlaubte fremde Hilfe und nur mit den Hilfen angefertigt zu haben, die ich in der Thesis angegeben habe. Alle Textstellen, die wörtlich oder sinngemäß aus veröffentlichten Schriften entnommen sind, und alle Angaben die auf mündlichen Auskünften beruhen, sind als solche kenntlich gemacht. Bei den von mir durchgeführten und in der Thesis erwähnten Untersuchungen habe ich die Grundsätze guter wissenschaftlicher Praxis, wie sie in der ‚Satzung der Justus- Liebig-Universität zur Sicherung guter wissenschaftlicher Praxis' niedergelegt sind, eingehalten. Gemäß § 25 Abs. 6 der Allgemeinen Bestimmungen für modularisierte Studiengänge dulde ich eine Überprüfung der Thesis mittels Anti-Plagiatssoftware.

Gießen, 24.10.2024

Magdalena A. Kuchta

I certify that I have made all reasonable efforts to secure copyright permissions for third-party content included in this thesis and have not knowingly added copyright content to my work without the owner's permission.

List of Abbreviations

5AR	5-α-reductase
ACTB	β-Actin
ANP	A-type natriuretic peptide
AR	Androgen receptor
ATP	Adenosine triphosphate
BNP	B-type natriuretic peptide
BPH	Bening prostatic hyperplasia
BSA	Bovine serum albumin
CaM	Calmodulin
CD	Cluster of differentiation
cDNA	Complementary DNA
cGMP	Cyclic guanosine monophosphate
CNP	C-type natriuretic peptide
CYP19	Aromatase
DAG	Diglyceride
DAPI	4',6-diamidino-2-phenylindole
DHT	Dihydrotestosterone
DMEM	"Dulbecco's Modified Eagle's Medium"
DMSO	Dimethyl sulfoxide
DNA	Deoxyribonucleic acid
dNTPs	Desoxyribonucleoside triphosphate
E2	Estradiol
EDS	Ethane dimethane sulfonate
EDTA	Ethylenediaminetetraacetic acid
EGF	Epidermal growth factor
eNOS	Endothelial NOS
EPBS	ELISA-PBS
ER	Endoplasmic reticulum
ERα/β	Estrogen receptor
FBS	Fetal bovine serum
FGF	Fibroblast growth factor
GAPDH	Glyceraldehyde 3-phosphate dehydrogenase
GC	Guanylyl cyclase
GC-A	Guanylyl cyclase A
GC-B	Guanylyl cyclase B
GPCR	G-protein-coupled receptor
GTP	Guanosine triphosphate
HAoSMC	Human aortic smooth muscle cells
HEPES	4-(2-hydroxyethyl)-1-piperazineethanesulfonic acid
HPR	Horseradish peroxidase
HPrSMC	Human prostate smooth muscle cell
IBMX	3-isobutyl-1-methylxanthine

IDE	Insulin degrading enzyme
IGF-I	Insulin-like growth factor
IL	Interleukin
iNOS	Inducible NOS
IP3	Inositol-1,4,5-trisphosphate
IP3R	IP3 receptor
IRAG	Inositol 1,4,5-triphosphate receptor associated 1
KGF	Keratinocyte growth factor
KO	Knockout
LUTS	Lower urinary tract symptoms
MEM	"Minimum Essential Medium Eagle"
MLC	Myosin light chain
MLCK	Myosin light chain kinase
MLCP	Myosin light chain phosphatase
mRNA	Messenger RNA
NA	Noradrenalin
NADP+	Nicotinamide adenine dinucleotide phosphate
NF-κB	Nuclear factor kappa-light-chain-enhancer
NEP/MME	Neutral endopeptidase (Membrane metalloendopeptidase)
nNOS	Neuronal NOS
NO	Nictric oxid
NOS	NO-synthase
NP	Natriuretic peptide
NPRC	Clearance receptor
OD	Optical density
PAP	Prostatic acid phosphatase
PBS	Phosphate buffered saline
PCR	Polymerase chain reaction
PDE	Phosphodiesterase
PFA	Paraformaldehyde
PIP2	Phosphatidylinositol 4,5-bisphosphate
PKC	Protein kinase C
PKG I	Proteinkinase G I
PLB	Phospholamban
PLC	Phospholipase C
PSA	Prostate specific antigen
RIA	Radioimmunoassay
RNA	Ribonucleinacid
ROCK	Rho-associated protein kinase
ROS	Reactive oxygen species
RPLP0	Ribosomal protein lateral stalk subunit P0 (60 S)
RT	Reverse Transcriptase
RT-qPCR	Real Time quantitative PCR
sGC	Soluble guanylyl cyclase
SMA	Smooth muscle actin

SMC	Smooth muscle cell
T	Testosterone
TAE	Tris-acetate-EDTA
TDF	Testis-determining factor
TGF-β	Transforming growth factor-β
TMB	3,3’,5,5’-Tetramethylbenzidin
TNF	Tumor necrosis factor
TRIS	Tris(hydroxymethyl)aminomethane (2-Amino-2-(hydroxymethyl)propane-1,3-diol)
TUR-P	Transurethral resection of the prostate
TWEEN®20	Polyoxyethylene (20) sorbitan monolaurate
VNP	Vasonatrin
WT	Wild type

List of Figures

List of Tables

Abstract

This thesis investigated the cGMP signalling pathway via CNP/GC-B as a new therapeutic option for benign prostatic hyperplasia. Expression analyses showed that in prostatic smooth muscle cells, CNP/GC-B components are higher expressed than others, such as GC-A or sGC. Furthermore, CNP treatment delayed the growth of HPrSMCs. *Ex vivo* experiments with a rat model demonstrated that CNP and its analogue VNP led to significant relaxation of the prostate glands. As both characteristics of BPH (increased proliferation and muscle tone) can be addressed by the CNP/GC-B pathway, it presents another option for the treatment of BPH.

1 Introduction

1.1 Overview of the male reproductive system

1.1.1 General overview of the male reproductive tract

The male reproductive tract of vertebrates include the penis, testis, epididymis, vas deferens, and accessory glands, which may vary between species. In the following sections, the male reproductive tract of humans and rats will be explained in more detail. Differences between the male reproductive tracts of humans and rodents will also be indicated.

1.1.2 Human male reproductive system

As in all male vertebrates, the male reproductive tract in humans consists of the penis, testis, epididymis, vas deferens which expands into the ampulla ductus deferentis, and additionally the accessory glands, which include the prostate, bulbourethral gland, and seminal vesicles (Fig. 1) (Kirsch et al. 2017).

The paired testicles are responsible for the production of male sex hormones (androgens) and sperm cells. The immature sperm are then transported to the epididymis, which lies along the testicles, and sperm matures on its way through the epididymis. In the last section of the epididymis, the mature sperm are stored until ejaculation. During two-phase ejaculation process, the sperm first flows out of the epididymis through the vas deferens to the proximal part of the urethra. The vas deferens ends in the urethra, which is enclosed by the prostate in this part. At this opening, which is known as the seminal colliculus, the urethra is enlarged. On this pathway, the sperm are mixed with other fluids from the accessory glands. The fluids from accessory structures including the prostate, and seminal vesicles are mix together with the sperm and ends in the urethra at the seminal colliculus. The fluid from the bulbourethral glands end at the pars spongiosa in the urethra (Aumüller et al. 2020). In the second phase, the expulsion phase, the mixed components are expelled from the body through the urethra (Giuliano and Clément 2005; Alwaal et al. 2015; Kirsch et al. 2017).

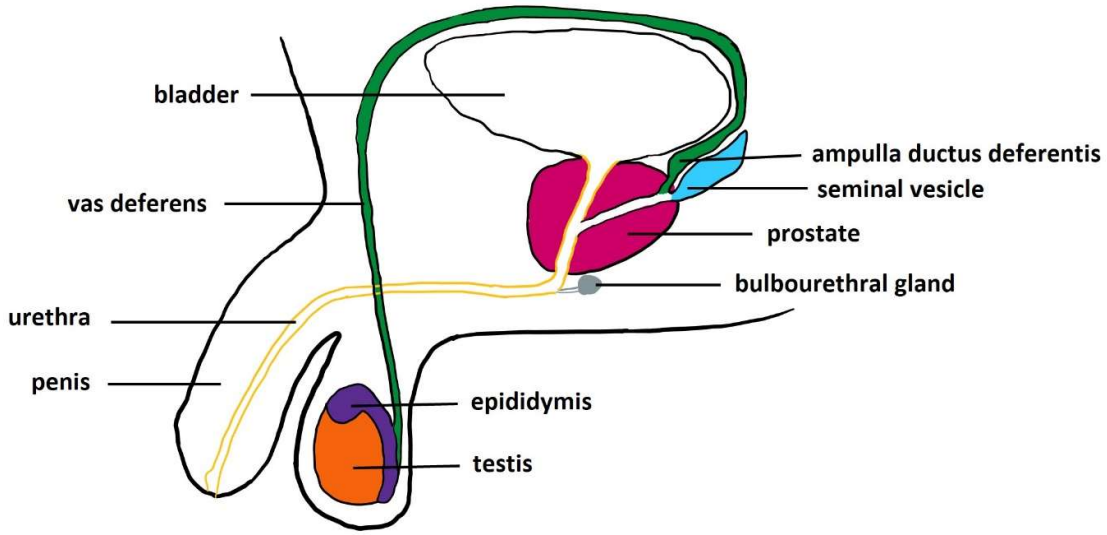

Figure 1 | General overview of the human male reproductive tract. The human male reproductive system includes the penis, testis (orange), epididymis (purple) and vas deferens (green), which expands into the ampulla ductus deferentis. The accessory glands, seminal vesicle (blue), the prostate (red), and the bulbourethral gland (grey) are also part of it.

To show the embryonic origin of the male reproductive tract of humans, next the development of this system will be described. The embryonic development of the urogenital tract, whereby urinary and genital organs are combined because they are structurally and functionally dependent on each other in the early developmental phase, begins with the formation of the tripartite system from the intermediate mesoderm. First, the pronephros is formed, which, however, is only rudimentary and has no function. After this, the mesonephros is formed, although part of it is also formed back again. The majority remains and the ureteral duct, which is also known as the Wolffian duct, is the precursor of the epididymal duct. Overlapping in time with the regression and transformation of the mesonephros, the metanephros is formed, from which the final kidney develops (Ulfig and Brand-Saberi 2017).

Initially, the paired gonadal ridges, which are from the intermediate mesoderm, develop in the same way in both biological sexes. Through the immigration of the gametes into the gonadal ridges, the gonads differentiate into the testes following the upregulation of the *SRY* gene and coding for the testis-determining factor (TDF). During this development, all the necessary cells are already formed and the Sertoli cells, the prespermatogonia and the Leydig cells are developed in the testis (Pask 2016; Ulfig and Brand-Saberi 2017).

The development of the male accessory glands is driven by the androgens testosterone (T) and dihydrotestosterone (DHT) via the androgen receptor (AR). The seminal vesicles develop from an invagination of the Wolffian duct shortly before it enters the urogenital sinus. The prostate, like the other male accessory sex gland, develops in an androgen-dependent manner from several origins. The development of the prostate starts early around week 8-9 of pregnancy (Cunha et al. 2018; Buskin et al. 2021). It starts with the development of prostate buds and the glandular epithelium from the urogenital sinus that are of endodermal origin. The surrounding mesenchyme, which is also influenced by androgens, develops into the stroma of the prostate (Pask 2016; Cunha et al. 2018). At birth, the human prostate is well developed, weighing only about 2 g in boys during childhood and during puberty, age-dependent growth occur, when T levels increase, the prostate changes mainly in size, reaching a weight of 20 g (Berry et al. 1984; Vickman et al. 2020).

In the next section, a short general description of the male reproductive tract of the rat is described.

1.1.3 Rat male reproductive system

Since the very similar human reproductive tract has already been described in detail in 1.1.2, this section only roughly describes the rodent reproductive tract. The male reproductive tract in rodents is shown and explained here based on the example of the rat. This tract here also consists of the penis and the paired testis (orange), epididymis (purple), vas deferens and additionally the accessory sex glands. In rats, the accessory glands include seminal vesicles (blue), the preputial gland, the prostate (red), glandula ampullaris, and bulbourethral gland (Fig. 2) (Jesik et al. 1982; Bosland MC et al. 1998).
The male sex hormone T and immature sperm cells are produced in the paired testis. On their way through the epididymis, the sperm cells mature and are stored in the last segment. During ejaculation, the sperm are ejected from the epididymis and transported through the vas deferens towards the urethra. Along the way, the sperm mix with the fluids from the seminiferous vesicles, preputial gland, and prostate. In the last step, the ejaculate is expelled from the body through the urethra.
Since the urogenital system of the rat has the same embryonic origin as in humans, it will not be described again here.

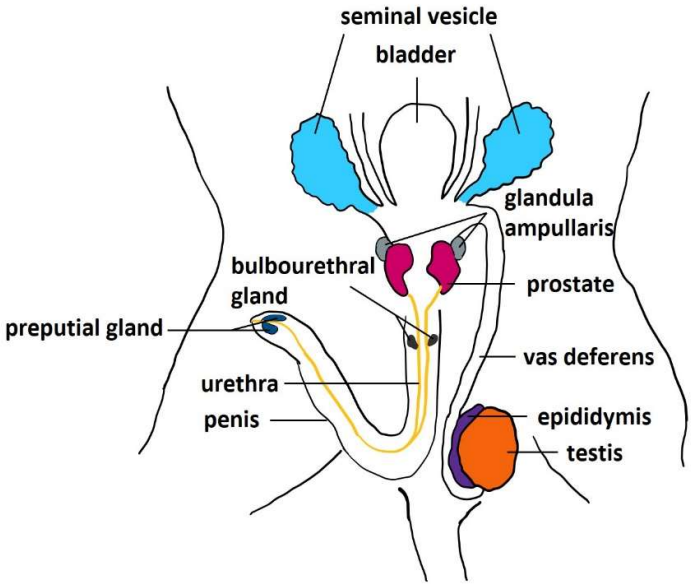

Figure 2 | General schematic overview of the rat male reproductive tract (ventral view). The rat male reproductive system consists of the penis, testis (orange), epididymis (purple) and vas deferens. The reproductive tract also includes the accessory glands, seminal vesicles (blue), preputial gland (dark blue), glandula ampullaris (light grey), bulbourethral gland (dark grey), and the prostate (red).

1.2 The Prostate gland

The prostate belongs to the accessory glands and is the largest accessory organ in the male reproductive system. It is an exocrine gland found only in mammals which secretes a fluid for the ejaculating fluid to support the sperm. However, there are species-specific differences in anatomy and physiology between mammals.

1.2.1 Anatomy, histology, and function of the human prostate

The human prostate is located caudally to the bladder, anterior to the rectum, posterior to the symphysis and thus encloses the first part of the urethra. It weighs about 20 g in a healthy man and is about 4 cm (transverse) x 3 cm (vertical) x 2 cm (anteroposterior). It is often compared in shape and size with a walnut (Kirsch et al. 2017). Because of its embryonic origin from the glandular epithelium and the surrounding mesenchyme, the prostate, as already described by McNeal et al. in 1981, consists of 70 % glandular elements and 30 % fibromuscular stroma. Based on the macroscopic anatomy the prostate is characterised into four zones because of its histological heterogeneity. According to McNeal et al., it is still usual to divide the prostate into the peripheral zone, central zone, transition zone and anterior fibromuscular stroma (Fig. 3). The whole prostate is enclosed by a fibromuscular capsule, which also divides the prostate into smaller regions or so-called lobules (McNeal 1988; McNeal 1981). The outermost zone, the peripheral zone, consists of about 70 % of the glandular volume and encloses the central zone and transition zone. The peripheral zone is predisposed to diseases and 70 % of prostate carcinomas occur in this zone. Prostatic chronic inflammation (prostatitis) is mainly found in this zone, too. About 25 % of the prostate consists of the central zone. This zone is located posterior to the transition zone, where the different ducts that open into the urethra are located. Here, in the central zones, the pars prostatica is found, which has the largest diameter, and in the middle is the colliculus seminalis. In this zone, the ductus deferens and the ducts of the seminal vesicles join and open into the urethra at the colliculus seminalis. Diseases such as Benign Prostatic Hyperplasia (BPH) or carcinomas are rare in this zone. The transition zone accounts for 5 % of the gland and surrounds the distal part of the preprostatic urethra. This zone is also predisposed to diseases and especially BPH occurs here. The smallest part with about 1 % is the anterior fibromuscular stroma. It fills the space between the peripheral zone and the urethra. In this zone, there are no glandular parts, only fibromuscular structures (McNeal 1988; Selman 2011; Kirsch et al. 2017; Alves et al. 2018).

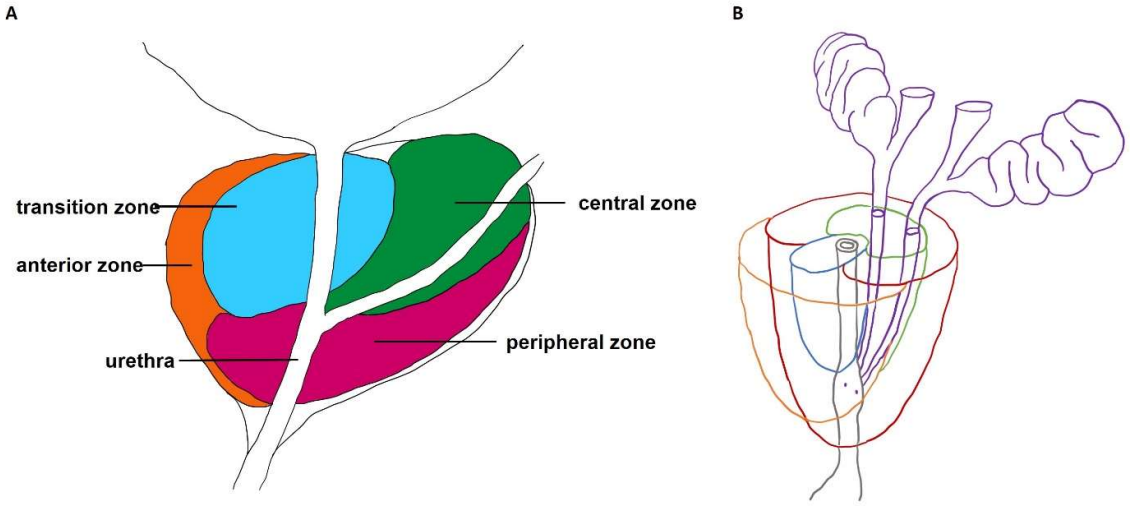

Figure 3 | (A, B) Detailed anatomy of the human prostate after McNeal et al. (1981). The prostate is located under the bladder and surrounds the urethra. The prostate gland can be divided into the transition zone (blue), central zone (green), peripheral zone (red), and anterior zone (orange), also called the fibromuscular stroma. The entire prostate is enclosed by a layer of collagenous fibres.

The prostate can be also differentiated into different areas and cell types in its microscopic anatomy. It consists of 30–50 tubuloalveolar glands which are mainly located in the peripheral zone. These glands are constructed of secretory acini which are composed of lined columnar epithelial cells that comprise the lumen. The epithelial cells produce prostatic secretion and release it into the lumen. The tubuloalveolar glands run into the prostatic excretory ducts (mainly found in the central zone), which end in the urethra with 15–30 openings. Depending on the zone, a dense stroma is found in the prostate consisting of fibroblasts, collagen fibres and smooth muscle cells (SMCs) in varying proportions. Furthermore, the prostate is strongly innervated by the autonomic nervous system (Kirsch et al. 2017; Alves et al. 2018). Through the numerous SMCs and innervation, the human prostate contracts spontaneously (Lee et al. 2017; Kügler et al. 2018)

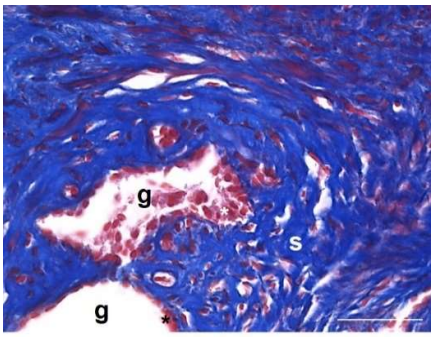

Figure 4 | Histology of the human prostate by azan staining. The adult prostate consists of glandular and stromal part. The glands (g) are surrounded by epithelial cells (*). A stromal compartment (s) can be found between the glands.

The prostate, as the largest accessory sex organ, plays a key role in the fertilization of sperm. The fluid produced by the luminal cells, called seminal plasma, accounts for about 30 % of the ejaculate. It is a milky liquid, is lightly acidic with a pH of approximately 6.4, and contains numerous proteins and enzymes. These secretory products include mainly the prostate-specific antigen (PSA), prostatic acid phosphatase (PAP), citrate and zinc (Kirsch et al. 2017).

PSA is a serine protease produced by the secretory epithelial cells in the acini of the prostate and cleaves the protein semenogelin-1 and -2, making the ejaculate thinner (Balk et al. 2003).

The acid phosphatase family hydrolyses a wide range of organic phosphomonoesters under acidic conditions, but the exact function of PAP in seminal plasma is not known (Vihko et al. 1978; Zelivianski et al. 1998; Kong and Byun 2013). The latest studies show that PAP could have an effect on sperm motility. A review by P. J. Hanley from 2023, which summarized the research around PAP in recent years, suggests a role of PAP in auto- and paracrine cholinergic signalling. It is suggested that PAP converts phosphocholine (PC) into choline, which in turn activates the choline signalling pathway in sperm. Choline can in turn be converted to acetylcholine (ACh) in sperm and thus stimulate signalling pathways (Hanley 2023).

The epithelial cells of the prostate are also able to produce a high amount of citric acid. In seminal plasma, high concentrations of citric acid of 40-150 mM were found. In contrast, the citric acid concentration in blood plasma is only 0.2 nM. The function of citric acid is to maintain a slightly acidic pH and it plays a crucial role in the Krebs cycle for the production of ATP (Costello and Franklin 2009).

In addition to these factors, a high concentration of zinc was also found in the seminal plasma, which originates from the prostate, which has the highest zinc concentration of any organ. Zinc concentrations in the prostate are 300-fold and in the ejaculate 100-fold higher than in blood plasma (140 µg/mL). Numerous studies show a multifaceted role of zinc on male fertility. Zinc affects the stability of biological membranes by influencing the fluidity of lipids, and also the stability of sperm chromatin (Costello and Franklin 2009; Zhao et al. 2016). Moreover, zinc could play an antibacterial role, as studies have shown that such high concentrations of zinc have an antibacterial effect on gram positive and gram negative bacteria, whereby it damages the membrane (Prins and Lindgren 2015; Mendes et al. 2022). However, more precise mechanisms about the function and mode of action of zinc and its high concentration in the prostate and seminal plasma are not known.

The fluid also contains carbohydrates, with high amounts of fructose, prostaglandins, electrolytes, polyamines, lipids and growth factors. All these products help to protect, nourish the sperm and maintain their motility in the vaginal environment (Prins and Lindgren 2015).

1.2.1.1 Role of sex hormones on the human prostate

The prostate, as an androgen-sensitive and -dependent organ, is already controlled by androgens during its embryonic development. Expression of the AR can be detected in the stroma as early as 11.5 weeks and additionally in the epithelium from 16 weeks onwards (Adams et al. 2002). DHT probably plays a more important role than T because it has a two- to five-fold higher affinity for AR and a two- to ten-fold higher potency than T. DHT is synthesised by the enzyme 5-α-reductase (5AR), which converts T to DHT. A 5-AR deficiency indicates that DHT is critical for normal prostate development, and important for initiation of prostate differentiation. Prostates from patients with 5AR deficiency are only rudimentarily developed (Imperato-McGinley et al. 1992; Cunha et al. 2018; Vickman et al. 2020).

Receptors for oestrogens (ERα and ERβ) have also been found in the embryonic prostate, although there is some controversy about their initial expression. Adams et al. detected ERβ as early as week 13 in epithelial cells of the prostate, whereas ERα could not be detected in the human fetal prostate and expression of ERα could only be detected postnatally (Adams et al. 2002). Another study by Shapiro et al. shows expression of ERβ as early as week 8 in the prostatic buds and initial expression of Erα could be detected at week 15 and was strong by week 19 (Shapiro et al. 2005). The exact role of oestrogens in embryonic prostate development is not completely understood, but the increase in estradiol (E2) from maternal source during pregnancy has been found to stimulate extensive squamous metaplasia in prostate development (Prins and Korach 2008).

At birth, the human prostate is well developed, and it is not until puberty, when T levels rise, that the prostate increases further in size and volume (Berry et al. 1984; Vickman et al. 2020).

T mainly produced in the testis reaches the prostate through the bloodstream and can act on both epithelial and stromal cells. In the stromal cells, T can be converted by 5AR into the predominantly active DHT. DHT acts either in an autocrine manner on stromal cells or in a paracrine manner on neighbouring epithelial cells (Fig. 5) (Roehrborn 2008). T or DHT bind to the receptor AR and cause a conformation change so AR can form a homodimer. Together with other components AR enters the nucleus and acts as a transcription factor and induces various signalling pathways (Vickman et al. 2020). The target genes contain hormone response elements to which the AR can bind and regulate the activity of these genes. The two androgen-dependent processes cell proliferation and apoptosis are a delicate balance that must be maintained. Cell proliferation is regulated by the activation of various growth factors, such as fibroblast growth factor (FGF), keratinocyte growth factor (KGF), epidermal growth factor (EGF) and insulin-like growth factor (IGF-I). To regulate apoptosis, DHT in a complex with the AR receptor can activate the production of transforming growth factor-β (TGF-β) (Kim et al. 1996; Niu et al. 2001; Carson and Rittmaster 2003).

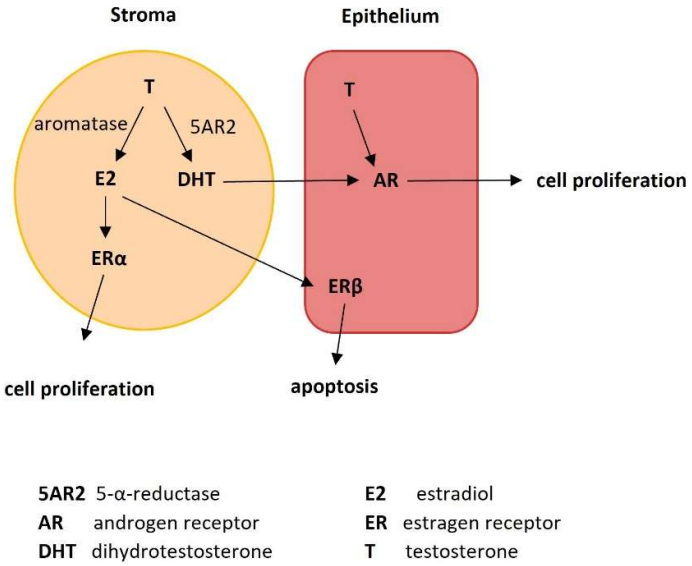

Figure 5 | Schematic overview of the regulation of the human prostate by sex hormones. Testosterone (T) can diffuse into prostatic stroma and epithelium cells. It can be converted either by aromatase into estradiol (E2) or by 5-alpha-reductase to dihydrotestosterone (DHT). These two androgens are binding to the androgen receptor (AR) regulating cell proliferation. Estradiol binds either to the oestrogen receptor alpha (ERα) regulating also cell proliferation in different cell types or to ERβ promoting apoptosis.

In addition to androgens, the human prostate is also regulated by oestrogens such as E2 (Fig. 5). The synthesis of E2 from T occurs mainly in stromal cells and is catalysed by the enzyme aromatase (CYP19) (Matzkin and Soloway 1992). In the human prostate, two different receptors for E2 can be found, depending on the cell type. ERα is expressed in stromal cells and ERβ is found in epithelial cells and also some stromal cells. These receptors are also transcription factors that enter the nucleus after binding with E2 and subsequent dimerization. By recruiting additional cofactors, the receptors bind with high affinity to their target genes and activate their synthesis. Thus, activation of ERα is associated with cell proliferation in stromal cells via the production of cyclinD1. Activation of ERβ, on the other hand, seems to regulate and induce apoptosis in epithelial cells (Prins and Korach 2008; Da Silva and Souza 2019).

1.2.2 Anatomy, histology, and function of the rat prostate

The rat prostate is also the largest accessory sex gland and is located partly under the bladder. The rat prostate can be divided into four lobes, whereby the localisation around the urethra, which is not completely enclosed, plays a role. Thus, the paired lobes can be divided into the ventral, lateral, dorsal, and anterior lobes (or coagulating gland), whereby the individual lobes differ slightly from each other histologically. Around the subdivided prostate, there is a thin membrane of connective tissue and surrounding fatty tissue (Fig. 6) (Jesik et al. 1982; Ginja et al. 2019).

Histologically, the rat prostate is a tubuloalveolar gland and composed of epithelium-lined acini, which produce the prostatic fluid and release it into the lumen. Surrounding these acini is a stroma consisting of various cell types. The main part is made up of SMCs, but fibroblasts, collagen fibres and blood vessels can also be found. The individual acini are surrounded by a single-cell layer of SMCs, which can spontaneously contract (Kügler et al. 2018). In addition to the acini, there are ducts in the rat prostate into which several acini merge. These ducts are surrounded by a multi-cell layer of SMCs and end in the urethra (Ginja et al. 2019).

During ejaculation, the fluid produced by the prostate flows out of the lumen, through the ducts into the urethra and is mixed with the sperm and other fluids from the accessory sex glands. The composition of the light acidic prostatic secretion plays an important role in the fertilisation of sperm. The prostate gland of rodents, as explained here in the rat, is embryologically derived from the urogenital sinus. Through epithelial budding and the resulting prostate buds, the prostate gland develops from an endodermal origin. The surrounding mesenchyme develops into the stroma of the prostate. However, this development does not progress much prenatally and at birth, the prostate is in the initial stage of budding. After birth, the prostate continues to develop into lobes with ducts and differentiation of the epithelial cells and ends around day 30 postpartum (Hayashi et al. 1991).

Since the rat is often used as an animal model, the next section will highlight the similarities and differences between the human prostate and the rat prostate.

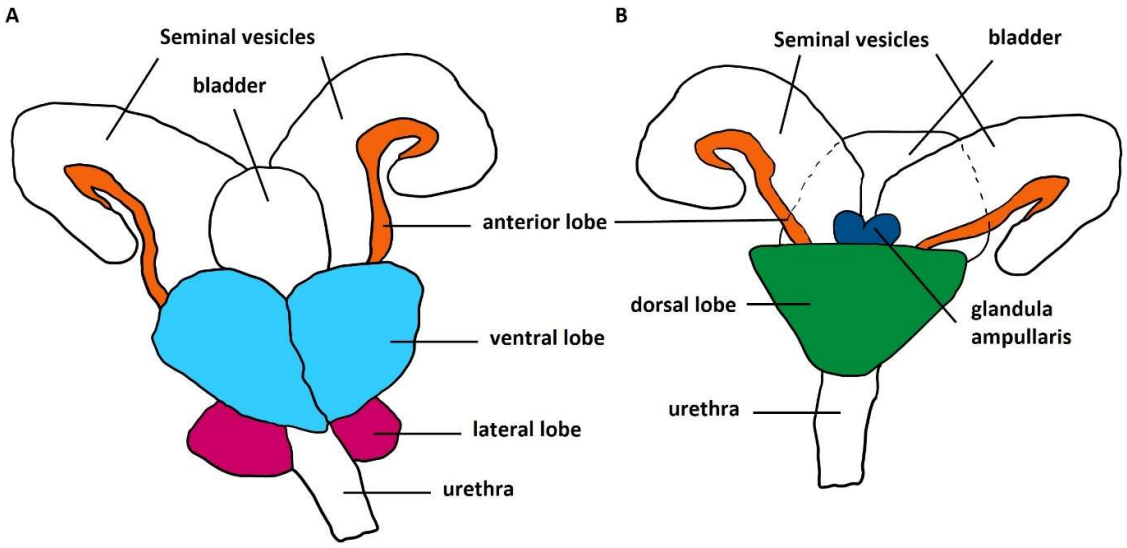

Figure 6 | Detailed anatomy of the rat prostate. (**A, B**) The prostate gland can be divided into the dorsal lobe (green), ventral lobe (blue), lateral lobe (red), and anterior lobe (orange), also known as the coagulating gland. (**B**) In this part of the reproductive system of the male rat, the glandula ampullaris (dark blue) can be seen on the dorsal side.

1.2.3 Comparison between human and rat prostate

Looking at the anatomy first, many similarities can be observed. The human and rat prostates can be divided into four different zones (ventral, lateral, dorsal and anterior) depending on their position (Jesik et al. 1982; McNeal 1988). For the research and also here in these studies, the ventral lobe of the rat prostate was used. Previous studies by our group have shown that the ventral lobe of the rat is best suited for such experiments, as it contracts spontaneously and responds appropriately to the investigated substances (Kügler et al. 2018; Seidensticker et al. 2022).

The differences between humans and rats become clear when considering the outer layer of the prostate. In rats, the individual lobes are surrounded by a thin, connective tissue-like membrane (Jesik et al. 1982), whereas in humans the entire prostate is surrounded by a capsule. Due to, among other things, this unique covering of the entire prostate, humans develop BPH and moreover it only occurs spontaneously in dogs and in chimpanzees (see section 1.4 for a more detailed explanation) (Steiner et al. 1999; Mahapokai et al. 2000).

Differences can also be observed in development. Although both the human and the rat prostate have the same embryonic origin in the urogenital sinus, the development of the human prostate is almost complete at birth. Only during puberty, when T levels increase, the human androgen-dependent prostate increases in size again (Berry et al. 1984; Cunha et al. 2018; Vickman et al. 2020). The prenatal development of the rat prostate stops early and only progresses to the initial stage of budding. After birth, the prostate further differentiates into lobes with ducts and increases in size (Hayashi et al. 1991).

Functionally, the human and rat prostates fulfil the same purpose. They are responsible for the production and secretion of prostatic fluid, which makes up 30 % of the seminal plasma. In both, this fluid is produced by the epithelial cells and contains several proteins and enzymes essential for sperm fertility.

1.3 Smooth muscle cells – contraction and relaxation

The contraction and relaxation of smooth muscle cells have an essential function in many organs. Smooth muscle cells are found in structures such as blood vessels, intestine, lungs, uterus, and ureter, but also in the male reproductive organs. Here, smooth musculature is found in the testis around the testicular tubules (Virtanen et al. 1986; Middendorff et al. 2002), epididymis (van Velde and Risley 1963), vas deferens (RICHARDSON 1962; Devine et al. 1971) and in the prostate (Hutch and Rambo 1970; Hafen and Burns 2024).

These muscle cells have a spindle-shaped basic form with one central elongated, rod-shaped cell nucleus in the cytoplasm. Due to their morphology, smooth muscle cells arrange themselves into easily recognisable bundles, which partially branch (Hafen and Burns 2024; Pape et al. 2019).

A smooth muscle cell is mainly composed of myofilaments, which consist of actin and myosin components. The actin filaments are anchored as bundles in dense plaques in the cell membrane. The actin filaments are interconnected via the dense bodies located in the cytoplasm. Dense bodies are the Z-discs of smooth muscle. They consist of intermediate filament desmin. Myosin filaments run between the actin filaments, whereby one myosin filament is cross-linked with several actin filaments (Fig. 7).

Furthermore, a functional classification can be made between two types of smooth muscle: the single-unit and the multi-unit type. In the single-unit type, the individual cells are electrically connected via a gap junctions and contract as a unit. This is possible through the rapid exchange of ions and second messenger molecules. These cell groups are activated by pacemaker cells, which in turn are controlled by the autonomic nervous system (Hafen et al. 2024). The single-unit type is found mainly in the intestinal wall, uterus and small blood vessels (Pape et al. 2019).

The multi-unit type consists of independent cells that can contract individually. This allows for more precise coordination of contractions as the cells are individually innervated. This type is found in the iris of the eye, larger vessels, and bronchi (Hafen et al. 2024).

This musculature fulfils different functions in the various tissues, but the signalling pathways are the same. For instance, smooth musculature is responsible for food transport through wave-like contractions in the gastrointestinal tract, but also for maintaining vascular resistance in the entire circulatory system. Although smooth muscle is an involuntary non-striated type of muscle, it can still be controlled. It can be controlled by various factors, such as the autonomic nervous system, and can also be influenced by neurotransmitters and hormones (Hafen et al. 2024).

The signalling pathways for contraction by the signalling molecule noradrenaline and relaxation by the natriuretic peptides and nitric oxide will be explained in more detail in the next sections.

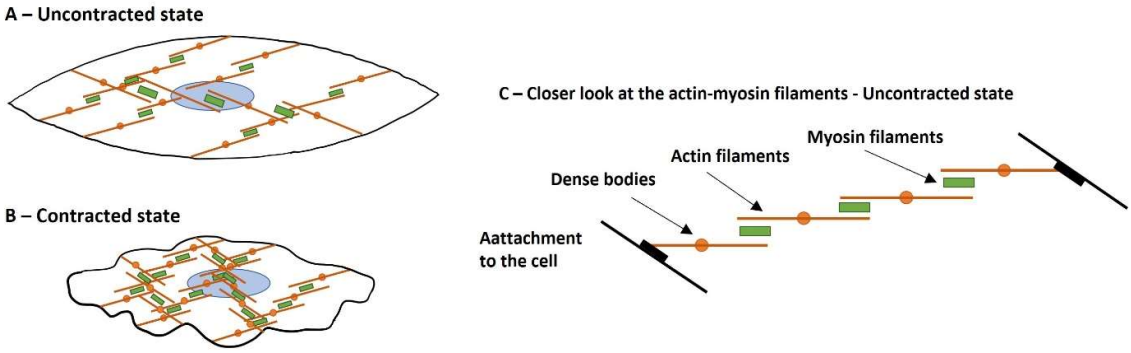

Figure 7 | Schematic overview of the structure of myofilaments and the simplified process of contraction in a smooth muscle cell. (**C**) The myofilaments consist of actin and myosin components. The actin filaments (orange) are anchored to the cell membrane via dense plaques. The actin filaments run as bundles over dense bodies and myosin filaments (green) run between the actin filaments. (**A**) Cell with actin and myosin filaments in an uncontracted state. (B) In the contracted state, the myosin filaments pull along the actin filaments and the cell contracts.
Figure 7A and 7C were modified according to https://de.wikipedia.org/wiki/Glatte_Muskulatur (05.05.2024)
Figure 7B was modified according to https://en.wikipedia.org/wiki/Smooth_muscle (22.06.2024)

1.3.1 Contraction pathways in smooth muscle cells of the prostate

The contraction of smooth muscle can be induced by the adrenergic signalling pathway and the signalling molecule noradrenaline (Fig. 8) (Christ and Andersson 2007; Webb 2003). This molecule can bind to the adrenoceptor α1, a G-protein-coupled receptor (GPCR), and mediates a signalling cascade. First, GPCR activates membrane phospholipase C (PLC), which cleaves phosphatidylinositol 4,5-bisphosphate (PIP2) into two further signalling molecules inositol-1,4,5-trisphosphate (IP3) and diglyceride (DAG). IP3 migrates through the cell to the smooth endoplasmic reticulum (ER). There it binds to the IP3 receptor (IP3R) on the membrane of the ER and induces a calcium release into the cytoplasm. The Ca^{2+} ions bind to the calmodulin (CaM) present in the cytoplasm. The Ca^{2+}/CaM complex diffuses and activates the myosin light chain kinase (MLCK), which triggers SMC contractions by phosphorylating the myosin light chain (MLC). At the same time, the Ca^{2+}/CaM complex inhibits caldesmon and calponin, which would inhibit actin ATPase. This interaction between the phosphorylated MLC and the active actin ATPase allows a molecular interaction between myosin and actin and thus leads to the contraction of the muscle cells. The cleavage of DAG from PIP2 in turn activates protein kinase C (PKC). Through another intermediate enzyme, the myosin light chain phosphatase (MLCP) is inhibited, which would dephosphorylate the MLC and thus deactivate it again (Christ and Andersson 2007; Webb 2003).

The Ca-independent rho-kinase signalling pathway via RhoA/Rho-associated protein kinase (ROCK) inhibits MLCP, which dephosphorylates MLC. Thus, MLC remains phosphorylated and contractions are stimulated. RhoA is a GTPase and is actually in a deactivated state, forming a complex of RhoA/GDP. Through the activated GPCR receptor, RhoA is activated by binding to RhoGTPase guanine nucleotide exchange factors. The active RhoA/GTP binds to the serine/threonine kinase ROCK and in smooth muscle cells this leads to contractions by further inhibition of MLCP. This signalling pathway also influences the regulation of the actin cytoskeleton and cell proliferation through the two ROCK1 and ROCK2 proteins (Christ and Andersson 2007).

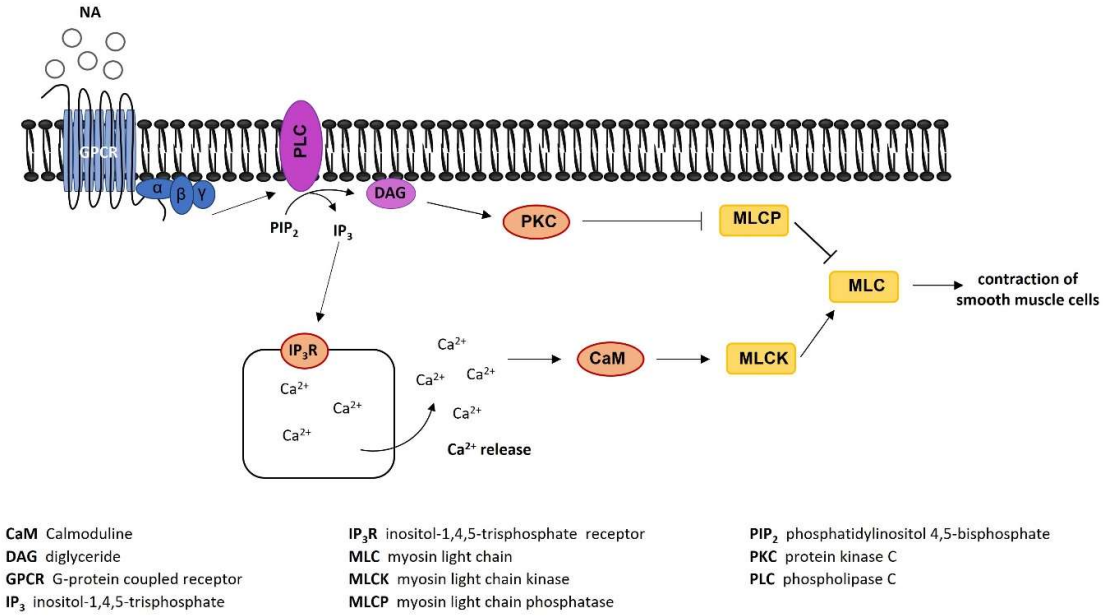

Figure 8 | Smooth muscle contractility coordinating via the adrenergic signalling pathway. The adrenergic pathway acts via adrenergic receptors that are G-protein coupled receptors (GPCRs) and are activated by noradrenaline (NA). GPCR activates the phospholipase C (PLC), which cleaves phosphatidylinositol 4,5-bisphosphate (PIP2) into the substrates inositol-1,4,5-trisphosphate (IP3) and diglyceride (DAG). IP3 initiates Ca2+ release through the IP3 receptor (IP3R) from the endoplasmic reticulum (ER) and Ca2+ can bind to calmodulin (CaM). CaM in turn interacts with the myosin light chain kinase (MLCK) which in turn results in smooth muscle contraction. DAG also contributes to the contraction of smooth muscle cells as it activates the protein kinase C (PKC) which inhibits myosin light chain phosphatase (MLCP). This prevents the MLPC from blocking MLC.

The movement of actin and myosin filament can be explained in more detail using the filament-slip theory. Already in the resting state, actin and myosin filaments are connected, whereby ATP is bound to the myosin head and a 90° angle to the actin is created. The active MLCK phosphorylates the myosin neck, thereby achieving a higher affinity to the actin filament, and the active ATPase cleaves the ATP at the myosin head to ADP + P, which provides the necessary energy. The resulting conformational change flips the myosin head forward and the actin and myosin filaments slide into each other. After ATP hydrolysis, the ADP + P diffuses out of the myosin heads. To return to the initial state, a new ATP binds to the myosin head and a conformational change follows in which the myosin head is again at a 90° angle to the actin filament (Pape et al. 2019).

This well-described pathway induces contractions in SMCs of many organs. This signalling pathway via noradrenaline induces contractions in the ureter (Canda et al. 2007), uterus (Dupuis et al. 2008), bronchioles (Brieva and Wanner 2001), iris dilator muscle (McDougal and Gamlin 2015) and the seminal tract resulting in ejaculation (Sanbe et al. 2007; Seidensticker et al. 2022). The prostate also has adrenergic innervation and alpha1A is the most common adrenoreceptor subtype in the human prostate and mediates contractions (Lepor et al. 1993a; Lepor et al. 1993b).

Spontaneous contractions in the fibromuscular stroma also occur in the prostate, and have been studied by our group. These spontaneous contractions are thought to be responsible for mixing of prostatic secretions in the lumen (Kügler et al. 2018). Spontaneous contractions in the prostate have also been studied in guinea pigs in the group of Dr. Betty Exintaris. Studies have shown that these spontaneous contractions are initiated by spontaneous Ca^{2+} transients and suggest the presence of pacemaker cells (Lang et al. 2006; Nguyen et al. 2011; Lam et al. 2011). However, pacemaker cells in the human prostate remain controversial. It was found that the spontaneous contractions in the transition zone of the prostate are non-neurogenic in nature and are probably caused by accessible extracellular Ca^{2+}. This was shown in experiments in which the human prostate no longer showed spontaneous contractions after Ca^{2+} removal from the organ bath (Chakrabarty et al. 2019).

When the SMCs contract, they must be able to relax again. Other signalling pathways such as natriuretic peptides or NO are responsible for this. These signalling cascades and their significance will be explained in the next section.

1.3.2 cGMP signalling pathway in smooth muscle relaxation via natriuretic peptides

Besides contraction, smooth muscle cells must be able to relax again. One signalling pathway that induces this is via the natriuretic peptides (NPs) (Fig. 9). The NP´s family consists of three members. First, the Atrial- or A-type (ANP) natriuretic peptide was discovered in 1981 by De Bold et al. (Bold et al. 1981). Only a few years later, Sudoh et al. discovered the Brain- or B-type natriuretic peptide (BNP) in 1988 (Sudoh et al. 1988) and only 2 years later the C-type natriuretic peptide (CNP) in porcine brain (Sudoh et al. 1990). All three have a similar structure with a 17-residue disulphide-linked ring, which is crucial for biological activity (Misono et al. 1984). Furthermore, ANP and BNP have two tails at the N- and C-termini, whereas CNP has only one tail at the N-terminus. Thus, all three NPs have a similar size, with ANP being 28, BNP 32 and CNP either 53 or 22 amino acids long (Potter et al. 2006). The two different-sized CNP forms occur because in some tissues the mature CNP-53 is cleaved to CNP-22 by a yet unknown enzyme. However, both CNP are equally capable of binding and activating their receptor GC-B (Yeung et al. 1996). Another similarity between the NPs is their synthesis. All three are synthesised as prepropeptides, then cleaved to a propeptide by different enzymes and finally cleaved to the active NPs by another specific enzyme (Potter et al. 2009). Interestingly, these peptides are also very conserved between species and human ANP differs from rat ANP by only one amino acid. CNP also shows high interspecies homology with 99 % (chimpanzee), 96 % (dog), 91 % (mouse) and 94 % (rat) in comparison to human (Potter et al. 2009). In the following years after the discovery of the NPs, the receptors for the peptides were discovered by different groups. Two membrane-bound receptors can mediate the relaxing signal pathway. The NPs ANP and BNP bind to the guanylyl cyclase GC-A and CNP to GC-B and activate them (Suga et al. 1992). These receptors have extracellularly a large (about 450 amino acid) ligand-binding domain and a single membrane-spanning region, which is about 20 residues long. Intracellularly, GC-A and GC-B consist of a 250-amino-acid large kinase homology domain, dimerization domain with 40 residues and approximately 250-amino-acid carboxyl-terminal guanylyl domain (Potter 2005). After binding the NPs, both guanylyl cyclases convert guanosine triphosphate (GTP) to cyclic guanosine monophosphate (cGMP), which binds to cGMP-dependent protein kinase I (PKG I) in the cytoplasm (Suga et al. 1992; Carvajal et al. 2000). This kinase can activate Ca^{2+} uptake into the ER. Phosphorylation of phospholamban (PLB) at the ER disassociates it from the ATPase, which is thereby reactivated. The activated Ca^{2+}-ATPase can thus transport Ca^{2+} from the cytoplasm into the ER again and thus lowers the intracellular concentration of Ca^{2+}. Furthermore, PKG I phosphorylates inositol 1,4,5-triphosphate receptor associated 1 (IRAG) and thus inhibits the IPR3-induced Ca^{2+} release from the ER (Komalavilas and Lincoln 1994; Murthy and Makhlouf 1998). A third important pathway through which PKG I leads to the relaxation of SMCs is through phosphorylation

and activation of MLCP. The MLCP, in turn, inhibits the MLC through dephosphorylation, which leads to relaxation (MacDonald and Walsh 2018).

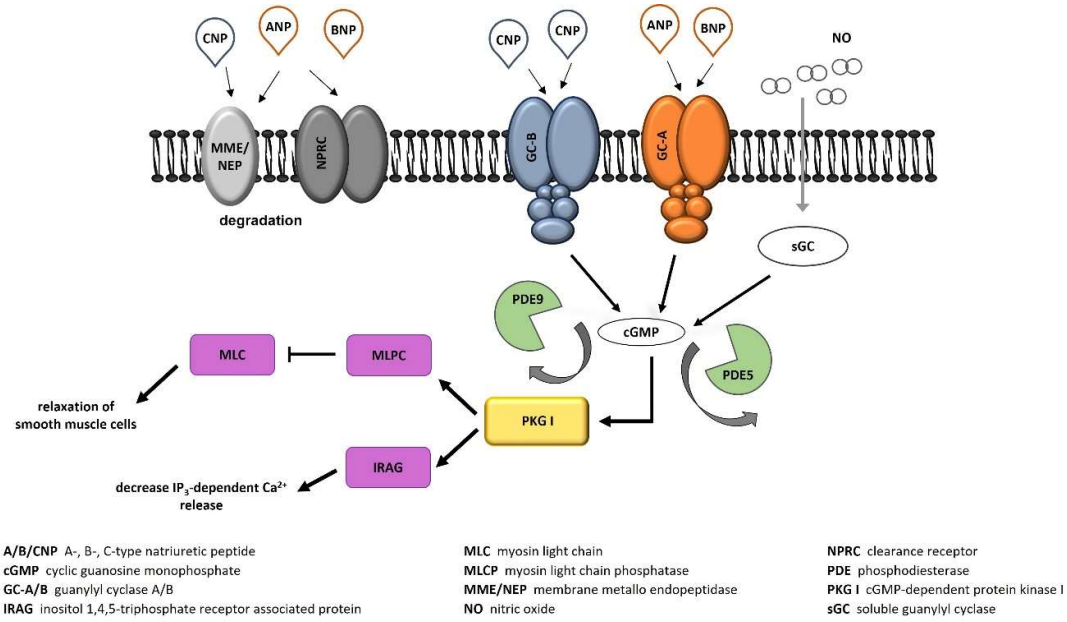

Figure 9 | Relaxation of smooth muscle cells through the cGMP signalling pathway activated by natriuretic peptides or nitric oxide. The production of the second messenger cyclic guanylyl monophosphate (cGMP) can be activated by nitric oxide (NO), that binds to the soluble guanylyl cyclase (sGC), or natriuretic peptides (A-, B- or C-NP). ANP and BNP bind guanylyl cyclase A (GC-A), whereby CNP only interacts with GC-B. The level of cGMP synthesized by GCs is either regulated by phosphodiesterases (PDEs), that hydrolyze cGMP in an inactive form or by the transmembrane enzymes membrane metallo endopeptidase (MME/NEP) and the Clearance receptor (NPRC). The activation of the cGMP-dependent protein kinase I (PKG I) by cGMP leads to the activation of myosin light-chain phosphatase (MLPC) that in turn inhibits the myosin light chain (MLC) resulting in smooth muscle relaxation. PKG I can also phosphorylate inositol 1,4,5-triphosphate receptor-associated protein (IRAG) and can thereby decrease the inositol triphosphate (IP3)-dependent Ca2+ release that is relevant for smooth muscle contraction.

The cGMP signalling pathway can be regulated at different levels. The first level already takes place extracellularly during the binding of the NPs to the GCs. Besides the receptors that mediate the signalling pathway, there are two other membrane-bound enzymes to which the NPs can bind.

In addition to the GCs that synthesise cGMP, there is a third receptor, NPRC, which is similar to the GCs. Like the other two GCs, NPRC also has a large extracellular ligand-binding domain, which is 30-35 % similar to GC-A and GC-B. The single membrane-spanning region is also the same. However, unlike the other two GCs, NPRC has only a 37 amino acid long intracellular domain and there is no known enzymatic activity of NPRC (Fuller et al. 1988; van den Akker 2001). It is responsible for the elimination of extracellular circulating NPs through receptor-mediated internalisation and subsequent

degradation (Matsukawa et al. 1999). Differences in the affinity of NPs for NPRC can be observed, although it is identical in humans and rats: ANP ≥ CNP > BNP (Bennett et al. 1991; Suga et al. 1992).

Furthermore, NPs can also be proteolytically degraded by NEP (Watanabe et al. 1997). It is also a membrane-bound, zinc-containing enzyme that cleaves substrates on the amino side of hydrophobic residues. For example, seven cleavage sites were identified for ANP, whereby the first cleavage leads to a break in the ring and thus inactivates the peptide (Stephenson and Kenny 1987; Vanneste et al. 1988). For CNP, six cleavage sites were found, whereby the initial cleavage site also cleaves the ring structure and inactivates the peptide (Kenny et al. 1993; Watanabe et al. 1997). In addition to the membrane-bound NEP, the insulin-degrading enzyme (IDE) can be found in the cytoplasm, which can cleave NPs. Studies showed that ANP is the preferred substrate for IDE and is cleaved at four sites. In contrast, BNP and CNP are only cleaved by IDE at three and two sites, respectively (Müller et al. 1992).

Furthermore, the signalling pathway can be regulated by the hydrolysis of cGMP. This is done by the phosphodiesterases (PDEs), which cleave phosphodiester links of intracellular cAMP or cGMP. There are eleven PDEs known, of which PDE5, PDE6 and PDE9 are cGMP specific. The hydrolysis and subsequent degradation reduce the intracellular cGMP level and thus interrupt the signalling pathway to relaxation (Maurice et al. 2014).

For the relaxation of prostatic SMCs, PDE5 is of particular interest, as there are many studies on this PDE. Initially, the exact localisation of PDE5 in the prostate was controversial, as early studies in the human prostate found PDE5 in glandular epithelial areas (Uckert et al. 2006) and not in the stromal part of the prostate. However, later studies also showed PDE5 expression in SMCs and thus in the stromal part (Zenzmaier et al. 2010), and a previous study by our group was able to show a clear co-expression and co-localisation of PDE5 and SMA in the human prostate and also the rat prostate (Kügler et al. 2018).

Another interesting cGMP-specific PDE that has the highest affinity for cGMP is PDE9 (Singh and Patra 2014). So far, the highest expression of this PDE has been found in the brain, spleen, small intestine and kidneys (Fisher et al. 1998; Rentero et al. 2003). Further studies also show expression of PDE9 in the urinary tract, like bladder and prostate (Nagasaki et al. 2012). Functionally, PDE9 is associated with cardiovascular diseases, insulin-resistance syndrome and diabetes, obesity, neurodegenerative disorders (Singh and Patra 2014). It was shown that the use of the PDE9 inhibitor BAY 73-6691 resulted in increased learning and memory capability (van der Staay et al. 2008). Interestingly, a new study shows that PDE9 plays a role in the regulation of SMCs in the bovine trachea and that the use of BAY 73-6691 led to a relaxation of bovine tracheal SMCs (Tajima et al. 2018).

The natriuretic peptides play an important role in other areas besides SMC relaxation, and next the effects of the individual NPs will be described in more detail.

1.3.3 Functions of natriuretic peptide in the body

ANP and BNP are also known as cardiac peptides because their origin is mainly in cardiac tissue. These NPs are stored in specific atrial granules of cardiomyocytes and released when needed (Bold et al. 1981; Bold et al. 2001). In addition to continuous release, the NPs are released in increased amounts during mechanical stress, such as stretching of the myocardium (Bold et al. 1996). An increase in BNP, but not ANP, is also observed during inflammatory processes in which proinflammatory cytokines are released (Kuhn 2016). The released NPs bind to the receptor GC-A and mediate various functions in the cardiovascular system as autocrine/paracrine hormones. In addition to the cardiovascular system, the expression of GC-A has also been detected in other tissues such as kidney, lung, brain, vasculature, liver, adipose tissue and testis (Kuhn 2004; Potter 2011). Thus, ANP and BNP also act as endocrine hormones. The most important role of these NPs, which is mediated via GC-A, is the effect on blood pressure and blood volume. This becomes clear when ANP or GC-A is knocked out and the mice suffer from increased blood pressure (Steinhelper et al. 1990; Ogawa et al. 1994; Potter et al. 2006). The precise actions by which ANP/GC-A system mediates an effect on blood pressure includes actions on endothelial permeability, vasodilation, diuresis, inhibition of the renin-angiotensin-aldosterone system, and thereby stimulation of renal function (Kurtz et al. 1986; Lanfear 2010; Kuhn 2016). One of the most important roles of ANP is its relaxant effect on vascular SMCs, which is evident in the relaxation of aortic rings after treatment with NPs and induces vasodilation (Drewett et al. 1995; Lopez et al. 1997). KO in mice of ANP or GC-A therefore leads to cardiac hypertrophy, chronic arterial hypertension and sudden death (Oliver et al. 1997; Kuhn 2004). Overexpression of GC-A, on the other hand, has an antihypertrophic effect (Kishimoto et al. 2001) and the treatment of cultured cardiomyocytes and fibroblasts with ANP shows an antiproliferative effect (Calderone et al. 1998). Surprisingly, BNP, which acts via the same receptor shows different effects. Deletion of BNP in mice shows that it is a local anti-fibroblastic factor in the heart (Tamura et al. 2000; Kuhn 2004). Because of their strong association with cardiac function, ANP and BNP are used as therapeutic agents in acute heart failure. BNP is used as a marker for heart diseases (Vuolteenaho et al. 2005) and, for example, Carperitide, a recombinant human ANP is used for the treatment of acute heart failure mainly in Japan (Kuwahara 2021).

In addition to the role of NPs in the cardiovascular system, ANP also shows a relaxing effect on the epididymis. Treatment with ANP led to a significant reduction of contraction in the epididymis (Mietens et al. 2014).

Only a few years after the discovery of CNP, the CNP level in seminal plasma was investigated. Interestingly, a study by Chrismann et al. (1993) showed that CNP is found in high amounts in porcine seminal plasma (Chrisman et al. 1993) and cattle seminal plasma (Codognoto et al. 2020). However, the role CNP might play there was not addressed. In the following years, the occurrence of CNP was further investigated and a study by Nielsen et al. (2008) showed that CNP is found in various porcine tissue types and that CNP is mainly present in male sex organs. CNP was found to be concentrated in the epididymis and testis. However, the highest amounts of CNP were detected in the seminal vesicles and the prostate (Nielsen et al. 2008). Only one year later, Nielsen et al. showed the presence of CNP also in human prostate tissue (Nielsen et al. 2009). The expression of the CNP receptor GC-B was also detected in various tissues, such as brain, bone, heart, kidney, lung, liver, the vascular system, testis and also in the female reproductive organs uterus and ovaries (Potter et al. 2009; Kuhn 2016). Previous studies by our group investigated the expression of components of the cGMP pathway in the male reproductive tract of the rat. It was shown that the analysed components, such as GC-A, GC-B, sGC, but also PDE5, PKG I and NOS3 are expressed in the rat prostate (Müller et al. 2011).

Functional studies on CNP and its receptor GC-B initially showed an inhibitory effect of CNP on the proliferation in different tissues. In studies with rats, it has been shown in vascular SMCs (Furuya et al. 1991) and cardiomyocytes (Horio et al. 2003). Furthermore, this effect has also been demonstrated in bovine aortic SMCs (Porter et al. 1992) and rodent cardiac fibroblasts (Tokudome et al. 2004), whereby CNP suppresses DNA synthesis.

A relaxing effect of CNP has also been found in male reproductive organs such as the penile arteries and epididymis. The study by Kun et al. (2008) showed a relaxing effect of CNP on human penile arteries, whereby it hyperpolarises the penile arteries. Furthermore, expression of CNP and its receptor GC-B RNA and protein level was found in the corpus cavernosum. First, this was demonstrated in 1998 in a study by Kim et al. in rat corpus cavernosum. CNP increased the production of cGMP and led to the relaxation of SMCs in the corpus cavernosum in organ bath experiments (Kim et al. 1998). Küthe et al. (2003) also demonstrated this effect in human corpus cavernosum. Here, too, treatment with CNP led to increased cGMP production and SMCs strips showed relaxation after CNP treatment in organ bath experiments. This study even suggests a possible therapeutic approach to treat patients with erectile dysfunction via this CNP/GC-B pathway (Küthe et al. 2003).

Furthermore, a relaxing effect of NPs was also shown in the epididymis. It has already been mentioned that ANP led to a relaxation in the epididymis, but CNP also showed a relaxing effect, although this was weaker than that of ANP (Mietens et al. 2014).

Recent studies on CNP show that it has an anti-inflammatory effect in the epididymis in epididymitis caused by *E. coli* bacteria. The application of CNP reduced the bacterial activity and decreased the

number of bacteria. It also suppressed the expression of some pro-inflammatory factors (NF-κB, IL-6, TNF-α and IL-1β) in macrophages and prevented their invasion (Mei et al. 2021).

The clearest effect of CNP or GC-B is seen in KO mice. Both the knock-out of GC-B and CNP results in dwarfism. Already in 2001, a study by Cusho et al. showed the effect of CNP KO on mice, whereby the effect was particularly evident during the growth process when CNP KO mice had reduced longitudinal growth. The vertebrae, tail, femurs, tibiae and limb bones were affected, and the mice showed significantly reduced naso-anal length. Since the KO mice had no changes in cranial growth, it was concluded that CNP affects endochondral ossification but not membranous ossification. In addition, the CNP KO mice died earlier than the wild-type mice (Chusho et al. 2001). Only a few years later, KO GC-B mice were generated in the study by Tamura et al. (2004). Again, the affected mice showed dwarfism, which became more prominent over the days after birth and is comparable to the results of the CNP KO mice. The naso-anal length was significantly shortened and the body weight was also significantly reduced. In addition, the GC-B KO mice died earlier. This study also looked at the histological changes in growth-plate cartilage, which were identical between CNP and GC-B KO mice. It is suggested that the changes in growth-plate cartilage are caused by a disturbed differentiation phase during endochondral ossification (Tamura et al. 2004).

This phenotype is found in humans with achondroplasia and possible therapy with Vosoritide, a recombinant C-type natriuretic peptide analogue, is being considered. A study was published in 2019 on a phase II clinical trial (Savarirayan et al. 2019) and a phase III trial (Savarirayan et al. 2020) is also already available. Vosoritide was administered subcutaneously to these children with achondroplasia. The treatment shows no serious side effects and there have been no deaths, so this treatment option is being pursued further.

1.3.3.1 Vasonatrin – a natriuretic peptide analogue

Vasonatrin (VNP) is a synthetic chimeric peptide of ANP and CNP. It was first synthesised in 1993 by Wei et al. and has the 22 amino-acid ring structure of CNP with the addition of the C-terminal end of ANP (Wei et al. 1993). Therefore, VNP is called a chimeric peptide. In the next few years, studies showed a relaxing and natriuretic effect of VNP. First, this was demonstrated in rings of femoral, saphenous, and renal arteries and veins of dogs. Compared to ANP and CNP, VNP also had a relaxing effect in a dose-dependent manner (Wei et al. 1993). Furthermore, work was carried out with Wistar rats to demonstrate cardiovascular and renal effects. It was shown that the treatment of rats with VNP also led to a relaxation of rings cut from the aorta. Furthermore, the treatment with VNP caused a decrease in mean arterial pressure and right arterial pressure. In addition, VNP also had a natriuretic effect and led to an increase in urine flow and sodium excretion. An RIA was used to determine the cGMP concentration, which was increased after treatment with NPs or VNP (Wei et al. 1993; Wei et al. 1994). In the following years, further studies showed effects of VNP, e.g. on cultured rat pulmonary artery SMCs. Hypoxia-induced cell proliferation and collagen synthesis were inhibited by the administration of VNP. A Comparison with ANP and CNP showed that VNP was stronger in its effect on the parameters investigated (Lu et al. 2005).

Other effects of VNP include the positive effect on diabetic hearts in rats. Here, VNP showed a protective effect against ischemia-reperfusion injury by inhibiting ER stress and apoptosis via the cGMP-PKG I signalling pathway (Shi et al. 2015).

Several years later, a group focused on the interactions and binding affinity of VNP to the two receptors GC-A and GC-B. Simulation analyses of VNP to GC-A or to GC-B showed a higher binding affinity of VNP to GC-B than to GC-A. In addition, the simulation showed VNP/GC-A to have a more flexible structure, whereas VNP/GC-B had a more stable structure, which can be attributed to the 35 pairs of H-bonds in VNP/GC-B. Further experiments in cultured cells in which GC-A or GC-B was specifically expressed showed that VNP leads to a higher production of cGMP via GC-B in comparison to GC-A (Jiang et al. 2014).

Due to its affinity for both receptors and its stronger effect on relaxation via the cGMP pathway, VNP may be suitable as a therapeutic approach in benign prostatic hyperplasia.

1.3.4 cGMP signalling pathway in smooth muscle relaxation via nitric oxide

Besides the NPs as activators of the cGMP signalling pathway, which among other things leads to relaxation in SMCs, nitric oxide (NO) is also known to initiate this pathway (Fig. 9). NO synthases (NOS), which are homodimers are responsible for the formation of this molecule and catalyse the production of NO. The amino acid L-arginine is used as the substrate and with oxygen and the co-substrate NAPDH it is converted to NO, citrulline, H_2O and NADP+ (Potter 2011; Förstermann and Sessa 2012).

There are three isoforms of NOS, which are present and named according to the site of production: endothelial NOS (eNOS), inducible NOS (iNOS) and neuronal NOS (nNOS).

In the neuronal tissue and system, nNOS is present and constitutively expressed. The NO synthesised by nNOS is associated with synaptic plasticity in the central nervous system, such as neurogenesis, learning and memory (Zhou and Zhu 2009), central regulation of blood pressure and vasodilation of blood vessels via peripheral nitrergic nerves (Togashi et al. 1992; Förstermann and Sessa 2012). An abnormality of NO synthesis by nNOS is associated with stroke, multiple sclerosis, Alzheimer's, and Parkinson's diseases (Steinert et al. 2010). In addition to neuronal functions, effects on SMCs and relaxation of SMCs are also known. In the male reproductive tract, for example, nNOS is involved in penile erection through relaxation of the SMCs in the corpus cavernosum (Kim et al. 1991; Rajfer et al. 1992). This signalling pathway is also already used therapeutically for the treatment of erectile dysfunction. PDE5 inhibitors are used, which prevent the degradation of cGMP by the PDE5 and cGMP accumulates in the SMCs (Davies 2015). In addition, there are newer therapeutic approaches to use the NO signalling pathway differently. The administration of L-arginine as a semi-essential amino acid and subtract in the synthesis of NO, has a positive effect on the amount of NO produced. The combination and administration of a PDE5 inhibitor (sildenafil) and L-arginine in patients with erectile dysfunction resulted in a significant improvement in the grade of erectile dysfunction (El-Wakeel et al. 2020; Muncey et al. 2021).

In contrast to nNOS and eNOS, iNOS is usually not produced in most cells. As the name suggests, the expression of this NO synthase can be induced by various factors. Among other things, inflammatory conditions ensure the expression of iNOS, whereby large amounts of NO are produced in macrophages, for example. Such conditions include signals through bacterial lipopolysaccharides and cytokines. This NO can enter neighbouring cells such as parasites, tumour cells, bacteria cells and cause damage by interacting with the DNA (Nathan and Hibbs 1991; Wink et al. 1991; Fehsel et al. 1993).

Although eNOS is mainly expressed in endothelial cells, it has also been found in other cell types such as cardiac myocytes, platelets, some neurons in the brain and tubular epithelial cells of the kidney. NO produced by eNOS is involved in many systems and functions. It plays an important role in the cardiovascular system, where it is responsible for vasodilation of all types of blood vessels (Furchgott

and Zawadzki 1980; Förstermann et al. 1986; Ignarro et al. 1986; Shesely et al. 1996). In this context, NO is also an inhibitor of platelet aggregation and adhesion to the vascular wall, thus acting as a preventer of thrombosis (Alheid et al. 1987; Radomski et al. 1987). In this vascular system, NO synthesised by eNOS may have anti-inflammatory and anti-atherosclerotic effects by preventing the adhesion of leukocytes to the vessel wall (Kubes et al. 1991) and by an apoptosis-suppressing effect (Dimmeler and Zeiher 1999). In addition to these functions, eNOS and NO have been shown to control the proliferation of vascular SMCs. NO has antiproliferative effects and inhibits DNA synthesis, mitogenesis and thus proliferation (Garg and Hassid 1989; Nakaki et al. 1990; Nunokawa and Tanaka 1992). An abnormality in eNOS activity is associated with several cardiovascular risk factors, such as diabetes mellitus, hypertension and hypercholesterolaemia (Förstermann and Sessa 2012).

The molecule NO can easily diffuse through the cell membrane of the cell and interact with its intracellular targets. Although NO can interact with many proteins and enzymes, only one receptor for NO is known. It is soluble guanylyl cyclase (sGC), which occurs as a heterodimer and consists of one α- and one β-subunit. Two of the α- and β-subunits are known (α1, α2, β1, β2), which can freely bind to each other. In humans, the α1 and β1 subunits are found in most tissues and the α2 and β2 subunits are expressed tissue-specifically. High expression of the α2 subunit occurs in brain, lung, colon, heart, spleen, uterus and placenta (Budworth et al. 1999; Derbyshire and Marletta 2012). The β2 subunit is poorly expressed, but is primarily found in kidney (Yuen et al. 1990).

This guanylyl cyclase also converts GTP to cGMP and the signalling pathway via PKG I as already described in 1.3.2 is activated. As described above, this signalling pathway activates various effects.

1.4 Benign prostatic hyperplasia

1.4.1 Definition and Etiology

Benign prostatic hyperplasia, also known as BPH, is one of the most common diseases of aged men. About 40 % of men have BPH in their 40s and the risk increases as they get older, so that 70-80 % of men have BPH by the age of 80 (Madersbacher et al. 2019).

BPH develops in the periurethral and the transition zone of the prostate (McNeal 1988) and is characterised by an uncontrolled proliferation of stromal and epithelial cells (Bartsch et al. 1979). These two characteristics can be divided into the static and dynamic components (Fig. 10) (La Vignera et al. 2016). The static component includes the increased proliferation of cells in the stromal and epithelial areas. The enhanced muscle tone is responsible for the dynamic component of the obstruction. During the development of BPH, the relationship between the glandular and stromal areas changes so that the stromal area becomes more dominant because of the increased proliferation of stromal cells (Bartsch et al. 1979). Due to the special anatomy and capsule around the human prostate, the cells also grow inwards and press on the urethra. Thus, the prostate can grow from its normal size (comparable to a walnut) and weight of 20 g up to 200 g and become as big as a tennis ball (Fig. 10) (Roehrborn 2008). Another characteristics in BPH is increased muscle tone of the prostate caused by adrenergic innervation of the prostate and among other things, that will be discussed in the further course (Lepor et al. 1993b). This symptomatology is already targeted in therapy (see next section 1.4.2 for more information). Due to the characteristics of BPH, lower urinary tracts symptoms (LUTS) can occur and cause symptoms such as poor urinary flow, frequency, hesitancy initiating flow, post-void dribbling and nocturia. These symptoms are also summarised as voiding LUTS. These BPH-induced LUTS also affect the patients' quality of life and have other implications, such as nocturia, which negatively affects a patient´s concentration and energy levels during the day (Devlin et al. 2021).

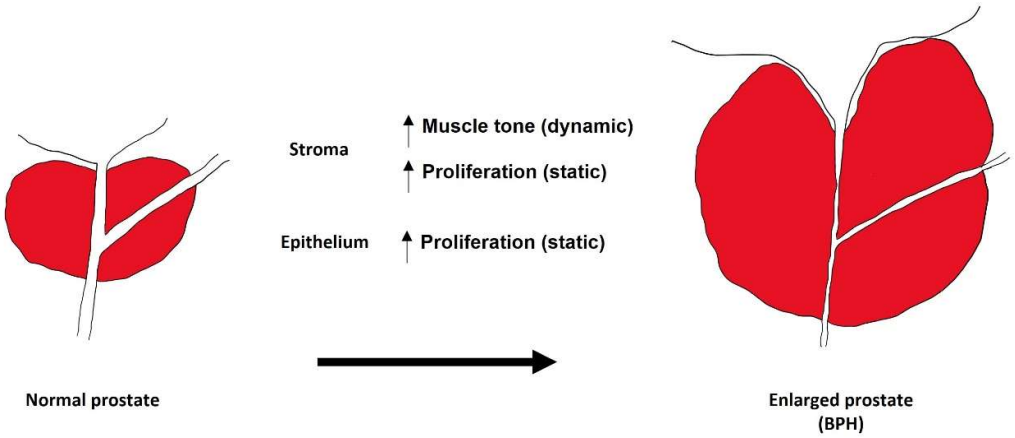

Figure 10 | Schematic view of the development of benign prostatic hyperplasia (BPH). In BPH, uncontrolled cell proliferation of the stromal and epithelial cells occurs (static component). The dynamic component of this disease includes an increased muscle tone. Because of a layer of collagenous fibres, the prostate grows inwards and presses on the urethra.

The exact cause leading to the development of BPH is still unclear. Since the prostate is an androgen-dependent gland, altered androgen levels in old age are associated with BPH but are controversially discussed. In addition to T, DHT also plays a decisive role in the prostate, as it binds to AR with an affinity up to 10 times higher than T. The 5-α-reductase (5AR), which has two subtypes (5AR1 and 5AR2), is responsible for the conversion of T to DHT, whereby 5AR2 is predominantly expressed in the prostate (Imperato-McGinley et al. 1992; Vickman et al. 2020). According to the saturation theory, the androgen-sensitive prostate is already saturated by the relatively low local hormone levels of T and DHT (Morgentaler and Traish 2009). Although the level of T in both serum and prostate decreases with age, the level of DHT is not affected (Hammond et al. 1978; Ryl et al. 2015). In fact, it seems to be the opposite, as higher levels of DHT have been measured in the prostate of BPH patients compared to healthy men (Siiteri and Wilson 1970). This delicate balance between T and DHT seems to play an important role in the development and progression of BPH (Roehrborn 2008). Interestingly, men with low T levels, such as post-castrated patients before puberty or eunuchs, do not develop BPH (Wilson and Roehrborn 1999).

In addition to androgens, oestrogens are also suspected to influence the development of BPH. In the cells, aromatase can convert T into E2, which can bind to two different receptors depending on the cell type (ERα and ERβ) (Simpson et al. 1994). Due to the reduced serum levels of T in old age, the ratio of T and E2 also changes, which disturbs the hormonal balance (Roberts et al. 2004). The specific localisation of the ERα and ERβ receptors strengthens a link between E2 and the development of BPH but they have opposite effects (Ellem and Risbridger 2009). ERα is mainly expressed in the stromal part of the prostate and can thus promote the proliferation of the cells (Song et al. 2016; Devlin et al. 2021).

Increased aromatase expression was also found in these cells (Hiramatsu et al. 1997). In contrast, ERβ is expressed in the basal epithelial cells and has a different effect (Song et al. 2016). It induces apoptosis of cells and the activation of ERβ by an antagonist induces apoptosis in BPH tissue (McPherson et al. 2010). However, since aromatase is expressed more in the stromal cells and thus ERα is activated more, the effects of ERα and ERβ do not balance each other out.

Besides hormonal influences, an impact of insulin and diabetes is also suspected. The effects of the insulin pathway are mediated by insulin growth factor 1 (IGF-1). A correlation between a high level of insulin / IGF-1 and BPH was found. In addition, the levels of insulin / IGF-1 could predict the size of the prostate, as higher levels of insulin / IGF-1 were found with increasing prostate size. This relationship could be explained by the local expression of the receptor for IGF-1 in the stromal components of the prostate, thus promoting proliferation of these cells (Clemmons and Maile 2005; Sreenivasulu et al. 2017).

Another factor that could lead to the development and initiation of BPH is chronic inflammatory processes in the prostate. The initial inflammatory response could be caused by various bacterial or viral pathogens, but the exact cause leading to BPH is still unclear. However, initial inflammation may be the trigger for BPH, as shown in a study in which 77.6 % of men had a chronically inflamed prostate before developing BPH (Nickel et al. 2008). A healthy prostate contains a large number of T-lymphocytes, which protect the prostate from pathogens from the urogenital tract. Clusters of differentiated CD8+T cells in periglandular areas form the majority and some CD4+T cells are found in the stroma. In BPH patients, however, more CD4+T cells were found than CD8+T, indicating chronic inflammatory processes. The activated T-cells release cytokines and interleukins, which lead to stromal and epithelial growth via other factors such as basal fibroblast growth factor 2 (FGF-2). The renewed growth of the prostate creates a hypoxic environment which leads to the release of ROS and further release of growth factors. A self-repeating cycle occurs, leading to chronic inflammation and uncontrolled increase in prostate volume (Steiner et al. 2003; Madersbacher et al. 2019; Devlin et al. 2021).

The factors listed here are the most likely to lead to BPH. However, it is not possible to explain why and how BPH develops, and other factors may also play a role. The following section discusses the possible and currently used treatment strategies.

1.4.2 Treatment options for benign prostatic hyperplasia

Nowadays, two strategies are applied in the treatment of BPH. Medications can be given that act on signalling pathways to reduce further growth and/or the basal tension of the prostate. If medication does not work or if micturition disorders are severe, a transurethral resection of the prostate (TUR-P) is performed to remove prostate tissue.
In the following sections, the medication treatment options are explained first and then the surgical procedure for a TUR-P is explained in more detail.

1.4.2.1 Medical strategies for BPH treatment

The progressive enlargement of the prostate due to uncontrolled cell growth leads to various LUTS and, if the patient is increasingly affected, drug therapy is used first. The choice of medication depends on the symptoms, but some treatment options have proven effective.
The following information is taken from reviews by Miernik and Gratzke (2020) published in Deutsches Ärzteblatt International (Miernik and Gratzke 2020) and Miernik and Roehrborn (2022) published in European Urology Focus (Miernik and Roehrborn 2022).
The first and still used therapy strategies use α1-adreneroreceptor (short α1-blocker) antagonists to inhibit the adrenergic signalling pathway. α1-blockers used in BPH therapy include terazosin, doxazosin, alfuzosin, tamsulosin and silodosin. These substances are antagonists to noradrenaline. Thus, these substances inhibit the NA-induced signalling pathway that leads to smooth muscle contraction by binding to the α-1-adrenergicreceptor and preventing signal transduction. The tissue tone of the prostate and bladder outlet can thereby be reduced. Because of their rapid and efficient action, α1-blockers are recommended for patients with moderate to severe LUTS. However, these substances have serious side effects. The most common side effects include asthenia, dizziness, and ejaculatory dysfunction.
Another approach to reduce muscle tone in the prostate is to use PDE5 inhibitors, such as tadalafil. Here, the cGMP signalling pathway, which also leads to smooth muscle relaxation, is modulated. By inhibiting PDE5, the hydrolysis of the second messenger cGMP is prevented and the signalling pathway remains active. Although these substances also lead to side effects such as headaches, dyspepsia or back pain, they do not lead to ejaculatory or erectile dysfunctions, since PDE5 inhibitors were first used in the treatment of erectile dysfunction. For the treatment of BPH, PDE5 inhibitors are used when the patient suffers from moderate to severe LUTS, as these substances also have fast and efficient effects.
In addition to short-term and rapid treatment strategies, 5-α-reductase inhibitors are used in long-term therapy. These inhibitors include the drugs finasteride and dutasteride and are used in patients

with predominantly voiding dysfunction and a large prostate volume above 40 mL. In this therapeutic option, the conversion of T to the more effective DHT is disrupted by inhibiting the responsible enzyme, 5-α-reductase. Since DHT activates signalling cascades that lead to cell proliferation, the growth of the prostate is inhibited and it was even observed that apoptosis was induced in prostate cells. Nevertheless, even these drugs have side effects, and among the most common and serious are decreased libido, erectile and ejaculatory dysfunction due to lower androgen levels. However, this treatment takes a long time (several months) to show effects and is therefore only suitable as a long-term therapy.

In order to optimise the treatments, combinations of these drugs are also used. Although side effects and drug interactions have to be taken into account, combinations of α1-blockers + 5-α-reductase inhibitors and 5-α-reductase inhibitors + PDE5 inhibitors have been proven to be beneficial.

A novel combination of PDE5 inhibitors (tadalafil) and α1-blockers (tamsulosin) promises a new approach to the treatment of BPH with LUTS and erectile dysfunction. This combination shows good tolerance and safety and the study by Sebastianelli et al., suggests an even more coordinated treatment of patients by switching to monotherapy after combination therapy (Sebastianelli et al. 2020).

α1-blockers + 5-α-reductase inhibitors have an increased risk of side effects, but the need for surgery is reduced and therefore this combination therapy is used in moderate to severe cases with an increased risk of progression (prostate volume < 40 mL). The approach with 5-α-reductase inhibitors + PDE5 inhibitors is also used in such moderate to severe LUTS.

Another option is the double or even triple combination with a muscarinic receptor antagonist or β3-adrenoceptor agonist (mirabegron). The muscarinic receptor M3 is expressed by the detrusor muscles of the urinary bladder and inhibition of this receptor prevents mediated contraction and this helps to empty the bladder. However, side effects include constipation, urinary problems, dizziness and nasopharyngitis.

To induce direct relaxation of the detrusor muscle, β3-adrenoceptor agonists can be used. The use of such a substance can improve storage symptoms. Side effects such as urinary tract infections, hypertension and nasopharyngitis must also be expected with the administration of this drug.

Current therapies result in undesirable side effects that limit patients' lives (ejaculatory and erectile dysfunctions). One possible way to circumvent this is to modulate the cGMP signalling pathway. This is already done by PDE5 inhibitors without serious side effects. Another approach considered in studies is to activate the cGMP pathway to relax SMCs via NO donors. These have been used to show that they first increase cGMP levels in tissues and further lead to relaxation in the prostate in various species such as rats, dogs and even humans. In a placebo-controlled study of the use of isosorbide dinitrate as

an NO donor in BPH patients, the drug was shown to have a beneficial effect on peak flow rate, enabled spontaneous voiding and decreased the volume of residual urine (Roshani et al. 2010; Tadayyon et al. 2012; Ückert et al. 2020).

The question arises whether the activation of the cGMP signalling pathway could also be mediated in another way, such as via the natriuretic peptides (see section 1.3.2). These peptides lead to relaxation of SMCs in other tissues. Together with PDE5 inhibitors, the cGMP pathway could be more strongly utilised as a possible treatment option for BPH.

1.4.2.2 Surgical Interventions

In the case that the symptoms of BPH, such as micturition disorders, are severe and the medication is not sufficient for treatment, a TUR-P will be performed, which is considered a standard procedure.

In this endoscopic procedure, a resectoscope with a wire acting as a resection loop is inserted through the urethra. Pieces of the prostate from the transition zone and the periurethral zone are removed. The resection loop is used to pass an electric current through the prostate to remove and ablate the tissue. The removal of the excess tissue that presses on the bladder and urethra relieves the pressure and provides relief to the patient (Braeckman and Denis 2017; Miernik and Gratzke 2020).

2 Aims

This thesis initially deals with the hormonal state in prostate of patients with BPH, focusing on the sex hormones testosterone and estradiol. Furthermore, the main focus is on the CNP/GC-B signalling pathway, which acts via the second messenger cGMP. This highlights the therapeutic potential of this relaxing signalling pathway, as a target in the future treatment of BPH.

- Local hormone levels of testosterone and estradiol will be determined in the prostate of patients with BPH, and the expression of the respective receptors will be measured at the mRNA level.
- Gene expression of key components of the CNP/GC-B signalling pathway in human prostate samples and correlation to the hormonal state.
- Functional assay such as cGMP ELISA will be performed with a primary human prostatic smooth muscle cells (HPrSMCs), derived from a young healthy man, in comparison to human aortic SMCs (HAoSMCs). These cells will be treated with ANP or CNP to demonstrate the dose-dependent cGMP production.
- Long-term exposure of SMCs to NPs will reveal potential effects on cell proliferation and expression of the cGMP pathway components.
- For the verification of the SMC phenotype immunofluorescence staining against SMC markers will be/was performed.
- To additionally proof the relaxing properties of the NPs, live imaging using rat prostate glands. To capture the contractility of the tissue imaging will be performed using a live imaging technique established in our working group. The resulting movies were analysed using the newly developed method for contraction analysis by Dr. Beatrix Bester and Cameron Nowell (Monash University).

3 Materials

3.1 Chemicals and Substances

The used chemicals are listed in the table 1 below.

Table 1 l Used Chemicals and substances

Chemical	Company
3,3',5,5'-Tetramethylbenzidin (TMB)	Carl Roth, Karlsruhe, Germany
3-isobutyl-1-methylxanthine (IBMX)	Sigma, St. Louis, USA
4-(2-hydroxyethyl)-1-piperazineethanesulfonic acid (HEPES)	Sigma, St. Louis, USA
Acetic acid	Merck, Darmstadt, Germany
Agarose	Carl Roth, Karlsruhe, Germany
Aniline	VWR, Radnor, USA
Aniline blue	Merck, Darmstadt, Germany
ANP	Bachem, Bubendorf, CH
Azocarmine G	Merck, Darmstadt, Germany
BSA	Merck, Darmstadt, Germany
cGMP	Biolog (Bremen, Germany)
CNP	Bachem, Bubendorf, CH
DAPI	Roche, Karlsruhe, Germany
Dimethyl sulfoxide (DMSO)	Carl Roth, Karlsruhe, Germany
dNTPs	Invitrogen, Waltham, USA
DPBS	Gibco, Thermo Fisher Scientific, Waltham, USA
Ethanol	Carl Roth, Karlsruhe, Germany
Ethylenediaminetetraacetic acid (EDTA)	Merck, Darmstadt, Germany
Eukit	Sigma, St. Louis, USA
Formaldehyde	Carl Roth, Karlsruhe, Germany
Glacial acetic acid	Merck, Darmstadt, Germany
Glycerol for immunofluorescence	Merck, Darmstadt, Germany
goat anti rabitt IgG antibody	Invitrogen, Waltham, USA
Hydrochloride acid	Merck, Darmstadt, Germany
Hydrogen peroxide	Carl Roth, Karlsruhe, Germany
iQ™ SYBR® Green Supermix	Bio Rad, Hercules, USA
MEM	Gibco, Thermo Fisher Scientific, Waltham, USA
Methanol	Sigma, St. Louis, USA
Noradrenalin	Sigma, St. Louis, USA
Oligio(dT)$_{12-18}$	Invitrogen, Carlsbad, Kalifornien, USA
Orange G	Merck, Darmstadt, Germany
Paraformaldehyd	Carl Roth, Karlsruhe, Germany
Parrafin	Merck, Darmstadt, Germany
Penicillin/Streptomycin	Gibco, Thermo Fisher Scientific, Waltham, USA
Phosphotungstic	Carl Roth, Karlsruhe, Germany
Picric acid	neofroxx, Einhausen, Germany
RNase, DNase free water	Invitrogen, Carlsbad, Kalifornien, USA

Sodium acetate	Merck, Darmstadt, Germany
Sodium bicarbonate	Merck, Darmstadt, Germany
Sodium chlorid	Merck, Darmstadt, Germany
Sodium dihydrogen phosphate monohydrtae	Merck, Darmstadt, Germany
Sodium hydroxid	Carl Roth, Karlsruhe, Germany
Sodium triphosphate	Carl Roth, Karlsruhe, Germany
Thimerosal	AppliChem, Darmstadt, Germany
TRIS	Carl Roth, Karlsruhe, Germany
Triton X-100	Sigma, St. Louis, USA
Trypsin-EDTA solution	Sigma, St. Louis, USA
TWEEN® 20	Carl Roth, Karlsruhe, Germany
VascuLife® SMC Medium Complete Kit	LifeLine Cell Technology, Frederick, USA
VNP	Bachem, Bubendorf, CH
x10 DMEM/F12	Gibco, Thermo Fisher Scientific, Waltham, USA
Xylol	Carl Roth, Karlsruhe, Germany
β-Mercaptoethanol	Carl Roth, Karlsruhe, Germany

3.2 Consumables

Table 2 l Used Consumables

Name	Company
8 well Chamber Slide	Sarstedt AG & Co. KG (Nuembrecht, Germany)
Cell culture flasks (25 and 75 cm3)	Sarstedt AG & Co. KG (Nuembrecht, Germany)
Delta T dish	Bioptechs Inc. (Buttler, USA)
Greiner Tubes	Greiner Bio-One International GmbH (Frickenhausen, Germany)
Immuno 96 well plates	Thermo Fisher Scientific (Waltham, USA)
Pipette tips	StarLab (Hamburg, Germany)
Reaction tube (1, 2.5 and 5 mL)	Sarstedt AG & Co. KG (Nuembrecht, Germany)
Reaction tube for qPCR & stripes	Greiner Bio-One International GmbH (Frickenhausen, Germany)
Serological pipettes	BD GmbH (Heidelberg, Germany)
x-well plates (48 and 96 well)	Greiner Bio-One International GmbH (Frickenhausen, Germany)

3.3 Tissue

In this thesis, human prostate tissue from BPH patients was used. After sampling, the tissue was placed in MEM medium and stored for a short time at 4°C. The samples were blotted as soon as possible and frozen in nitrogen within 1 hour.

Prostate tissues from rats 8-12 weeks old were used. The prostates were removed, prepared from fat and blotted to dry. The prostate samples were frozen in nitrogen until further use.

The samples were stored at -80°C until further use. A detailed list of the human and rat prostate samples with their respective ethics numbers can be found in Table 3.

Table 3 l Tissue which was used

Tissue	Species	Ethics
Prostate	Human	AZ 55/13
Prostate	Wistar rats (Rattus norvegicus)	469_M
		487_M
		505_M
		506_M
		507_M
		510_M
		955_GP

3.4 Cell lines

In these studies, primary human prostatic smooth muscle cells (HPrSMCs) and primary human aortic smooth muscle cells (HAoSMCs) obtained from Life Line Cell Technology (Frederick, USA) were used.

3.5 Antibodies

Table 4 l Primary Antibodies for Immunofluorescence. Diluted in Dilution Buffer for Immunofluorescence

Antibody	Dilution	Species	Company
Anti-Smooth Muscle Actin (SMA)	1:1000	Mouse monoclonal	Sigma (St. Louis, USA)

Table 5 l Secondary Antibodies for Immunofluorescence. Diluted in PBS Buffer

Antibody	Dilution	Species	Company
Alexa Flour 488	1:250	Goat-anti-mouse	Thermo Fisher Scientific (Waltham, USA)
Goat-anti-Rabbit IgG (H+L)			Invitrogen (Waltham, USA)

3.6 Oligonucleotides

The oligonucleotides for RT-qPCR used in this work were designed at Primerblast (https://www.ncbi.nlm.nih.gov/tools/primer-blast/) or sourced from a publication, whereby they should result in a product with a size of 70 – 350 bp. Some of the primer pairs result in a bigger product but the tests show good efficiency. The sense and antisense sequences for human (Table 6) and rat (Table 7) samples are listed below. More details about testing primers can be found in 4.2.1.3.1 Methods section.

Table 6 l Human oligonucleotides for RT-qPCR

Gene	Sense (5'-3')	Antisense (5'-3')	Product size	Origin
Beta-Actin	TCC CTT CCT GGG CAT GGA GT	TAC AGG TCT TTG CGG ATG TC	90	
RPLPO	CCT CGT GGA AGT GAC ATC GT	ATC TGC TTG GAG CCC ACA TT	178	
AR	GACATGCGTTTGGAGACTGC	TTCCCTTCAGCGGCTCTTTT	164	
ERα	TGGGAATGATGAAAGGTGGGAT	GGTTGGCAGCTCTCATGTCT	129	
ERβ	CATGCGAGTAACAAGGGCAT	TGGGAGCCCTCTTTGCTTTT	176	
GC-A	CAC CCT GGA CTG GAT GTT CC	CGT CCA CAG CTT TTT GGC AT	220	
GC-B	GAT GCT GGA GAA GGA GCT GG	TGG CGA CAA CAT TTC CCT TG	206	
NPRC	TCC CTG CAA ATC ATC AGG TGG	TCC TAG TAA AGC CCC CAC GA	70	
PKG I	CTC CAC CTA GAC AAG CTT CCA	GGG CTC ATT CCG ATT TCA TA	90	(Franko et al. 2018)
CNP	TGG AGT TAA GCG AGC AGC AAC	CCC ATT TGC CCA AGG AAT AGA G	236	(Xia et al. 2016)
PDE9A1	GTA CTG CAA CTC CAG CGA CA	GGA GAT GGT CGT GTT CCG AG	73	
PDE5	TGTTAGAAAAGCCACCAGAGAA	AGGGGCACTGTTATCTGCAC	148	
sGCβ1	GAG GTG TGG GAA GAC ATC AAA	GCA GCA GCA ACC AAA TCA TA	107	(Schermuly et al. 2008)

Table 7 l Rat oligonucleotides for RT-qPCR

Gene	Sense (5´-3´)	Antisense (5´-3´)	Product size	Origin
Beta-Actin	CCTA GGC ACC AGG GTG TGA T	TGG CCT TAG GGT TCA GAG GG	232	
Gapdh	CTT GTG CAG TGC CAG CCT C	ACC AGC TTC CCA TTC TCA GC	230	
Gc-a	CCA GAT TCT GCC TCA CTC CG	GCC CTG ACA CCA CCA TGT AA	248	

Gc-b	TCT TTG CCA ACA CCG GTC AC	AGA AAG GCC ATA CCC TTC ACA A	295	
Nprc	ATG ATG CTC GCT CTG TTC CG	ACA TGA TCA CCA CTC GCT CA	223	
Pkg I	GGA CTC ATC AAG CAC ACC GA	GTT CTT ACA TCC TCC CCC TGC	293	
Sgcβ1	CTG TAG TCG CTG TCT GGG TC	CCA GCA TTG AGG TTG AGG ACT	266	
Pde9a1	TGG GTG GAC TGT TTA CTG G	CGG TCT TCA TTG TCT TTC G	347	(Zhu et al. 2017)

3.7 Standard systems and Kits

Table 8 l Used Standard systems and Kits

Name	Company
iQ™ SYBR® Green Supermix	Bio Rad (Hercules, USA)
RNase-Free DNase Set	Qiagen (Hilden, Germany)
RNeasy Mini Kit	Qiagen (Hilden, Germany)
SuperScript™ II Reverse Transcriptase	Invitrogen (Carlsbad, USA)

3.8 Buffers and Solutions

Table 9 l Used Buffers and solutions

Buffer	Composition
Aniline blue – Orange G Solution	0.5 g Anilonblue 2 g Orange G 8 mL Glacial acetic acid 100 mM Aqua dest.
Aniline-alcohol	0.1 mL aniline 100 mL 90 % ethanol
Azocarmine Solution	0.1 g Azocarmine G 100 mL aqua dest. Heat until the solution boils, then add 1 mL glacial acetic acid / 100 mL of filtered solution
Bouin´s Solution	30 mL saturated picric acid 10 mL glacial acetic acid 2 mL 37 % formaldehyde
Dilution Buffer for Immunofluorescence	0.2 % BSA 0.1 % NaN_3 In PBS
ELISA Blocking Buffer	0.1 M NaH_2PO_4 x H_2O

	0.066 M NaOH
	0.15 M NaCl
	0.8 % BSA
	1 nM EDTA
	0.08 % Tween 20
	0.0025 % Thimerosal
ELISA Coating Buffer	50 mM $NaHCO_3$ pH 9.6
	6,7 µg/mL Goat-anti-rabbit IgG
ELISA Washing Buffer	0.5 % NaCl
	0.02 % Tween 20
ELISA-PBS Buffer (E-PBS)	0.1 M Na_3PO_4 x 12 H_2O
	0.15 M NaCl
	0.005 M EDTA
	0.2 % BSA
	0.01 % Thimerosal
	pH 7.0 (adjust with HCl)
HPR Substrate Solution	0.01 M Sodium acetate
	0.45 mM citric acid
	0.00038 % H_2O_2
	0.0001 % TMB (in DMSO)
PBS	0.136 M NaCl
	0.05 M Na_2HPO_4 x 2 H_2O
	pH 7.4 (adjust with 1 N HCl)
TAE	40 mM Tris
	20 mM acetic acid
	1 mM EDTA

3.9 Devices

Table 10 l Used Devices

Device	Company
Biological Safety Cabinet	Nuaire, Plymouth, USA
Centrifuge 5804 R	Eppendorf, Hamburg, Germany
Concentrator 5301	Eppendorf, Hamburg, Germany
DH Autoflow CO_2 Air-Jacketed Incubator	Nuaire, Plymouth, USA
DIAS Microplate reader	Dynatech, Denkendorf, Germany
Digital Camera C-400 200 M	Olympus, Hamburg, Germany
Electrophoresis Power Supply 300 V - 500 mA E835	Consort, Turnhout, Belgium
Fluorescence microscope, Axioskop 2 plus	Zeiss, Muinch, Germany

Heating Immersion Circulatior ED Water Bath	Julabo, Seelbach, Germany
Heating/Cooling Dry Block CH-100	Biosan, Riga, Latvia
iCycler 5 IQ™ Real-time PCR detection system	Bio Rad, Hercules, USA
Mastercycler gradient 5331	Eppendorf, Hamburg, Germany
Mikro 20 Centrifuge	Hettich Zentrifugen, Tuttlingen, Germany
Mikrotom Leica RM 2255	Leica, Wetzlar, Germany
Mixer Mill MM400	Retsch (Haan, Germany)
Motic binocular light microscope SMZ-171	Motic, Wetzar, Germany
Moticam 3 digital camera	Motic, Wetzar, Germany
MultiImage Light Cabinet Alpha DigiDoc™	Biozym Scientific, Hessisch Oldendorf, Germany
Nanodrop 2000 Spectrometer	Thermo Scientific, Waltham, USA
Olympus BX50WI microscope	Olympus, Tokio, Japan
Seperation Sytem B1	Owl Separations Systems Inc. (Portsmouth, USA)
Table centrifuge with vortex	NeoLab, Heidelberg, Germany

3.10 Software

Table 11 l Used Software

Software	Company
GraphPad Prism	GraphPad Software, San Diego, USA
Axiovision LE software	Zeiss, Muinch, Germany
Fiji Image J	https://www.fiji.sc
Motic Images Plus 2.0ML	Motic, Wetzar, Germany
qPCR System	Bio Rad, Hercules, USA
Revelation 2.0	Dynatech, Denkendorf, Germany

4 Methods

4.1 Cell Biological Methods

4.1.1 Cell culture

The adherent growing primary HPrSMCs and HAoSMCs used in these studies were cultured in VascuLife® SMC Medium Complete Kit supplemented with 1 % Penicillin-Streptomycin (in the further context referred to as `medium´) at 37°C and 5 % CO_2. The HPrSMCs were used until passage 15 and the HAoSMCs until passage 11. When the cells reached a confluence of 90 % they were washed with DPBS and detached from the surface with 0.5 % Trypsin / 0.2 g EDTA solution. Medium was added to stop the trypsinization. The cell suspension was centrifugated (5 min at 1000 g) and the cell pellet was resuspended with a defined volume of medium. A “Neubauer improved” counting chamber with 0.1 mm depth was used to count the cells. For further cultivation, the cells were seeded in new cell culture flasks.

4.1.2 Treatment

4.1.2.1 Treatment of cells for measurements of cGMP production

For subsequent cGMP ELISA 40,000 cells/well were seeded in a 48 well plate in 500 µL medium. On the fourth day, the medium was replaced by a medium without FBS (VascuLife® Basal Medium) to equilibrate and to avoid desensitisation of GC-B by FBS (Abbey and Potter 2003). After 4 h the medium was replaced with 200 µL/well medium with diluted natriuretic peptides. For the treatment, the natriuretic peptides ANP and CNP were diluted in a medium without FBS and with 0.25 mM of the phosphodiesterase inhibitor IBMX (Müller et al. 2004). The natriuretic peptides were diluted to 1 µM, 100 nM, 10 nM, 1 nM, and 0.1 nM. For control, the medium was replaced by a medium without FBS and with 0.25 mM IBMX. The cells were incubated for 1 h at 37°C and 5 % CO2; for termination 800 µL of 100 % ice-cold EtOH was added to each well. The plate was incubated for at least 1 h at -20°C. After that, the cells were resuspended and the suspension was transferred to a reaction tube. The suspension was stored at -80°C.

4.1.2.2 Treatment of cells for cell growth tests

To determine whether natriuretic peptides (CNP and VNP) have an effect on cell growth of HPrSMCs, 500,000 cells were seeded in a T25 cell culture flask. For these experiments, the medium (5 mL) in which the cells were cultured by standard was used. After the cells had settled on the surface after a few hours, they were treated with either 1 µM CNP or 1 µM VNP. For the control, WT HPrSMCs were

not treated. After culturing the treated cells for 3 days at 37°C and 5% CO2, the cells were detached from the surface with 0.5% trypsin / 0.2 g EDTA solution and the reaction was stopped with medium. A “Neubauer improved” counting chamber with 0,1 mm depth was used to count the cells. The cell suspension was used and harvested using the "RNeasy Mini Kit" according to the manufacturer's instructions with on-column DNase digestion. In the end, the RNA was eluted with 30 µL RNase-free water and stored at -80°C.

4.2 Molecular Biological Methods

4.2.1 Determination of mRNA abundance

To analyse mRNA abundance and differences, total RNA was isolated from tissue or cells and via reverse transcription synthesized into cDNA to be analysed by RT-qPCR.

4.2.1.1 RNA Isolation

4.2.1.1.1 RNA Isolation from Tissue

For human tissue samples from TUR-P patients (n = 40), special care was taken to use non-bloody samples to avoid isolation of RNA from platelets or larger blood vessels. For the RNA isolation, 57 – 116 mg of whole prostate tissue from BPH patients were used.

RNA was also isolated from rat ventral prostate (n = 15). For this, the prostate was first dissected from the animal and the ventral prostate was isolated. Larger blood vessels were excised and approximately 50 mg of tissue was weighed.

Human and rat prostatic tissues were frozen at -80°C to be used later for RNA isolation.

RNA was isolated from the tissue samples using the "RNeasy Mini Kit" (spin technology) according to the manufacturer's instructions with on-column DNase digestion with some adaptations in the beginning due to the consistency of the tissue.

First, the tissue was pulverized (under nitrogen) and then RLT buffer with 1 % β-Mercaptoethanol was added. A metal bead was added and the tissue was processed in a mixer mill at 30 Hz for 3 min. The lysate was centrifuged for 5 min at full speed (24,500 g) and the supernatant was transferred to a fresh reaction tube. This supernatant was used for further steps following the manufacturer's instructions. In the end, the RNA was eluted with 30 µL RNase-free water and stored at -80°C.

To determine RNA amounts, RNA was thawed at 65°C for 5 min, vortexed, and then cooled on ice for 5 min. Before the RNA concentration was measured, the RNA was vortexed again and then the concentration was determined using the NanoDrop 2000 spectrometer.

4.2.1.1.2 RNA Isolation from Cells

For RNA isolation from cells, 350,000 cells in a 25 cm^3 flask were cultivated. After the cells reached approximately 90 % confluence, they were harvested using the "RNeasy Mini Kit" according to the manufacturer's instructions with on-column DNase digestion. In the end, the RNA was eluted with 30 µL RNase-free water and stored at -80°C.
To determine RNA amounts, RNA was thawed at 65°C for 5 min, vortexed, and then cooled on ice for 5 min. Before the RNA concentration was measured, the RNA was vortexed again and then the concentration was determined using the NanoDrop 2000 spectrometer.

4.2.1.2 Reverse Transcription

For cDNA synthesis, the "SuperScript™ II Reverse Transcriptase" was used and 2 µg total RNA was added up to 11 µL RNAse free water. All steps were performed according to the manufacturer's instructions in a Mastercycler, using Oligo$(dT)_{12\text{-}18}$ as primer. The cDNA was diluted 1:10 with RNase-free water for use in the RT-qPCR and stored at -20°C.

4.2.1.3 Real-Time quantitative Polymerase Chain Reaction – RT-qPCR

For quantification of DNA molecules during amplification within a PCR, the molecular biological method of Real-Time quantitative polymerase chain reaction (RT-qPCR) can be used. With the results, the relative mRNA abundance in the sample can be calculated.

4.2.1.3.1 Bio-Rad Real-Time PCR System

For RT-qPCR the iCycler 5 IQ™ Real-time PCR detection system from Bio-Rad was used, which works with the iQ™ SYBR® Green technology. The big advantage of an RT-qPCR is to follow the DNA amplification in real-time. This is enabled by the fluorescent dye SYBR® Green, which emits only when it intercalates in double-stranded DNA (dsDNA). As the fluorescence intensity is proportional to the amplified dsDNA, the relative amount of mRNA in the samples can be calculated later.
The oligonucleotides, which were used in this study were designed at Primerblast or sourced from a paper. The sense and antisense sequences can be found in table 6 for human or in table 7 for rat samples. The primer pairs where designed to span an exon-exon junction to avoid genomic DNA contamination. All primer pairs were tested using a cDNA dilution series in RT-qPCR and as a control, a water sample was integrated. The resulting C_t value (threshold cycle) after a qPCR, indicates the cycle at which the fluorescence of the sample exceeds the threshold. According to the MIQE guidelines

better known as the C_q value (quantitative cycle). The PCR efficiency was calculated with the following formula:

$E = 10^{-1/m} - 1$ m – gradient

An efficiency of 2.0 means that the product doubles per cycle and thus corresponds to an efficiency of 100 %. Only primer pairs with an efficiency of 80 – 120 % were used. Furthermore, primer pairs that resulted in only one product were used. To analyse the specificity of primer pairs in the RT-qPCR a melt curve was performed. For this, the temperature was slowly and continuously increased to 95°C. Because the PCR products disassemble into their single strands with increasing temperature and a decrease in SYBR Green fluorescence can be observed, the number of peaks obtained can be used to conclude the number of products.

4.2.1.3.2 Measurement of mRNA abundance

To determine the mRNA abundance, the number of target transcripts and housekeeping gene transcripts (as controls) were measured in an RT-qPCR. For that, a master mix was prepared [consisting of 5 µL iQ™ SYBR® Green Supermix (Bio-Rad) and 0.06 µL of each of primer oligonucleotide (100 pmol/µL each)] and pipetted into a 96-well plate. Then 2.5 µL of diluted cDNA (end concentration 50 ng/well) was added, whereby duplicates were performed.
The measurement was done by the iCycler 5 IQ™ Real-time PCR detection system (Bio-Rad).

RT-qPCR program:
95°C 3 min
95°C 20 sec
60°C 20 sec
72°C 20 sec
} 40 cycles
55°C – 95°C – melt curve

4.2.1.3.3 Calculation of the relative mRNA quantity

To calculate the relative mRNA amount of genes of interest, the ΔC_t method was used. This method uses the difference between the target transcript and the control transcript, normalizing to the control transcript. For normalization of gene expression for comparative analyses β-actin was used as the housekeeping gene for samples of human origin and *Gapdh* for rat samples.
The relative mRNA amount was calculated with the following formula:

$$relative\ mRNA\ amount = 2^{-(C_tX - C_tK)}$$

X – target transcript

K – control transcript

4.2.2 Determination of cGMP production

Determination of cGMP concentrations in samples was carried out by competitive double-antibody cGMP ELISA with solid-phase technique. This type of ELISA can be divided into three steps. In the first step, the cGMP from the sample and a cGMP-biotin derivative compete for binding to the added cGMP antibody. The cGMP antibody is binding to a second antibody (IgG – goat anti-rabbit) with which the plates were coated. Next, horseradish peroxidase (HPR) coupled to streptavidin is added, which binds only to biotin-containing immunocomplexes. In the last step, the colourless substrate TMB is added, which is converted by the HPR to a blue dye. The addition of H_2SO_4 results in a yellow dye. The colour development of the chromogen is dependent on the amount of enzyme bound to the wells. Thus, it is inversely proportional to the cGMP concentration.

4.2.2.1 Plate coating for cGMP-ELISA

For the cGMP-ELISA coated immune 96 well plates were needed. For this 150 µL Coating buffer with 6,7 µg/mL of Goat-anti-rabbit IgG was added to each well. The plates were stacked, and the top plate was covered with a lid and incubated overnight in a dark chamber at room temperature. After that, 240 µL/well blocking buffer was added and again the plates were incubated overnight in a dark chamber at room temperature. The plates were emptied by draining and the remaining liquid was removed by tapping. The wells were washed with 350 µL/well washing buffer and again the liquid was removed. After that, the coated plates can be stored airtight at -20°C.

4.2.2.2 cGMP-ELISA

The stored suspension, as explained in the previous section, was centrifuged at 4°C for 30 min at 20,000 g and the supernatant was transferred to a fresh reaction tube. In this step, the suspension can be stored at -80°C or further processed. A concentrator was used to lyophilize the suspension, in which the samples were evaporated under vacuum at 60°C for 1.5 – 2 h. The pellets were resuspended in 140 µL EPBS and vortexed. For the cGMP ELISA, a coated Immuno 96-well plate had to be activated by 375 µL/well EPBS for 2 min and a cGMP standard (0.14; 0.42; 1.26; 3.78; 11.34 and 34.02 pM in EBPS) was prepared. The activated 96-well plates were loaded with 50 µL/well standard or samples in duplicates, 50 µL/well biotin tracer (170 fM in H_2O), and 100 µL/well cGMP antibody serum (1:80,000). For the blank (NSB), no standard or sample and no cGMP antibody serum was given in 2 wells. The plate was covered with a lid and stored in a wet, dark chamber. After overnight incubation (at least 18 h) at 4°C, the plate was aspirated and 200 µL of HPR-Streptavidin solution (0.152 µg/mL Streptavidin in EPBS) were added to each well. Again, the covered plate was incubated in a wet, dry chamber for 30 min at 4°C followed by 3 washing steps for 1 min. After the last washing step, the plate was left to stand for 3-5 min. In the meantime, the HPR substrate solution was prepared and 250 µL were added to each well. This was followed by incubation for 40 min in a wet, dry chamber at room temperature. As a final step, 50 µL/well of 2 M H_2SO_4 were added and the OD was measured at 450 nm by a DIAS microplate reader using the “Revelation 2.0” software.

4.2.2.3 Calculation of cGMP quantity

To determine the cGMP concentration in samples, the OD was measured at 450 nm by a microplate reader. The “Revelation 2.0” software was used, which calculates the cGMP concentration in each sample. In detail, the software performs a background correction with both the standard and the samples. A standard curve is created using the ODs of the standards and the specified values (Fig. 11). The cGMP amount of each sample, whereby the average of the duplicates is calculated, is obtained from the standard curve in pmol/mL.

$$B/Bo\,(\%) = \frac{OD_{Standard/Probe} - OD_{NSB}}{OD_{Nullstandard(Bo)} - OD_{NSB}}\ x\ 100$$

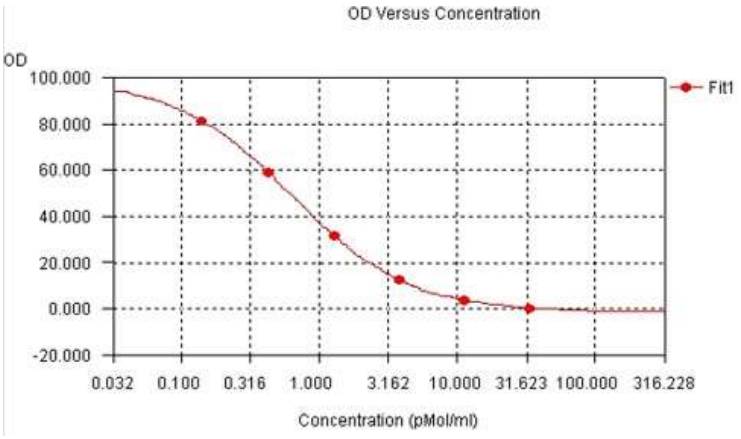

Figure 11 l Representative standard curve generated during cGMP-ELISA. The OD of the cGMP standard is plotted against the cGMP concentration (0.14; 0.42; 1.26; 3.78; 11.34 and 34.02 pM in EBPS) [pM/mL].

4.2.3 Measurement of hormone levels testosterone and estradiol via Radioimmunoassay

For the determination of local hormone levels of testosterone and estradiol in the human prostate, tissue samples were first processed and then handed over to Prof. Dr. Schuler's laboratory (Justus-Liebig University Giessen, Clinic of Veterinary Obstetrics, Gynecology and Andrology) for RIA measurement.

4.2.3.1 Sample preparation for hormone level evaluation

For the local hormone determinations, 100 mg of human prostate tissue was weighed for testosterone and 150 mg for estradiol. Using a mortar and adding nitrogen, the samples were powdered and resuspended in a reaction tube with either 300 mL PBS for testosterone samples or 450 mL for estradiol samples. A metal bead was added and the samples were processed for 4 min at 30 Hz in a mixer mill.

The metal bead was then removed and the samples could either be stored at -80°C or used for RIA. For the RIA, the samples were taken to Prof. Dr. Schuler's laboratory where the hormone levels of testosterone and estradiol were determined with a RIA. In the following sections, the RIA for testosterone and estradiol are briefly described as they are carried out in Prof. Dr. Schuler's laboratory.

4.2.3.2 RIA to determine Testosterone

For the determination of testosterones in the processed prostate tissue samples, an established protocol for RIA which was set up as a competitive assay was used (Roecken FE, Nothelfer H.-B., Hoffmann B. 1995; Hoffmann et al. 2010). First, the hormones were extracted. For this, Tuloul was used as extrusion medium with the sample or control. After mixing on a rotary mixer for 15 min, the samples were briefly centrifuged at 3,500 rpm. The supernatant was removed and dried down in a vortex evaporator (temperature ≤ 50°C). Following a precise pipetting scheme (working with duplicates), BSA buffer, tracer containing the H^3-testosterone and the antiserum were added to the sample, controls and blank. To the samples for the standard curve (10 fmol/0.1 mL; 20 fmol/0.1 mL; 40 fmol/0.1 mL; 80 fmol/0.1 mL; 160 fmol/0.1 mL; 640 fmol/0.1 mL; 1280 fmol/0.1 mL; 2560 fmol/0.1 mL) the tracer and the antiserum were added.

The plate was first shaken for 30 sec, then incubated for 20 min at 37°C in a heat shaker and finally for 60 min at 4°C in an ice water bath. Separation of the free hormone was done by adding an ice-cold carbon suspension, shaking briefly and incubating for 10 min at 4°C. The samples were then centrifuged at 3,200 rpm for 15 min at 4 °C and the supernatant removed for measurement. For the measurement, the sample was mixed with a scintillator, shaken, and left for 10 min. Subsequently, the H^{3-}pulses were measured for 3 min. The cross-reactivity to DHT in this assay is 47 % and the limit of detection was at 0.1 ng/mL.

The following formula was used for the evaluation:

$$[T\ nmol/L] = \left(Readout_{sample} - Readout_{blank}\right) * 10$$

4.2.3.3 RIA to determine Estradiol

The RIA for the determination of estradiol-17β followed the similar and established protocol (Hoffmann et al. 1992) with minimal differences in incubation times and centrifugation steps. Extraction was also performed with Tuloul and the supernatant was removed after the last centrifugation step. The reaction mixture was pipetted, adding only BSA buffer and antiserum to the sample and controls. To the samples for the standard curve (0.5 pg/0.1 mL; 1 pg/0.1 mL; 2 pg/0.1 mL, 4 pg/0.1 mL; 8 pg/0.1 mL; 16 pg/0.1 mL; 24 pg/0.1 mL; 32 pg/0.1 mL) only antiserum was given. The plate was shaken for 30 sec, followed by pre-incubation overnight at 4°C. The tracer with the H^3-estradiol was added to the individual samples, followed by shaking for 30 sec and incubation for 45 min at 4°C. The free hormone was separated after the addition of the ice-cold carbon suspension for 30 min at 4°C.

After centrifugation, the sample was added to the scintillator and left for 10 min. The H^3 pulses were measured for 4 min. The detection limit for this RIA was at 0.5 pg/0.1 mL.

The following formula was used for the evaluation:

$$[E2\beta\ pg/mL] = \left(Readout_{sample} - Readout_{blank}\right) * 4$$

4.3 Imaging Methods

For experiments on fresh prostate tissue, live methods were used to perform both contraction studies and calcium imaging experiments.
For both experiments, the tissue was embedded in collagen, which is described in the next section.

4.3.1 Preparation and collagen embedding of tissue for imaging

After sacrificing the animal, the prostate was dissected out with the bladder. To keep the tissue alive, MEM medium was used all the time. Under a binocular light microscope, the prostate was prepared and the fatty tissue was removed. The ventral lobes were extracted and individual glands were dissected from one of the ventral lobes. Care was taken to isolate individual glands that were on the same plane to ensure more accurate focusing during subsequent movie recordings. The prepared tissue was embedded in 300 µL of a mixture of rat collagen, x10 DMEM/F12, 0.1 % acetic acid, 0.5 M sodium hydroxide, and 1 M HEPES (Mietens et al 2014) in delta-T dishes. This was followed by incubation for 30 min at 37°C and 5 % CO_2 to allow the rat collagen to polymerize.

4.3.2 Live imaging

To investigate the contractility of tissue, *ex vivo* experiments were performed using isolated glands from the rat prostate. Tissue was prepared as described above and embedded in rat collagen. Because a diving objective was used, 100 µl of MEM, including 5 % penicillin/streptomycin, was carefully added to the polymerized collagen in the delta-T dish.

4.3.2.1 Live imaging recording

For live imaging recordings, the delta-T dish was fixed to an Olympus BX50WI microscope combined with a Moticam 3 digital camera and a diving objective. The system was connected to the Motic Images Plus 2.0ML software (Fig. 12). In each experiment 1 frame was recorded every second with a cycle time of 1800 frames (30 min) and later a video was generated from it.

First, spontaneous contractions (no treatment) were recorded for 10 min, which was later used as a baseline. Subsequently, the tissue was treated with natriuretic peptides at a final concentration of 100 nM or 1 µM. Again, the tissue response was recorded for 10 min. Finally, noradrenaline was added at a final concentration of 10 µM to check the tissue for viability.

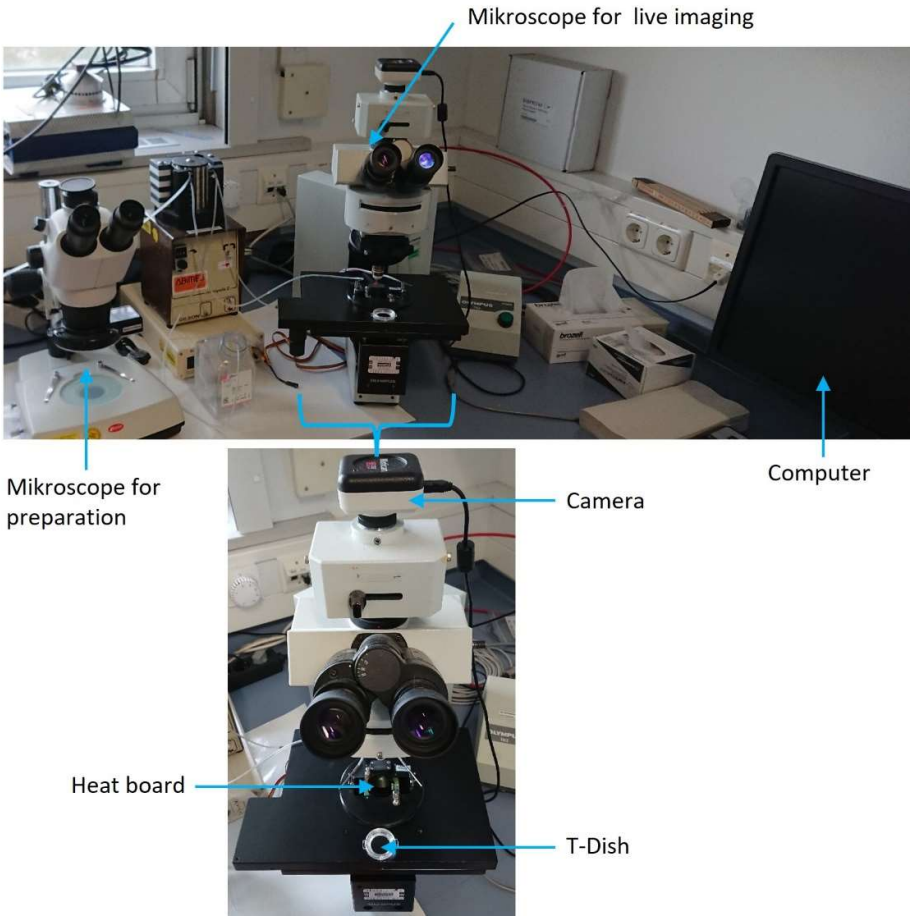

Figure 12 | Setup for live imaging. The delta-T dish was fixed to an Olympus BX50WI microscope combined with a Moticam 3 digital camera and a diving objective. The system was connected to the Motic Images Plus 2.0ML software.

4.3.2.2 Evaluation of live imaging movies

Since the prostatic tissue shows multidirectional movements at several points simultaneously, a newly published method was applied to analyse such contraction experiments (Stadler et al. 2021). For this purpose, based on the Wiggle Index (Denecke et al. 2015; Preston et al. 2015; Preston et al. 2016), the code was further developed https://doi.org/10.26180/13653614. Like the Wiggle index before, the adjustment compares the sum of movements (extracted from standard deviation scores) during different time points in the experiment. The entire field of view or a defined area can be analysed. In addition, due to the extension of the code, the fold change relative to the baseline (and to any other addition) can be measured separately for each pixel. Subtle differences in motion can thus be detected since the data are expressed as a population distribution. In addition to the fold change, the analysis can be illustrated in colour-coded heat maps that show the change in motion during the different segments of the experiment in one image. These heat maps can be used to identify the location and intensity of the motion. The colour-coded heat maps show strong contractions and movements in red, medium movements in green and weak movements in blue.

For further statistical analysis, the fold change of each data point was inserted and evaluated in GraphPad Prism software. Therefore, the raw standard deviation data point of each part of a single experiment was used to obtain a cumulative frequency distribution with the GraphPad Prism function "frequency distribution" and "cumulative frequency". The obtained histogram of data was used to perform a “nonlinear regression” (curve fit) using exponential one phase association testing with the command “Compare: Does one curve adequately fit all data set?” to calculate the static evaluation and to create the corresponding graphs. The profiles of the curves show the differences in the movements after the treatments, with slow rising curves indicating less movement, and fast rising curves representing high movement.

In this study, two different time periods were analysed in each movie. In the first analysis, 30 sec for calibration were skipped and 2 min analysed. This allowed an initial effect of treatment to be detected. In the second analysis, a later time point was selected. For this, 2.5 min were skipped and 5 min analysed to demonstrate a longer-lasting effect.

4.4 Histological Methods

Histological methods are used to examine tissue sections microscopically. Chemical staining methods, such as the azan stain according to Heidenhain, also allow conclusions concerning tissue structures.

4.4.1 Preparation of Paraffin Sections

Prostate tissue samples from BPH patients were prepared and fixed for 24 h in Bouin's solution. Afterwards, the tissue samples were placed in 70 % ethanol for at least 24 h. Before embedding in paraffin, the tissue was dehydrated with an ascending ethanol series (70 %, 80 %, 90 %, and 100 %) and cleared with xylol. For embedding, paraffin was melted at 65°C and the tissue was embedded in it. Before cooling down, the paraffin-embedded tissue was kept in a heating cabinet at 65°C for 12 h. The paraffin blocks in which the tissue was embedded were carefully trimmed with a razor blade. For cutting, the blocks were clamped in a microtome. The 5 µm thick paraffin sections were placed on a slide glass and transferred to a 40°C water bath for smoothing and positioning. For drying, the slides were placed on a 40°C hot plate. To dry out completely, the slides with the sections were stored in a drying cabinet at 30-40°C for overnight.

4.4.2 Azan Staining after Heidenhain

For staining, the sections were first deparaffinised with a descending alcohol series and sterile water. After a short washing step, the sections were incubated in aniline-alcohol (100 mL 90 % ethanol; 0.1 mL aniline) for 5 min and then in azocarmine solution for 10-15 min at 56°C in the warming cabinet. After a short washing step in water, the sections were differentiated in aniline alcohol until only nuclei were stained. Then the sections were first placed in 5 % phosphotungstic acid for 2 h and then in an aniline blue-orange mixture for 1-2 h. After a wash step in sterile water., the sections were incubated in aniline alcohol. After a washing step in sterile water., the differentiation was carried out in 96 % ethanol until the tissue components were clearly recognisable. Finally, sections were dehydrogenated in an alcohol series (isopropanol and xylol). The sections were covered with a cover slip using Eukitt® as the inclusion resin.

4.4.3 Immunofluorescence

For histological analysis of the cells by immunofluorescence, 20,000 cells/well were seeded into an 8-well chamber slide. When cells reached 80 – 90 % confluence, they were washed 3x for 10 min with PBS, then fixed with 4 % PFA for 10 min, and again washed 3x for 10 min with PBS. For possible storage, the wells were filled with PBS or the protocol was continued. The cells were washed 3x for 10 min, and then 250 µl/well of blocking solution (2 % normal goat serum in PBS) was added for 1 h at room temperature. The primary antibody SMA (Kügler et al. 2018) was diluted 1:1000 (table 4) in the buffer for immunofluorescence and then 200 µL/well was pipetted into the appropriate well. For control 1 well per coverslip was filled with PBS instead of primary antibody. The cells were incubated overnight at 4°C with the primary antibodies and then washed 2x for 10 min with PBS. Because secondary antibodies are light-sensitive, from this step on the work was done in darkened rooms. Dilutions for secondary antibodies are listed in table 5. In double-staining, care was taken to ensure that the primary antibodies had different origins, and for the secondary antibodies, attention was paid to different coupled fluorophores. A total of 200 µL/well of the secondary antibodies was added and the cells were incubated in the dark for 1 h at room temperature with the secondary antibody. All used secondary antibodies were added to the control well to exclude possible non-specific binding of them. After the cells were washed again 2x for 10 min with PBS, everything was fixed with 4 % PFA for 10 min. Before cells were coverslipped using glycerol for immunofluorescence, they were washed 2x for 10 min with PBS. The cells stained with immunofluorescence were observed on a fluorescence microscope Axioskop 2 plus and images were acquired using Axiovision LE software.

The coverslipped cells can be stored at 4°C in the dark for later re-viewing of the fluorescence signals.

4.5 Statistic

For all analyses, GraphPad Prism (GraphPad Prism 9, Version for Windows, GraphPad Software, La Jolla, California, USA, www.graphpad.com) was used.

Outliers were identified using the “Identify Outliers” function and excluded in data from human and rat prostate samples. The “Rout Test” was used because there was more than one outlier.

To confirm the normal distribution of data, the D´Agostino & Pearson test was used. Because the data sets did not show a normal distribution Mann-Whitney test was performed to detect differences in gene expression and treatment effects on cGMP production. Furthermore, 2-way ANOVA was performed to analyse cGMP ELISA results. For the calculation of the EC_{50} value, as the half maximal effective concentration, the function "log(agonist) vs. response (three parameter)" was used in Graph Pad Prism.

For pairwise comparison of gene expression, the Wilcoxon test was used.

Correlation analyses for non-normally distributed data sets were performed by Spearman correlation. Differences were considered significant if: $p \leq 0.05$ (*); $p \leq 0.01$ (**); $p \leq 0.001$ (***) and not significant if $p > 0.05$ (n.s.).

5 Results

Benign prostatic hyperplasia (BPH) is the most common disease in men and around 80 % over the age of 80 are affected. This disease is mainly characterised by uncontrolled proliferation of the stromal components and increased muscle tone. Since it is suggested that the altered hormone levels of testosterone and estradiol with age may play a role in the development of BPH, first prostate samples from BPH patients were prepared and the local levels of T and E2 were determined by RIA. Furthermore, the gene expression of the corresponding receptors was measured. Previous work by our group has shown a correlation between the expression of components of the cGMP signalling pathway, which is responsible for SMC relaxation, and T in rat models. The absence of T after Leydig cell depletion by EDS (ethane dimethane sulfonate) injection led to increased expression of, among others, PKG I and PDE5 in the prostate (Müller et al. 2011). Based on this previous work, correlation analyses were used to demonstrate a connection between T and the cGMP signalling pathway components.

In the further progress of the thesis, the focus was directed toward the cGMP signalling pathway, as this is also of interest from a therapeutic point of view for the treatment of BPH. Already today, substances are used that influence this signalling pathway. The relative gene expression of different signalling pathway components was investigated in the human prostate of BPH patients, but also in HPrSMCs. For comparison with other SMCs, HAoSMCs were considered. The effects of natriuretic peptides on cGMP production were revealed by a specific cGMP ELISA to get information of the activity of the NP receptors. Furthermore, a rat model was used to demonstrate *ex vivo* the effects of NPs and analogues on prostate tissue.

5.1 Evaluation of sex hormone levels and receptor expression in the human prostate

To determine the local hormone levels of testosterone and estradiol, prostate samples from BPH patients were prepared together with Dr. Mathias Seidensticker from our group. In cooperation with Prof. Dr. Schuler's laboratory RIAs were performed to measure the local hormone levels as described in section 4.2.3. Prostate tissue from the same patients was also used to determine the relative gene expression of the receptors for T and E2 by RT-qPCR.

5.1.1 Sex hormone amounts in the human prostate

The measurement of local hormone levels in the human prostate (n = 54) resulted in a concentration between 0.1 and 0.51 ng/mL with a mean value of 0.21 ± 0.1 ng/mL for testosterone (Fig. 13A), with 3 samples below the minimum detection limit of 0.1 ng/mL. For estradiol, the RIA measurements showed concentrations between 0.008 and 0.18 ng/mL as well as a mean value of 0.038 ± 0.024 ng/mL (Fig. 13B).

Correlation analyses according to Spearman showed a positive correlation between T and E2 with a correlation coefficient (Spearman r) of 0.6214 and p = 0.0012 (Fig. 13C).

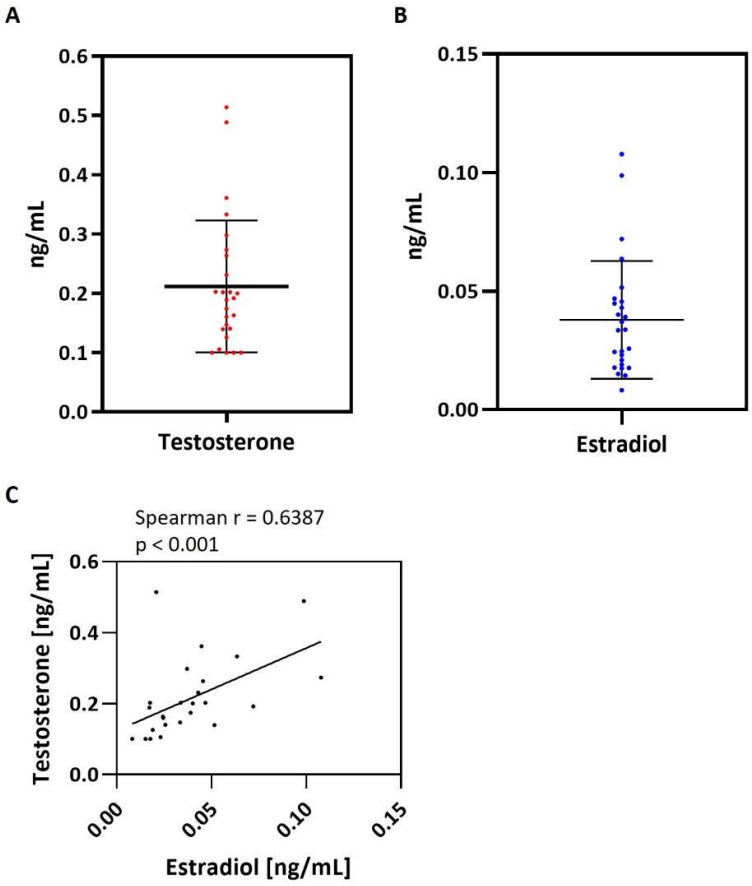

Figure 13 | Measurement of the local hormone testosterone and estradiol amounts in the prostate of BPH patients. Local levels of (**A**) testosterone and (**B**) estradiol in the human prostate were determined via a radioimmunoassay (n = 54). For detailed information see Materials and Methods. (**C**) Correlation analyses between testosterone and estradiol levels were performed using GraphPad Prism software. Spearman r and p-value are indicated in the figure.

5.1.2 Expression analysis of sex hormone receptors in the human prostate

To reveal the expression of the receptors for T and E2, RT-qPCR analyses were performed. The relative expression of AR and the two receptors for estradiol ERα and ERβ, both found in the prostate, was measured. These experiments showed that the *AR* is significantly higher expressed than the E2 receptors *ERα* and *ERβ* ($p \leq 0.001$) (Fig. 14A, B). There was, however, no significant difference between the relative expression of *ERα* and *Erβ* ($p = 0.8785$). Interestingly, Spearman's correlation analyses showed that the amount of the local T and the expression of *AR* correlate positively with a correlation coefficient $r = 0.4254$ ($p = 0.0484$) (Fig. 14C).

Since previous work of our group has shown a correlation between T levels and the expression of components of the cGMP signalling pathway (Müller et al. 2011), the relative gene expression of these components was subsequently measured in the human prostate, in the same patients and additionally in further ones.

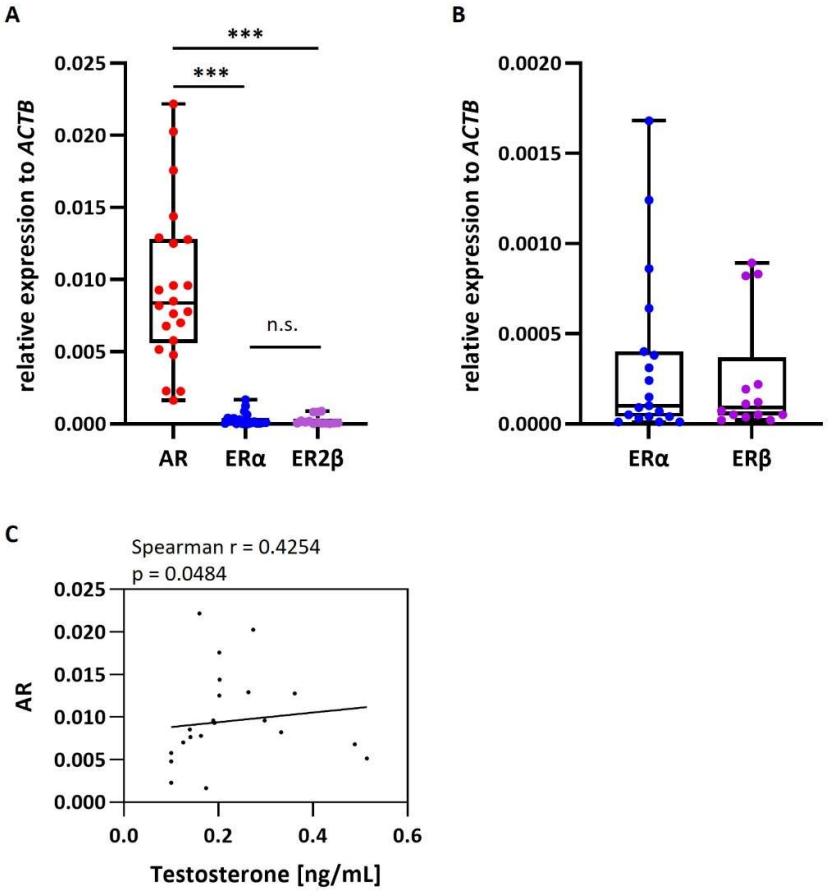

Figure 14 | Expression and correlation analysis of hormone receptors in the human prostate. RT-qPCR was performed with human prostate samples of BPH patients (n = 40) to measure the expression of the androgen receptor (*AR*) and the α- and β- estradiol receptor (*ERα* and *ERβ*). (**A**) Expression of all three investigated genes was compared and (**B**) expression of only *ERα* and *ERβ* was compared. *ACTB* was used as the reference gene for normalization and the relative gene expression was calculated by the ΔC_t method. Mann Whitney test was used to determine the statistical significances; (***) $p \leq 0.001$; (n.s.) not significant (**C**) Correlation analysis between *AR* and testosterone levels was performed. Spearman r and p-value are indicated in the figure.

5.2 Expression and correlation analysis of cGMP pathway components in human prostate tissue

Besides the receptors for the hormones testosterone and estradiol, components of the cGMP signalling pathway were also measured. Furthermore, attention was also paid to the NP CNP, which can activate the cGMP pathway. Interestingly, various studies were able to detect a high concentration of CNP in porcine seminal plasma (Chrisman et al. 1993), but also in male reproductive organs, with the highest amounts being found in the prostate and seminal vesicles (Nielsen et al. 2008). Thus, the local relative gene expression of the receptors for NPs *GC-A* and *GC-B*, but also other components of the signalling pathway, such as *NPRC*, *PKG I*, *PDE9A1,* and the *CNP* transcript were investigated in the prostate of BPH patients. As the cGMP pathway has already been targeted for the treatment of BPH, with Tadalafil as a PDE5 inhibitor (Sebastianelli et al. 2020), the therapeutically relevant components *sGCβ1* and *PDE5* were also analysed.

The analysis of the relative expression by RT-qPCR showed that all investigated components were expressed (Fig. 15). Among the receptors *GC-A*, *GC-B*, and *sGCβ1*, *GC-B* showed the highest expression and was significantly higher expressed than the other receptors ($p \leq 0.001$) (Fig. 15B). No difference was found between the expression of *GC-A* and *sGCβ1*. Looking individually at the expression of the NP receptors *GC-A* and *GC-B*, it was found that in 27 out of 29 patients *GC-B* was significantly higher expressed than *GC-A* ($p \leq 0.001$) (Fig. 15D). Spearman correlation analyses also revealed a positive correlation between the two NP receptors *GC-A* and *GC-B* with Spearman $r = 0.7152$ ($p \leq 0.001$) (data not shown).

In addition to the cGMP-producing receptors, the expression of *NPRC* was also measured, which has no catalytic property to produce cGMP. Instead, it is known to degrade natriuretic peptides. The expression of *NPRC* was also detected, but in small amounts (Fig. 15A).

Furthermore, the expression of the cGMP-dependent protein kinase *PKG I* was detected (Fig. 15A). Interestingly, a Spearman correlation analysis showed a positive correlation (Spearman $r = 0.5224$; $p = 0.0018$) between the cGMP-producing *GC-B* and the cGMP-binding *PKG I* (Fig. 15F).

Since affecting the cGMP signalling pathway is used for the treatment of BPH, gene expression of the target genes, i.e. *sGCβ1* and *PDE5*, were investigated. As mentioned earlier, *sGCβ1* was significantly lower expressed than *GC*-B, suggesting a more important role of the CNP/GC-B signalling in the prostate. Furthermore, the cGMP-degrading enzyme *PDE5* showed a relatively lower expression than *PDE9A1* (Fig. 15C). In general, *PDE9A1* showed the highest expression compared to all components studied, but also the highest variance. A Spearman correlation analysis also showed a positive correlation (Spearman $r = 0.6992$; $p \leq 0.001$) between *PDE9A1*, which inactivates cGMP, and *GC-B*, which produces cGMP (Fig. 15G).

Since previous studies by our group found a correlation between T level and protein expression of cGMP pathway components in rat male reproductive organs (Müller et al. 2011), Spearman correlation analyses, now using E2 values, were performed in this study. E2 was found to correlate positively with *PKG I* (Spearman r = 0.4509, p = 0,0237) (Fig. 15E).

As the cGMP signalling pathway leads to SMC relaxation, the expression especially of GC-B (and CNP) was investigated in cultured primary HPrSMCs to show that the CNP/GC-B pathway could be a candidate for BPH therapy.

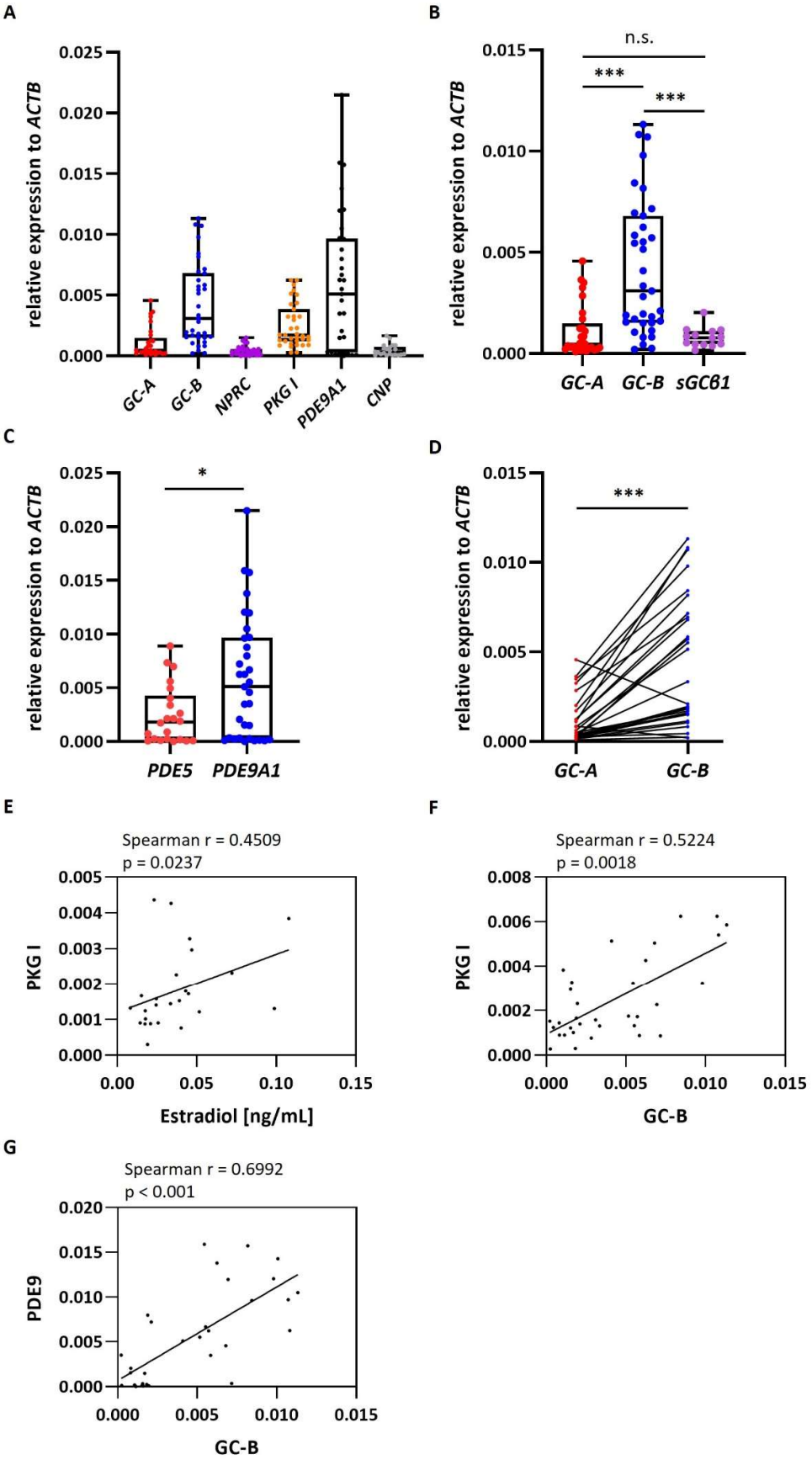
A
relative expression to ACTB
0.025
0.020
0.015
0.010
0.005
0.000
GC-A
GC-B
NPRC
PKG I
PDE9A1
CNP
B
relative expression to ACTB
n.s.
***
***
0.015
0.010
0.005
0.000
GC-A
GC-B
sGCβ1
C
relative expression to ACTB
*
0.025
0.020
0.015
0.010
0.005
0.000
PDE5
PDE9A1
D
relative expression to ACTB
***
0.015
0.010
0.005
0.000
GC-A
GC-B
E
Spearman r = 0.4509
p = 0.0237
PKG I
0.005
0.004
0.003
0.002
0.001
0.000
0.00
0.05
0.10
0.15
Estradiol [ng/mL]
F
Spearman r = 0.5224
p = 0.0018
PKG I
0.008
0.006
0.004
0.002
0.000
0.000
0.005
0.010
0.015
GC-B
G
Spearman r = 0.6992
p < 0.001
PDE9
0.020
0.015
0.010
0.005
0.000
0.000
0.005
0.010
0.015
GC-B

Figure 15 | Expression and correlation analysis of cGMP pathway components in human prostate tissue. (**A, B, C, D**) RT-qPCR was performed to measure the gene expression of GC-A, GC-B, sGCβ1, NPRC, PKG I, PDE9A1, PDE5 and the CNP transcript in the human prostate (n = 40). Relative gene expression was calculated by the ΔC_t method and normalized to ACTB. (**D**) Individual analysis of each patient and the relative gene expression of *GC-A* and *GC-B*, which were connected by a line. (**A-D**) Mann Whitney test was used to determine statistical significances; (***) p≤0.001; (*) p≤0.05. Correlation analysis between (**E**) *PKG I* / estradiol level, (**F**) *GC-B* / *PKG I* and (**G**) *GC-B* / *PDE9A1* were performed. Correlation index (Spearman r) and p-values are indicated in the figures.

5.3 Expression analysis of cGMP pathway components and effects of natriuretic peptides in cultured human prostatic and aortic smooth muscle cells

To investigate cell-type specifically the cGMP signalling pathway, further work was carried out with cultured human HPrSMCs, starting with the gene expression of the signalling pathway components.

5.3.1 Gene expression and correlation analysis of cGMP pathway related genes in human prostatic smooth muscle cells

Gene expression of *GC-A*, *GC-B*, *sGCβ1*, *NPRC*, *PKG I*, *PDE9A1*, and the *CNP* transcript was first examined in HPrSMCs over 6 passages from p8 to p13 (Fig. 16). In HPrSMCs the highest relative gene expression was found for GC-B, NPRC and PKG I. It was found that the relative expression of genes studied varied only slightly between the individual passages. Therefore, in further analyses for each gene the mean values of all single measurements independently of the passages were used.

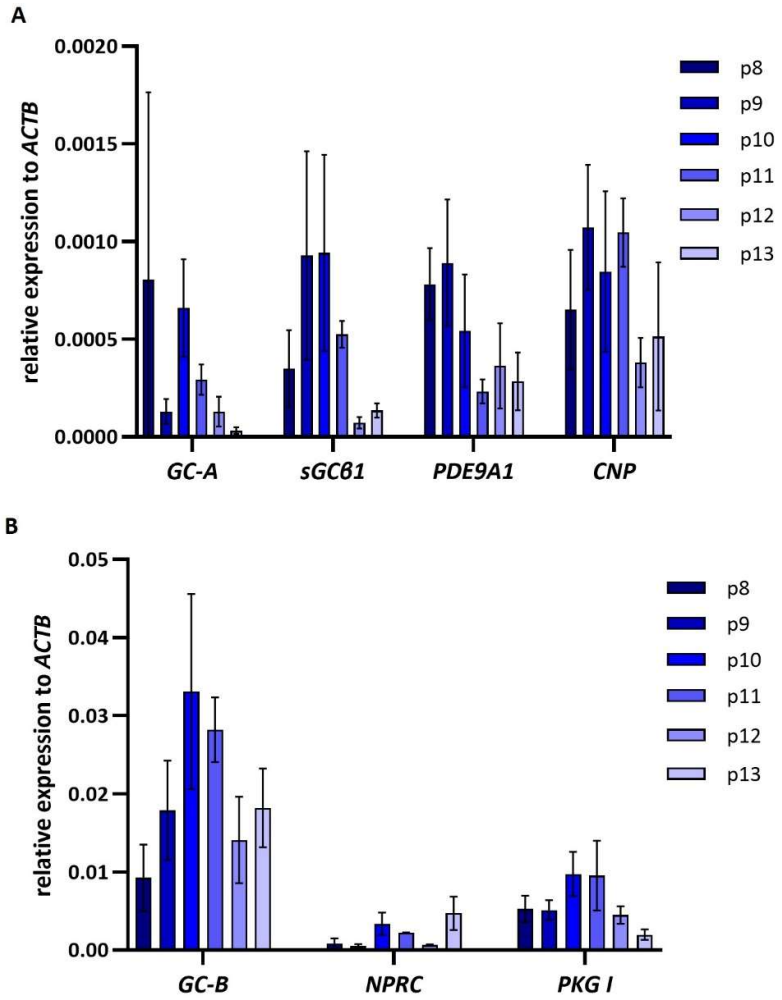

Figure 16 | (A, B) Gene expression analysis over six passages in human prostatic smooth muscle cells. RT-qPCRs were performed using human prostatic smooth muscle cells (HPrSMCs) and gene expression of (**A**) *GC-A, sGCβ1*, *PDE9A1, CNP* transcript and (**B**) *GC-B*, *NPRC*, and *PKG I*, the over six passages with three replicates was measured. Relative gene expression was calculated by the ΔCt method and normalized to *ACTB*.

The comparison of gene expression showed that *GC-B* was the most highly expressed gene studied in HPrSMCs (Fig. 17A). It showed a significantly ($p \leq 0.001$) higher expression than *GC-A* or *sGCβ1*. As in total human prostate samples (see. Fig. 17) there was no significant difference between the expression of *GC-A* and *sGCβ1* (Fig. 17B). Pairwise comparison of each sample between *GC-A* and *GC-B* also revealed a significantly higher expression of *GC-B* ($p \leq 0.001$) (Fig. 17C).

Furthermore, as in the human prostate (see Fig. 13), *NPRC*, *PKG I*, *PDE9A1* and *CNP* were also expressed in small amounts (Fig. 17A).

Interestingly, a positive correlation between the cGMP-binding *PKG I* and the cGMP-producing *GC-B* was also found in HPrSMCs with a Spearman correlation index $r = 0.4964$ ($p = 0.0361$) (Fig. 17D).

Since the C_t value of the reference gene *ACTB* in cells was too different to the C_t value in total human prostate (data not shown), a direct comparison of expression between these entities was not possible.

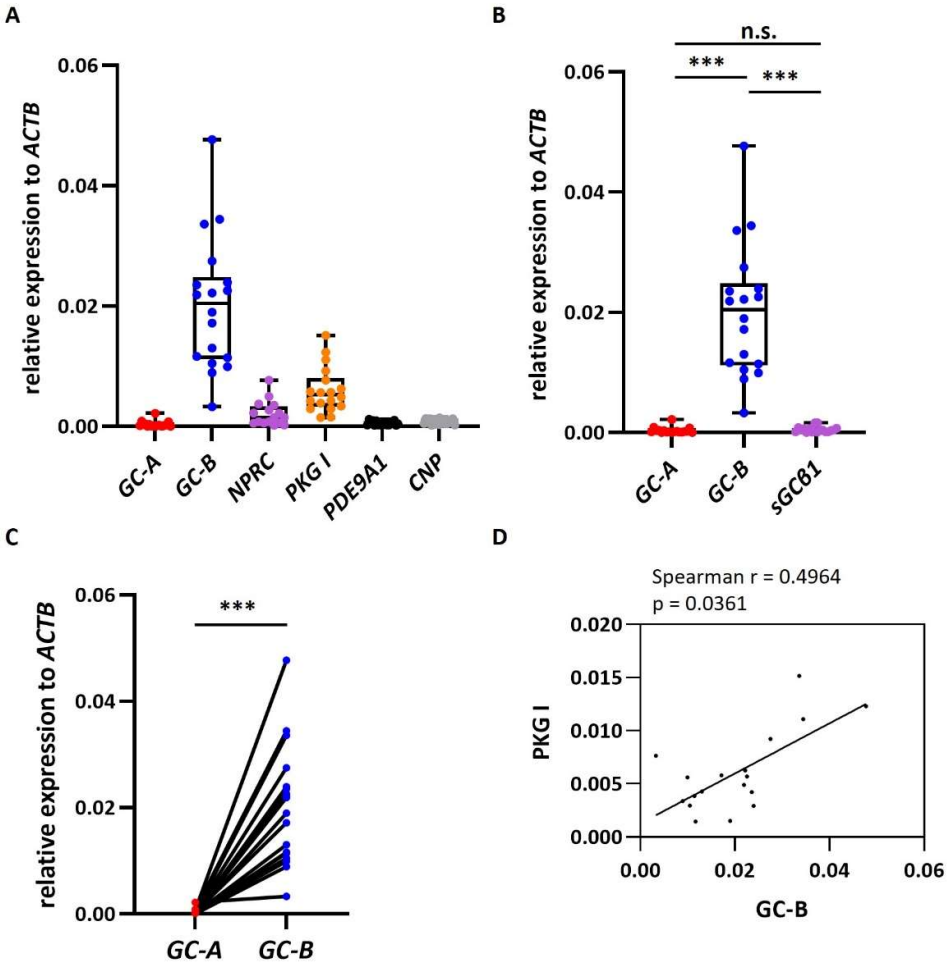

Figure 17 | Expression and correlation analysis of cGMP pathway components in human prostatic smooth muscle cells. (**A, B, C**) RT-qPCR was performed to measure the gene expression of *GC-A*, *GC-B*, *sGCβ1*, *NPRC*, *PKG I*, *PDE9A1*, and the *CNP* transcript in human prostatic smooth muscle cells (HPrSMCs) (n = 18). Relative gene expression was calculated by the ΔC_t method and normalized to *ACTB*. (**C**) Individual analysis of each patient and the relative gene expression of *GC-A* and *GC-B*, which were connected by a line. (**A-C**) Mann Whitney test was used to determine statistical significances; (***) p≤0.001; (n.s.) not significant. For pairwise comparison of gene expression, the Wilcoxon test was used; (***) p≤0.001. (**D**) Correlation analysis between *GC-B* and *PKG I* was performed. Correlation index (Spearman r) and p-values are indicated in the figure.

5.3.2 Effects of CNP and the synthetic natriuretic peptide VNP on human prostatic smooth muscle cells

In addition to the muscle relaxant signalling cascade, the cGMP signalling pathway via PKG I is also known to be involved in cell growth and in the inhibition of proliferation (Li and Sun 2005). To investigate these possible effects on cell growth in cultured HPrSMCs, cells were treated with either 1 µM of the NP CNP or the synthetic analogue VNP. After 3 days, cells were counted and RNA was isolated from these cells for measurements of relative gene expression (see chapter 4.1.2.2).
It was found that after treatment with both 1 µM CNP or VNP, the growth of HPrSMCs was significantly reduced. Interestingly, CNP had a more significant ($p \leq 0.001$) effect on cell growth than VNP ($p = 0.0016$). Treatments resulted in either a 30 % decrease of cell number with CNP or 25 % with VNP (Fig. 18).

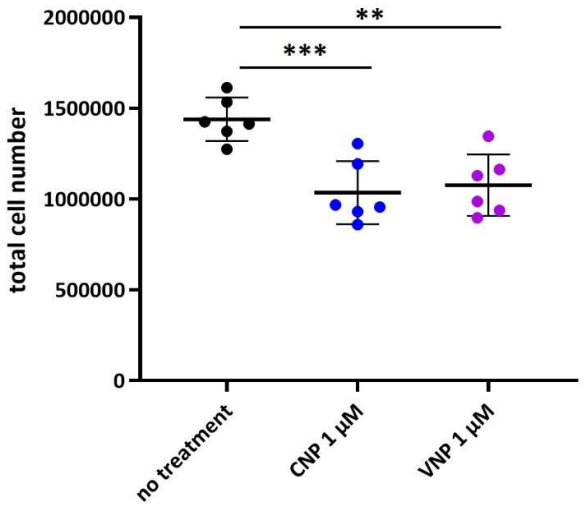

Figure 18 | Reduced cell proliferation of human prostatic smooth muscle cells after treatment with natriuretic peptides. Human prostatic smooth muscle cells (HPrSMCs) were cultured in flasks and treated for three days with 1 µM CNP or VNP. The total cell number was counted and compared with HPrSMCs without treatment. Student´s t-test was used to determine statistical significance; (***) $p \leq 0.001$; (**) $p \leq 0.01$. These cells were also used for RNA extraction and RT-qPCR measurements, see Fig. 17. For details see Materials and Methods.

Besides the effects on proliferation, the relative gene expression of components of the cGMP signalling pathway was also investigated. It was found that both the treatments with 1 µM CNP and VNP had a negative effect on the expression of *GC-A*, *GC-B*, *PKG I*, *NPRC*, *NEP*, *PDE5* and *PDE9A1* in HPrSMCs (Fig. 19).

For the expression of *GC-A*, it was observed that treatment with 1 µM CNP caused a significant decrease in expression of about 61 % ($p = 0.0013$). After 1 µM VNP, the expression significantly decreased by 76 % ($p \leq 0.001$). The treatment with CNP or VNP had a significant effect on the gene expression of *GC-B*. Again, VNP had a stronger negative influence on the *GC-B* expression. This decreased by 70 % after VNP ($p \leq 0.001$) and only by 38 % after CNP ($p = 0.0446$).

The decrease of gene expression by CNP or VNP was most impressive for *PKG I* in HPrSMCs. After both treatments, the expression decreased significantly by ~78 % ($p \leq 0.001$).

Treatment with either 1 µM CNP or VNP also influenced the gene expression of the NP-degrading enzymes *NPRC* and *NEP*. When HPrSMCs were treated with 1 µM VNP, *NPRC* expression decreased significantly by 47 % ($p = 0.0432$). The strongest effect was observed on the expression of *NEP*, it decreased by 70 % after CNP ($p \leq 0.001$) and by 79 % after VNP treatment ($p \leq 0.001$).

Furthermore, the expression of the cGMP-degrading enzymes *PDE5* and *PDE9A1* was also examined. Both peptides had a negative influence on the relative gene expression, but the influence of CNP was stronger. The expression of *PDE5* decreased by 88 % ($p = 0.0025$) after 1 µM CNP and by 35 % (n.s.) after VNP. Similar effects were also observed for *PDE9A1*. After treatment with CNP, gene expression decreased by 64 % ($p \leq 0.001$) and by 51 % after VNP ($p = 0.0034$).

In addition to HPrSMCs, primary human aortic SMCs were also studied for comparison with vascular SMCs and are presented in the next section.

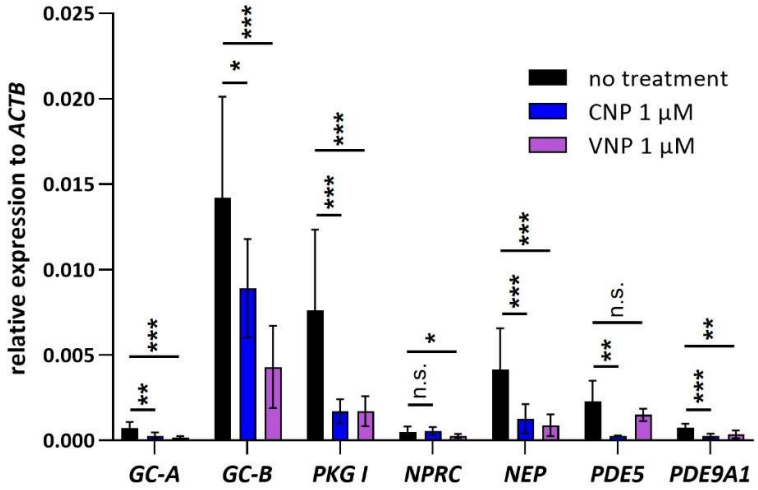

Figure 19 | Altered gene expression of cGMP pathway components in human prostatic smooth muscle cells after treatment with natriuretic peptides. RT-qPCR was performed and gene expression of *GC-A*, *GC-B*, *PKG I*, *NPRC*, *NEP*, *PDE5* and *PDE9A1* was measured in human prostatic smooth muscle cells (HPrSMCs; n = 9). Relative gene expression was calculated by the ΔC_t method and normalized to *ACTB*. Mann Whitney test was used to determine statistical significances; (***) p≤0.001; (**) p≤0.01; (*) p≤0.05; (n.s.) not significant.

5.3.3 Gene expression and correlation analysis of cGMP pathway related genes in human aortic smooth muscle cells

The primary HAoSMCs were cultured like HPrSMCs and used from p7 to p11. First, gene expression of the same cGMP pathway components as in HPrSMCs was investigated. It was found that *GC-A*, *GC-B*, *sGCβ1*, *NPRC*, *PKG I*, *PDE9A1*, and the *CNP* transcript were also expressed in these cells (Fig. 20 and Fig. 21). The comparison between the passages from p7 to p11 showed that there were only minor deviations (Fig. 20), that is why the data were summarised in the further course.

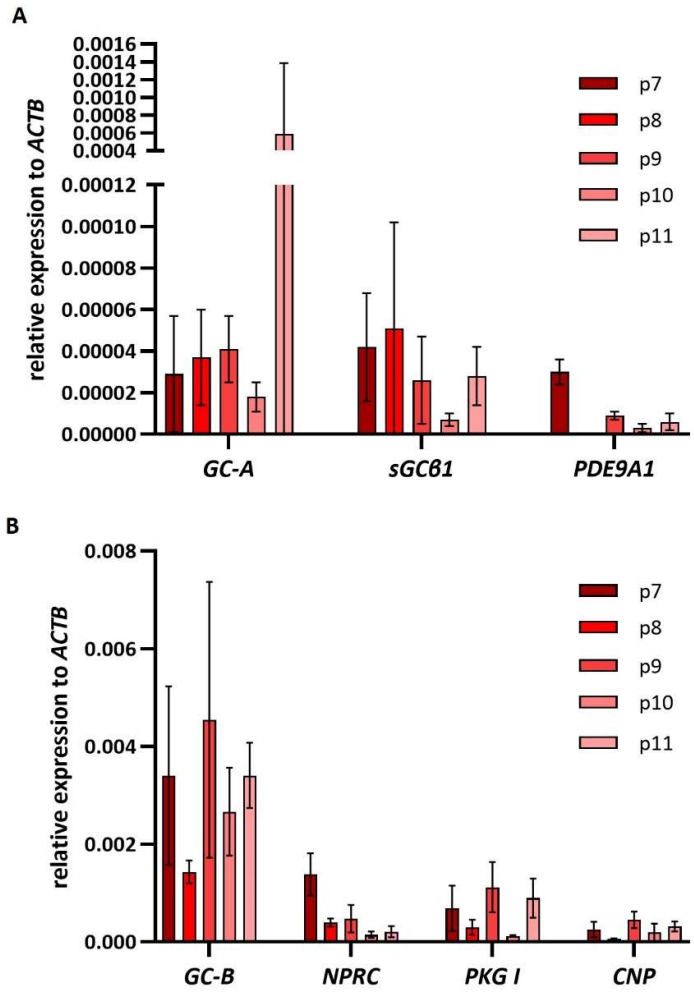

Figure 20 | (A, B) Gene expression analysis over six passages in human aortic smooth muscle cells. To detect possible changes in the gene expression pattern in human aortic smooth muscle cells (HAoSMCs), RT-qPCRs were performed and gene expression of (**A**) *GC-A*, *sGCβ1, PDE9A1* and (**B**) *GC-B*, *NPRC*, *PKG I*, and the *CNP* transcript over five passages with three replicates was measured. Relative gene expression was calculated by the ΔCt method and normalized to *ACTB*.

In HAoSMCs, *GC-B* was found to be the most highly expressed gene examined (Fig. 21A). It was significantly higher expressed than the other NP receptor *GC-A* ($p \leq 0.001$) and the NO receptor *sGC* ($p \leq 0.001$) (Fig. 21B). Pairwise comparison of each sample between *GC-A* and *GC-B* also revealed a significantly higher expression of *GC-B* (Fig. 21C). Both *GC-A* and *sGCβ1* were expressed at a very low level and no significant differences in gene expression were detected between them. Furthermore, expression of *NPRC* and *PKG I* could be measured. Interestingly, a positive correlation between *GC-B* and *PKG I* was also found in HAoSMCs, with a Spearman $r = 0.7582$ ($p = 0.0024$) (Fig. 21D).

In addition, expression of *PDE9A1* and the transcript of *CNP* could be determined.

The comparison of the expression of the investigated genes between HPrSMCs and HAoSMCs is presented in the next section.

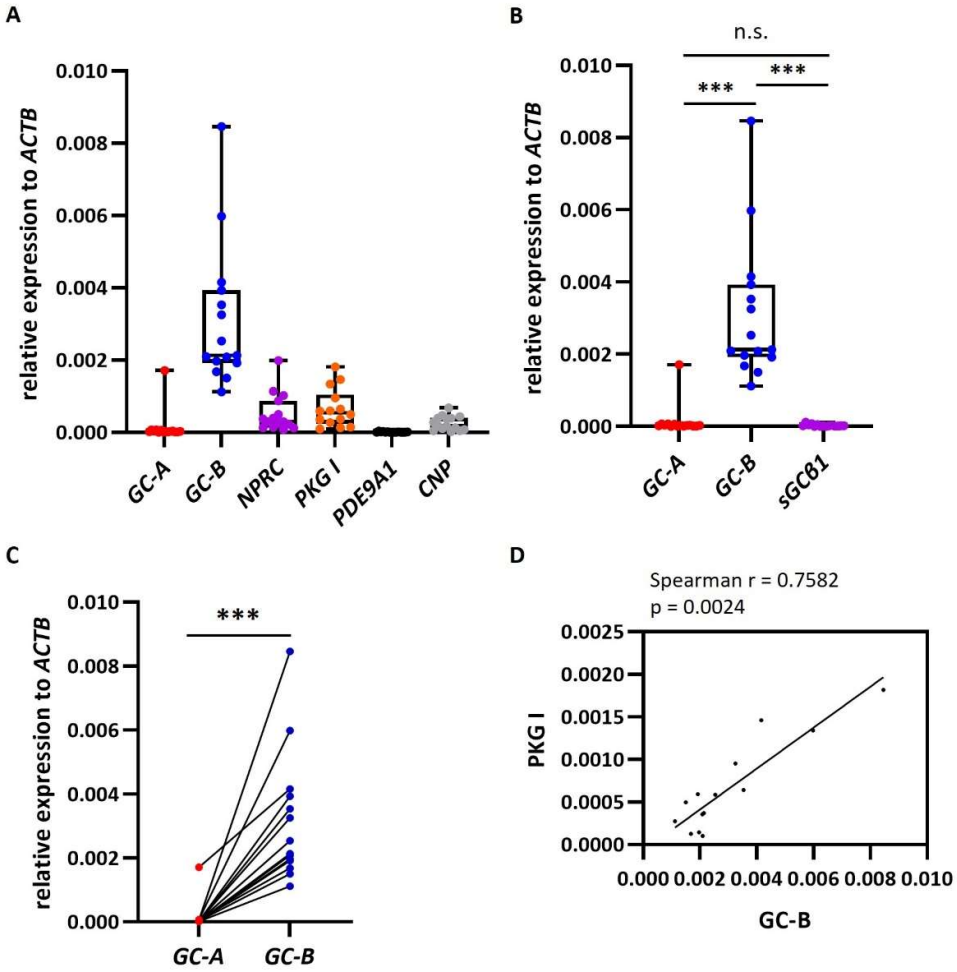

Figure 21 | Gene expression and correlation analysis of cGMP pathway components in human aortic smooth muscle cells. (**A, B, C**) RT-qPCR was performed to measure the gene expression of *GC-A*, *GC-B*, *sGCβ1*, *NPRC*, *PKG I*, *PDE9A1*, and the *CNP* transcript in human aortic smooth muscle cells (HAoSMCs; n = 15). Relative gene expression was calculated by the ΔC_t method and normalized to *ACTB*. (**C**) Individual analysis of each sample and the relative gene expression of *GC-A* and *GC-B*, which were connected by a line. (**A-C**) Mann Whitney test was used to determine statistical significances; (***) p≤0.001; (n.s.) not significant. For pairwise comparison of gene expression, the Wilcoxon test was used; (***) p≤0.001. (D) Correlation analysis between GC-B and PKG I was performed. Correlation index (Spearman r) and p-values are indicated in the figures.

5.3.4 Comparative expression analysis between cultured human prostatic and aortic smooth muscle cells

The question remains whether the human prostatic SMCs show specific features in the expression of certain cGMP signalling pathway components. Therefore, HPrSMCs were compared with HAoSMCs and the expression of *GC-A*, *GC*-B, *sGCβ1*, *NPRC*, *PKG I*, *PDE9A1*, and the *CNP* transcript was evaluated. This was possible because HPrSMCs and HAoSMCs had very similar and thus comparable expression of the reference gene *ACTB*.

There were significant differences in expression between HPrSMCs and HAoSMCs for all genes examined, and every gene was higher expressed in HPrSMCs (Fig. 22).

The NP receptor *GC-A* was 2.3-fold higher expressed in HPrSMCs than in HAoSMCs ($p \leq 0.001$). *GC-B* in HPrSMCs was the most highly expressed gene among the genes studied and 6.5-fold higher expressed in HPrSMCs than in HAoSMCs ($p \leq 0.001$). The *sGCβ1* was significantly higher expressed in HPrSMCs (15.8-fold; $p \leq 0.001$). The *NPRC*, which is responsible for the degradation of NPs, was 4-fold higher expressed in HPrSMCs than in HAoSMCs ($p = 0.0017$). The expression of *PKG I* also showed significant differences and was 9-fold higher in HPrSMCs than in HAoSMCs ($p \leq 0.001$). The clearest difference was found in the expression of *PDE9A1*. It was 51-fold higher expressed in HPrSMCs than in HAoSMCs ($p \leq 0.001$). The expression of the CNP transcript was also measured in HAoSMCs and was 3-fold lower than that in HPrSMCs ($p \leq 0.001$).

To get information about functional activity of NP receptors in these cells, HPrSMCs and HAoSMCs were treated with the NPs ANP and CNP. Using a cGMP ELISA, ANP- and CNP-induced cGMP production in these cells was measured.

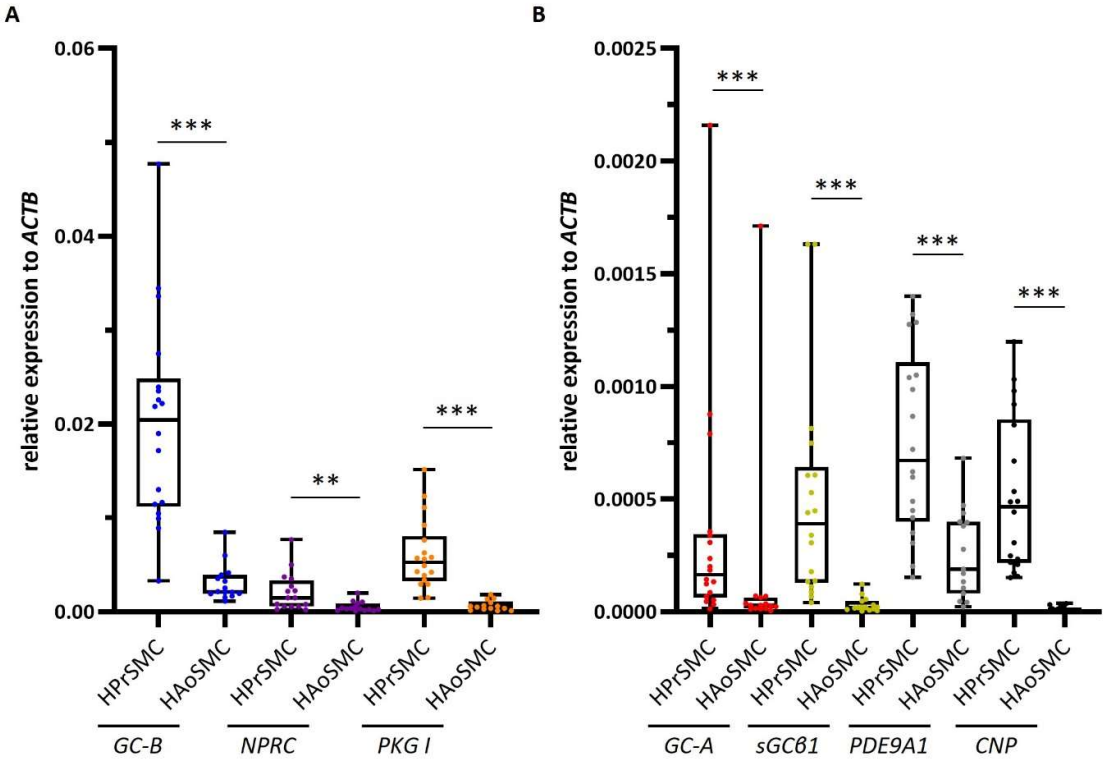

Figure 22 | (A, B) Comparative gene expression analysis between human prostatic smooth muscle cells and human aortic smooth muscle cells. RT-qPCR was performed to measure the gene expression of (**A**) *GC-B, NPRC, PKG I* and (**B**) *GC-A, sGCβ1, PDE9A1*, and the *CNP* transcript in human prostatic smooth muscle cells (HPrSMCs; n = 18) and human aortic smooth muscle cells (HAoSMCs; n = 15). Relative gene expression was calculated by ΔC_t method and normalized to *ACTB*. Mann-Whitney test was used to determine statistical significance; (***) p≤0.001; (**) p≤0.01.

5.4 Natriuretic peptide-induced cGMP production in cultured human prostatic and aortic smooth muscle cells

To get information about the cGMP-producing NP receptors GC-A and GC-B, HPrSMCs and HAoSMCs were treated with the NPs ANP and CNP. A cGMP ELISA was used to measure cGMP in these cells (see chapter 4.1.2.1 and 4.2.2).

In both HPrSMCs (Fig. 23A) and HAoSMCs (Fig. 23B), CNP was found to be more potent than ANP in increasing the concentration of cGMP in these cells. In HPrSMCs, even the lowest CNP concentrations of 0.1 nM led to a relevant cGMP production (0.47 pMol/mL), which was also significantly higher than after 0.1 nM ANP (0.16 pMol/mL). Even at the higher concentrations of 1 nM to 100 nM, cGMP production was significantly higher after CNP treatment than after ANP treatment. The first concentration where ANP treatment triggered significant cGMP production was 10 nM. At a concentration of 1 µM, both ANP and CNP treatment resulted in almost equal cGMP production (ANP - 6.5 pMol/mL; CNP - 6.3 pMol/mL) in HPrSMCs. The EC_{50}, describing the half maximum effective concentration, in HPrSMCs for CNO was 2.255×10^{-9} and for ANP 4.425×10^{-7}.

In HAoSMCs, CNP treatment also led to significantly higher cGMP production than ANP treatment at all concentrations (Fig. 23B). Even at the lowest concentration of 0.1 nM, CNP resulted in a significantly higher cGMP production compared to control cells (not shown). Treatment with 10 nM ANP was able to increase the cGMP level in HAoSMCs, which was significantly higher than the control value (not shown). The EC_{50} in HAoSMCs for CNP was 5.064×10^{-9} and for ANP 4.041×10^{-7}.

To exclude phenotypic changes, like a differentiation into other cell types, immunofluorescence was performed. For this purpose HPrSMCs were stained with the smooth muscle actin antibody and the phenotype was analysed in p9 and p11.

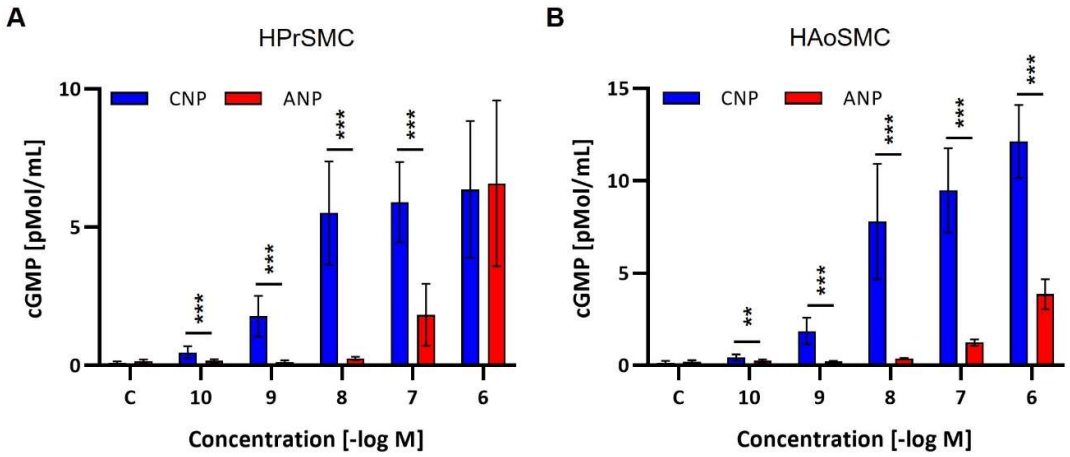

Figure 23 | Natriuretic peptide-induced cGMP production in human prostatic and aortic smooth muscle cells. Cultured primary (**A**) HPrSMCs and (**B**) HAoSMCs were stimulated for 60 min in medium (without FBS) with 0.25 mM IBMX, a phosphodiesterase inhibitor, and indicated concentrations of ANP or CNP. Each panel shows the means ± SEM of data pooled from four experiments. Five replicates were used in each passage over four passages. Cells were cultured as described and cGMP production was measured by an ELISA (see Materials and Methods).
A two-way ANOVA was used to determine whether there are differences between ANP- and CNP- induced cGMP production. Mann-Whitney test was used to calculate statistical significance; (***) $p \leq 0.001$.

5.5 Immunofluorescence in cultured human prostatic smooth muscle cells

For immunofluorescence investigations (section 4.3.3), cells were seeded in a chamber slide and grew for a few days until they reached confluence of about 80 %. HPrSMCs from p9 and p11, passages also used for qPCR and functional studies, were stained with an antibody against smooth muscle actin (SMA) to show their SMC phenotype. In addition, cell nuclei were stained with DAPI.

In nearly all HPrSMCs from p9 and p11, SMA was detectable, indicating the SMC characteristics of these cells (Fig. 24). Especially, more differentiated cells showed the typical SMC phenotype. As previously described the filamentous structure of SMCs was visible together with a centrally located nucleus.

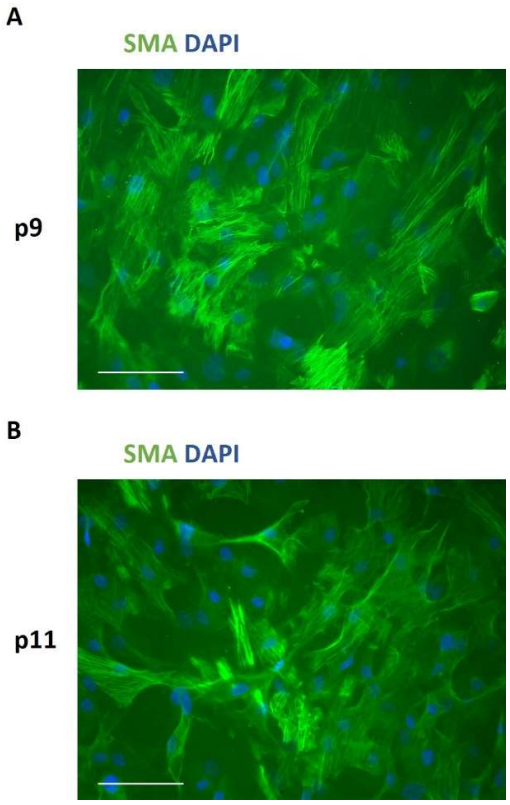

Figure 24 | Immunofluorescence for the smooth muscle marker SMA in human prostatic smooth muscle cells in passages 9 and 11. Cells were cultured in chamber slides and fixed with PFA once they reached 80-90 % confluence. Immunofluorescence was used to detect smooth muscle actin (green) in human prostatic smooth muscle cells (HPrSMCs). Pictures were taken over (**A**) passage 9 and (**B**) passage 11. DAPI (blue) was used to stain the nuclei (see Materials and Methods for details). Scale bars = 100 µm.

5.6 Expression and correlation analysis of cGMP pathway components in rat prostate

In RT-qPCR studies the rat prostate showed a similar expression pattern for *Gc-a*, *Gc-b*, *Sgcβ1*, *Nprc*, *Pkg I*, *Pde9A1* and *Pde5* compared to total human prostate tissue and cultured HPrSMCs.

Gc-b was significantly higher expressed than the other GCs *Gc-a* and *Sgcβ1* (Fig. 25B). The pairwise comparison between *Gc-a* and *Gc-b* in the same rat prostates showed that in 14 out of 15 prostates, *Gc-b* was higher expressed than *Gc-a* (Fig. 25B). The statistical test also showed a significant difference ($p \leq 0.001$). A significant difference in gene expression between *Gc-a* and *Sgcβ1* could also be measured, with *Gc-a* being higher expressed (Fig. 25B). As another component of the cGMP signalling pathway, the expression of the cGMP-dependent *Pkg I* was measured. This gene showed a moderate expression and it was only slightly lower expressed than *Gc-a* (Fig. 25A).

Furthermore, gene expression of the NP receptor *Nprc*, which is without a cGMP-producing domain but known to degrade NPs, was measured. It was found that *Nprc* is expressed at a low level and it is the lowest gene studied (Fig. 25A).

Gene expression of two other cGMP pathway components *Pde5* and *Pde9A1* which hydrolyse cGMP was also measured. The two PDEs showed a relatively high gene expression in the rat prostate, with *Pde9A1* being significantly higher expressed than *Pde5* ($p \leq 0.001$) (Fig. 25C).

Next, the effect of CNP and the synthetic analogue VNP on living tissue was investigated.

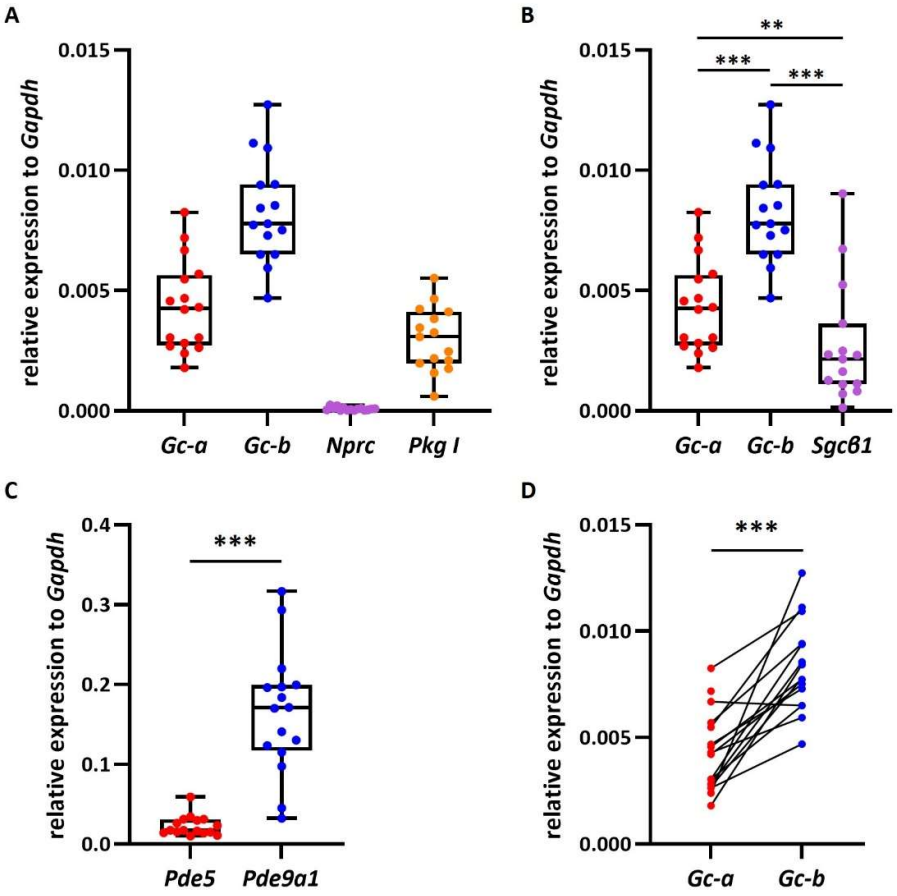

Figure 25 | Gene expression analysis in the rat prostate of cGMP pathway components. (**A, B, C, D**) RT-qPCR was performed to measure the gene expression of *Gc-a*, *Gc-b*, *Sgcβ1*, *Nprc*, *Pkg I*, *Pde5* and *Pde9a1* of rat ventral prostate (n = 15). Relative gene expression was calculated by the ΔC_t method and normalized to *Gapdh*. Mann Whitney test was used to determine statistical significances; (***) p≤0.001; (**) p≤0.01. For pairwise comparison of gene expression, the Wilcoxon test was used; (***) p≤0.001. (**D**) Individual analysis of each sample and the relative gene expression of *Gc-a* and *Gc-b*, which were connected by a line.

5.7 Live imaging – The effects of natriuretic peptides and analogues on the contractility of the rat prostate

As the expression of the investigated genes in the rat prostate showed a similar pattern as in the human prostate tissue and HPrSMCs, the rat tissue was used for further *ex vivo* experiments. In all three prostate entities investigated (human prostate tissue, HPrSMCs, rat prostate), GC-B showed significantly higher gene expression than GC-A. Since especially the NP CNP had a significant effect on cGMP production in both HPrSMCs and HAoSMCs, the effect of CNP on live rat prostate tissue was investigated. In other male reproductive organs, such as epididymis (Mietens et al. 2014) and penile arteries (Kun et al. 2008), a relaxing effect of the CNP could already be shown. In addition to the NP CNP, the synthetic analogue VNP was also used. For the first time, this peptide was synthesised in 1993 by Wei et al. and its relaxing effects on canine aortas and veins were demonstrated (Wei et al. 1993). Further studies have first shown that VNP can activate both GC-A and GC-B (Jiang et al. 2014) and further that in rat arteries, treatment with VNP leads to relaxation (Wei et al. 1994). Furthermore, it has even been shown in human radial arteries that VNP leads to relaxation (Yu et al. 2010).

For the live experiments, rat prostate from 3-month-old rats were used for this purpose. The prostates were removed, prepared and the still living tissue was fixed in rat collagen for *ex vivo* experiments (chapter 4.3.1).

First, spontaneous contractions of the prostate were recorded for 10 min. Then, 100 nM or 1 µM CNP or VNP was added and its effect was recorded for another 10 min. Finally, the vitality of the tissue was checked with the addition of 10 µM NA.

Two different time points were analysed in the recorded videos. In the first analysis, 30 sec were skipped and 2 min were analysed in each section. In the second analysis, the first 2.5 min were skipped and 5 min were analysed in each section. Thus, an early effect was captured by the first analysis and a later and longer effect in the second analysis.

For the analysis, a code was used that calculates the fold change for each individual pixel from the recordings and thus indicates the movement. These raw data sets with the fold change were analysed with GraphPad Prism, whereby first a cumulative frequency was calculated and with this a nonlinear regression (curve) was carried out to obtain the statistical evaluation of the corresponding graphs. In these graphs, the cumulative distribution is plotted against the movement score (for details see chapter 4.3.2.2).

In addition, colour-coded heat maps were generated showing strong contractions and movements in red, medium movements in green and weak movements in blue.

In the first section, the effects of CNP on the rat prostate glands are shown.

5.7.1 The effect of CNP on the spontaneous contractility

The evaluation of the effect of CNP on rat single prostate glands (Fig. 26A, upper right corner) showed that CNP had a significant relaxing effect on rat prostates. Treatment with 100 nM CNP resulted in a significant ($p \leq 0.001$) decrease in spontaneous contractions in a first analysis (Fig. 26A), in which 2 min were analysed starting 30 sec after treatment (Fig. 26B top). The corresponding heat maps for spontaneous contraction showed a relatively large number of green and red pixels prior to CNP treatment, indicating moderate movement of the prostate gland. After CNP treatment a significant decrease in the heat maps was visible as an increase of blue pixels, which indicate lower and weaker contraction of the prostate gland (Fig. 26B bottom).

However, the second analysis measuring a 5 min period 2.5 min after treatment (Fig. 26D) showed no significant difference between spontaneous movement and after 100 nM CNP ($p = 0.2629$) (Fig. 26E, top). In the corresponding heat maps, there are hardly any differences of green and red pixels between spontaneous movements and after CNP treatment (Fig. 26E, bottom).

To induce a greater and longer-lasting effect, the prostate glands were treated with 1 µM CNP. The first evaluation (Fig. 26A) showed that after 1 µM CNP the movements of the prostate gland decreased significantly ($p = 0.0101$) (Fig. 26C, top). The corresponding heat map showed a higher number of green and red pixels representing great spontaneous movements of the prostate gland. After CNP treatment movements decreased, which can be seen by an increased number of blue pixels (Fig. 26C, bottom). In the longer lasting time period (second analysis) (Fig. 26D) 1 µM CNP also led to a significant ($p = 0.0057$) decrease of spontaneous movements (Fig. 26F, top). The corresponding heat map showed (visible as a decreased number of green and red pixels) a reduction of contractions after treatment with 1 µM CNP (Fig. 26F, bottom).

In addition to CNP, rat prostate glands were also treated with a synthetic NP called VNP, in which the C-terminus of ANP was added to CNP. In this section, the effect of VNP on spontaneous contractions of prostate glands will be described.

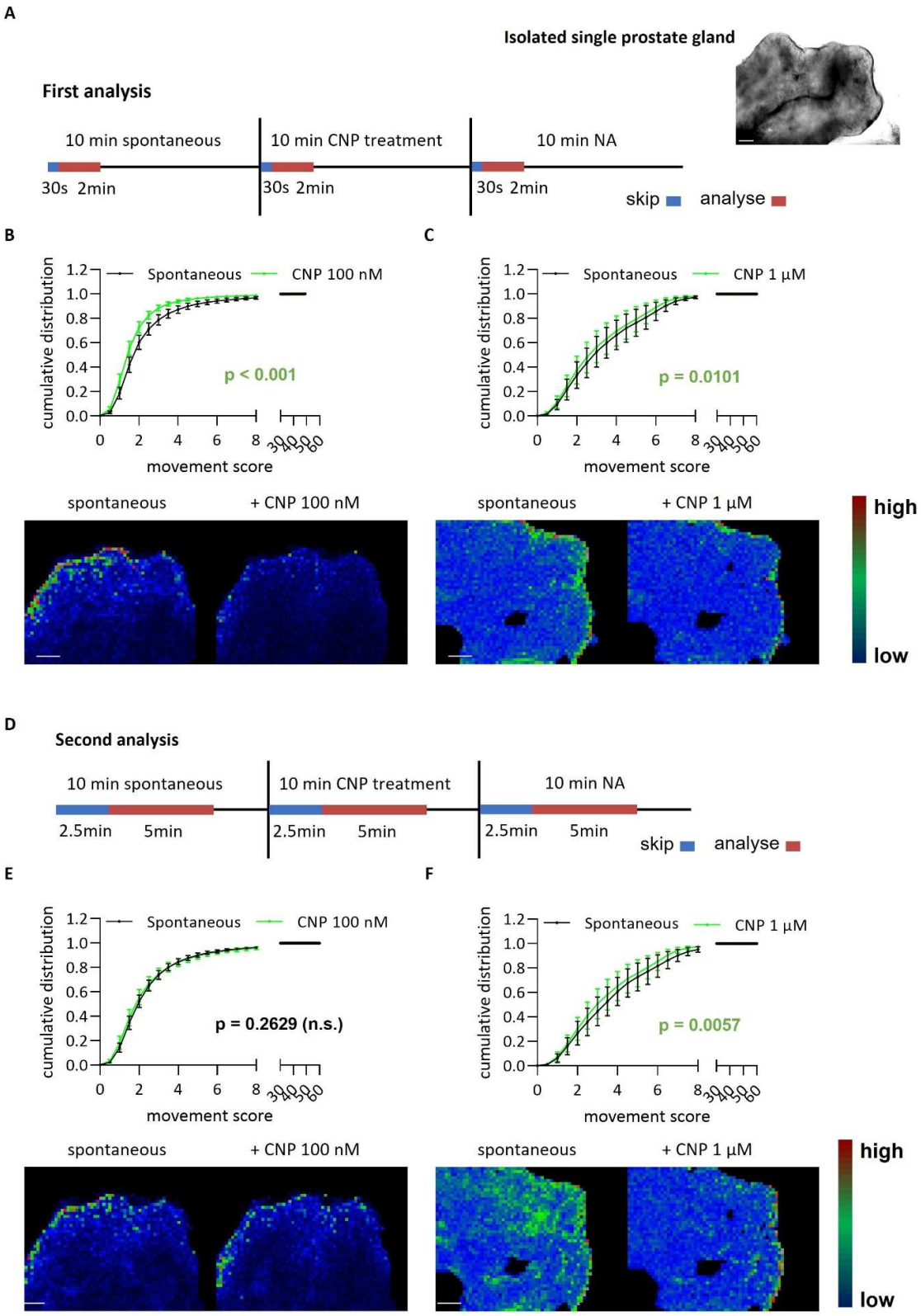
A
Isolated single prostate gland
First analysis
10 min spontaneous
10 min CNP treatment
10 min NA
30s 2min
30s 2min
30s 2min
skip
analyse
B
C
cumulative distribution
Spontaneous
CNP 100 nM
CNP 1 µM
p < 0.001
p = 0.0101
movement score
spontaneous
+ CNP 100 nM
+ CNP 1 µM
high
low
D
Second analysis
10 min spontaneous
10 min CNP treatment
10 min NA
2.5min
5min
2.5min
5min
2.5min
5min
skip
analyse
E
F
p = 0.2629 (n.s.)
p = 0.0057

Figure 26 | The relaxing effect of CNP on rat prostate glands demonstrated by live imaging. (**A, D**) Scheme of experimental setup of analyses for the two selected time periods and a representative view of a single isolated gland in transillumination (**A, right**). (**B, C**) Graphs of the cumulative distribution (± SEM) comparing spontaneous contractions and the effects of 100 nM and 1 µM CNP, respectively, on contractility over 2 min. CNP significantly decreased contractility. Representative heat maps are shown below the corresponding graphs. (**E, F**) Graphs of the cumulative distribution (± SEM) comparing spontaneous contractions and 100 nM or 1 µM CNP effects on contractility over 5 min after skipping 2.5 min. Only 1 µM CNP significantly decreased contractility. Representative heat maps are shown below the corresponding graphs.
Heat maps, showing the intensity of the sum of movements over the analysed time, were displayed in a color-coded manner with blue representing low intensity, green moderate and red high intensity movement. Scale bars = 100 µm. p-values are indicated in the figure (n.s. – not significant) and n = 10.

5.7.2 The effect of VNP on the spontaneous contractility

The treatment and evaluation with VNP followed the same scheme as previously described for CNP. After recording 10 min of spontaneous contractions, the rat gland was treated with 100 nM or 1 µM VNP and the effects were recorded for another 10 min. Again, the evaluation was performed at an early (Fig. 27A) and later (Fig. 27D) time point.

It was found that in the first scheme of analyses (Fig. 27A), in which 2 min were analysed 30 sec after treatment, 100 nM VNP had a significant ($p \leq 0.001$) relaxing effect on the rat prostate glands (Fig. 27B, top). Also, in the corresponding heat maps after VNP treatment, there is a clear decrease of green and red pixels, which indicate moderate to strong movements (Fig. 27B, bottom). In the second analysis, 2.5 min were waited before a longer time period of 5 min was analysed (Fig. 27D). The results showed that 100 nM VNP also led to a significant ($p = 0.0256$) reduction of spontaneous contractions in the prostate gland (Fig. 27E, top). The corresponding heat maps showed less green and red pixels after VNP treatment compared to the heat map for spontaneous contractions (Fig. 27E, bottom).

The prostate glands were also treated with 1 µM VNP using the same schemes of analyses (first and second analysis) The first analysis resulted in no significant ($p = 0.0516$) reduction of spontaneous contractions after treatment with VNP (Fig. 27C, top). In the heat maps, there was no difference in the number of coloured pixels between spontaneous contractions and VNP treatment (Fig. 27C, bottom). The second and longer analysis also starting at a later time point (Fig. 27D) showed that 1 µM VNP had a significant ($p = 0.0033$) relaxing effect on spontaneous contractions of the rat prostate (Fig. 27F, top). The associated heat maps of spontaneous movements and after VNP treatment showed a markedly lower number of green and red pixels after 1 µM VNP treatment (Fig 27F, bottom).

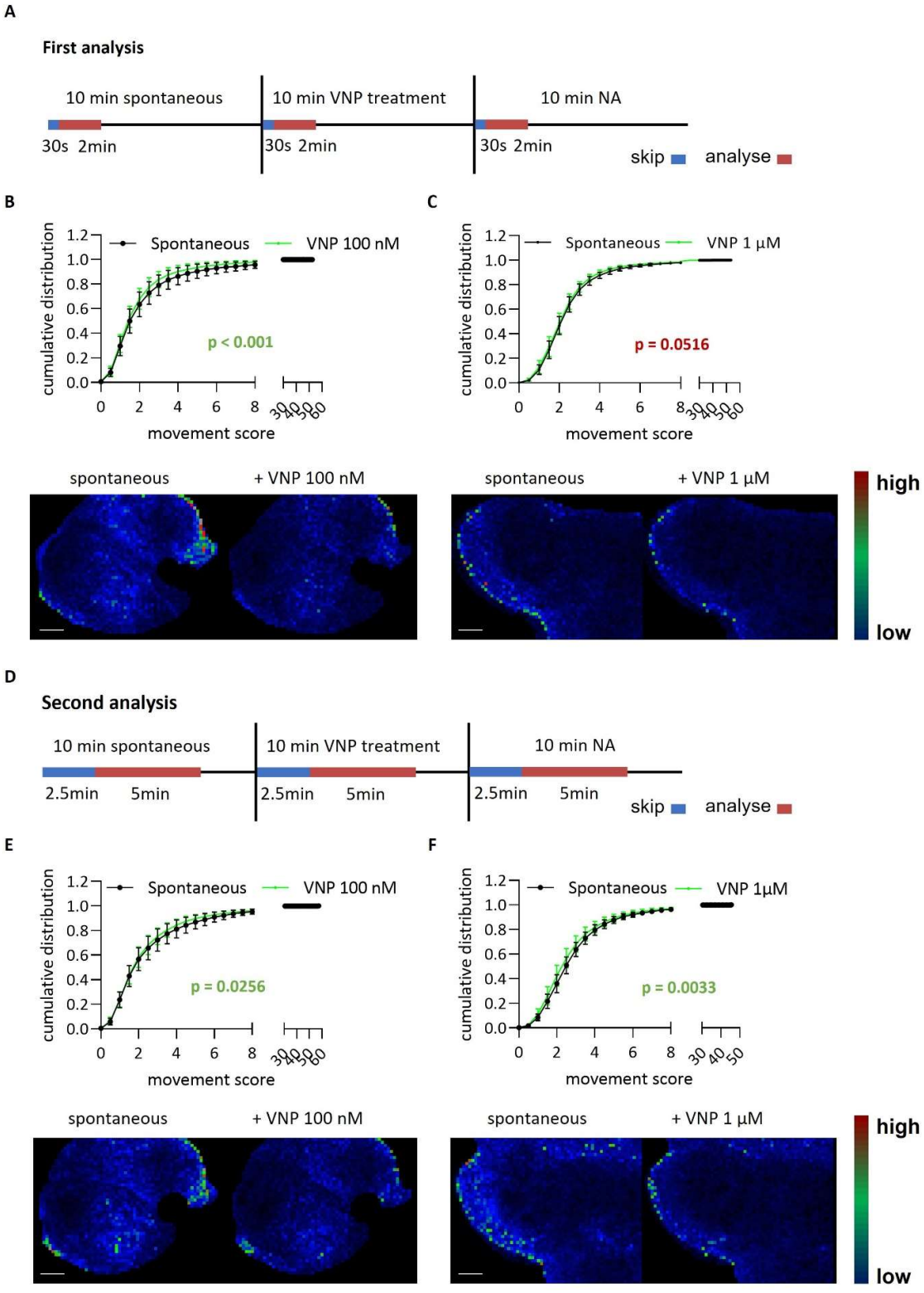
A
First analysis
10 min spontaneous
10 min VNP treatment
10 min NA
30s 2min
30s 2min
30s 2min
skip
analyse
B
C
cumulative distribution
Spontaneous
VNP 100 nM
VNP 1 µM
p < 0.001
p = 0.0516
movement score
spontaneous
+ VNP 100 nM
+ VNP 1 µM
high
low
D
Second analysis
10 min spontaneous
10 min VNP treatment
10 min NA
2.5min
5min
2.5min
5min
2.5min
5min
skip
analyse
E
F
VNP 1µM
p = 0.0256
p = 0.0033

Figure 27 | The relaxing effect of VNP on rat prostate glands demonstrated by Live imaging. (**A, D**) Scheme of experimental setup of analyses for the two selected time periods. (**B, C**) Graphs of the cumulative distribution (± SEM) comparing spontaneous contractions and the effects of 100 nM and 1 µM VNP, respectively, on contractility over 2 min. Representative heat maps are shown below the corresponding graphs. (**E, F**) Graphs of the cumulative distribution (± SEM) comparing spontaneous contractions and 100 nM or 1 µM VNP effects on contractility over 5 min after skipping 2.5 min. Representative heat maps are shown below the corresponding graphs.
Heat maps, showing the intensity of the sum of movements over the analysed time, were displayed in a color-coded manner with blue representing low intensity, green moderate and red high intensity movement. Scale bars = 100 µm. p-values are indicated in figures (n.s. – not significant) and n = 10.

6 Discussion

Benign prostatic hyperplasia, abbreviated as BPH, is an enlargement of the prostate gland that is observed in men with increasing age. By the age of 40 years, 40 % of men already suffer from BPH, and by the age of 80 years, 80-90 % of men are affected (Madersbacher et al. 2019). The origin of this disease is not known, but it is assumed that most likely a combination of initial chronic inflammation and hormonal changes occur in men as they age and led to changes in the prostate. In ageing men T level decrease, but plasma DHT levels remain the same. The androgenic signalling pathway via T and DHT can lead to proliferation, and may be responsible for uncontrolled growth and prostate enlargement, among other factors (Hammond et al. 1978; Ryl et al. 2015; Nickel et al. 2008). Considering the anatomy, the urethra passes through the prostate gland. The human prostate has a special characteristic as it is surrounded by a capsule. Uncontrolled growth, therefore, does not occur outwards but inward, and the urethra is compressed by the prostate. The urethra and indirectly the bladder are affected by this compression, which can intensify LUTS. The increased muscle tone in BPH also increases LUTS and treatments aim to reduce both growth and muscle tone (Lepor et al. 1993b; Roehrborn 2008).

The first and still first line medications for BPH target the adrenergic pathway. α1-blockers are used to reduce NA-induced contraction of the prostate. Further treatment options aim to reduce the formation of DHT in the prostate with 5-α-reductase inhibitors and thus inhibit growth. However, this treatment methods have some serious side effects, such as libido loss and ejaculation disorders, which negatively affect the lives of patients. Newer drugs that reduce muscle tone target the cGMP pathway, as it leads to relaxation in SMCs. PDE5 inhibitors are used to increase cGMP levels, leading to relaxation of SMCs in the prostate (Miernik and Gratzke 2020). This approach was further pursued in this work, and the cGMP signalling pathway and its activation especially by natriuretic peptides in the human prostate and rat were investigated. A special focus was placed on the NP CNP. This NP seems to play a special role in male reproductive organs. As early as 1993, Chrisman et al. found a high amount of CNP in the seminal plasma. Nielsen et al. underlined the special role of CNP when they measured a high concentration in the human prostate (Chrisman et al. 1993; Nielsen et al. 2008).

6.1 The impact of sex hormone on the human prostate

In healthy men, serum levels of total testosterone range from 2.7 to 10.7 µg/L, although they may decrease during the day. However, with age, the amount of T in the serum decreases, but the level of DHT does not change (Roehrborn 2008). According to the literature, serum estradiol level in man are 25 – 85 pmol/L (Behrends et al. 2021). In this work, the local hormone levels of T and E2 were measured in prostate tissues from 54 BPH patients. The local level of T in prostates of BPH patients varied from 0.1 to 0.51 µg/L with a mean value of 0.21 ± 0.1 µg/L. Thus, the local T level was 32-fold lower than the serum level; however the serum values refer to healthy patient data. Roberts et al. showed the levels of sex hormones in the serum of BPH patients. The bioavailable T level decreased from 0.538 to 0.412 µg/L with progressive age (Roberts et al. 2004). Since the prostate is also supplied by serum T, and serum T level decreases with age, it is expected that less T is found in the prostate, and thus the androgenic signalling pathway is impaired (Madersbacher et al. 2019). However, this is not the case because despite the decreasing serum T level in old age, the prostate continues to grow and develop BPH. The prostate, as an androgen-sensitive organ, converts T into DHT, which is many times more potent since it has a higher affinity for the AR. In further studies, the local prostate level of DHT could be measured as this might be more meaningful. In addition, the T/DHT ratio and whether this changes with age in BPH patients would be interesting.

Besides T and DHT, the hormone E2 is interesting. With age the level of E2 in men remains unchanged. This leads to hormonal changes and a shift in the ratio of T and E2 with age. This altered T/E2 ratio is considered to be one of the causes of the uncontrolled growth of the stroma, but also the epithelial component of the prostate, as the proliferation of these cells is stimulated via the E2 receptor ERα (Roberts et al. 2004; Zhang et al. 2016; Devlin et al. 2021). Measurement of local E2 in the human prostate revealed a mean value of approximately 0.038 ± 0.024 ng/ml, which was in the lower range of serum levels in a healthy man. Interestingly, local hormone measurements in this study showed a positive correlation between T and E2 levels. Although the relationship between serum T and E2 may change with age, the two hormones remain interdependent in the prostate, as the local enzyme aromatase converts T into E2 in the prostate. This would result in no change in the prostate T/E2 ratio. A study by Song et al. showed the expression of the receptors AR, ERα, and ERβ in human prostate tissue from young healthy men and patients with BPH. At both the RNA and protein levels, AR was higher expressed in BPH tissue than in normal tissue (Song et al. 2016). Consistent with previous findings, high relative expression of AR at the RNA level was also observed in this study. In addition, a correlation between local T level and *AR* expression was found. Thus, the local regulation of *AR* expression by T could be suggested. Since the regulation of testosterone synthesis via the hypothalamic-pituitary axis follows a negative feedback loop (Hauger et al. 2022), it is interesting that

T and *AR* are positively correlated in the prostates. This should be examined in further studies whether possible deregulation of this signalling pathway in the prostate could be one of the possible reasons for the development of BPH. Furthermore, this could indicate that the signal for further and uncontrolled growth, especially concerning the stroma, is partly due to local T and its receptor AR. Even if T decreases with age, the level of DHT remains the same, and the increased expression of the *AR* receptor mediates the increased proliferation of cells. Uncontrolled growth caused by DHT and receptor AR has been already targeted in BPH therapy. The use of 5-α-reductase inhibitors reduces the conversion of T to DHT. With this therapy, apoptosis is observed in epithelial cells, preventing prostate growth (Miernik and Gratzke 2020).

In the study by Song et al. high expression levels of ERβ were also found in BPH tissue which were higher than AR expression (Song et al. 2016). It seemed surprising that this study indicated that the receptors for E2 are higher expressed than the androgen receptor AR. In contrast, the current study showed that the relative expression of *ERα* and *ERβ* measured in total prostate tissue was significantly lower than A*R* expression, with no difference between the expression of *ERα* and *ERβ*. The similar expression of *ERα* and *Erβ* was unexpected as several studies have shown that ERα expression decreases and ERβ is higher expressed in BPH (Song et al. 2016; Devlin et al. 2021). In addition, ERα is expressed only in stromal components, whereas ERβ has been detected in different cell types of the prostate. However, most of these studies are based on immunological staining (Tsurusaki et al. 2003; Devlin et al. 2021). The different expression patterns of *ERα* and *ERβ* may explain why no differences in receptor expression were observed in this study. ERα is mainly expressed in the stroma of the prostate, which is predominant in BPH prostate. ERβ expression may increase, but the proportion of other cell types may decrease in BPH.

Besides the uncontrolled growth in the epithelium and stroma of the prostate, increased muscle tone in the stromal component is one of the main symptoms of BPH (La Vignera et al. 2016). This increased muscle tone is targeted as a new therapeutic option via the relaxing cGMP signalling pathway. PDE5 inhibitors are used to increase intracellular cGMP levels and thereby induce tissue relaxation (Sebastianelli et al. 2020). In this work, the focus was on this cGMP signalling pathway and to further characterise it in the prostate.

6.2 Differences between intact tissue and cultured cells regarding the gene expression of cGMP signalling pathway components

The cGMP pathway has been shown to relax SMCs of various origins, including the coronal vessels of the heart, lung, and the reproductive organs epididymis and penis (Cargill and Lipworth 1995; Drewett et al. 1995; Lopez et al. 1997; Kun et al. 2008; Mietens et al. 2014) Recently, this signalling pathway has been targeted for treatment of BPH and represents a new target. PDE5 inhibitors are used to increase intracellular cGMP levels by inhibiting the cGMP-hydrolysing enzyme PDE5. Additionally, PDE5 inhibitors and activation of the signalling pathway have been investigated as therapeutic options (Sebastianelli et al. 2020). Activation was mediated by an NO donor and the sGC. In different species such as rats and dogs, it was shown that cGMP levels were increased and the prostate relaxed. Moreover, in a placebo-controlled study in BPH patients the application of an NO donor, which increases cGMP levels, showed beneficial effect on peak flow rate, enabled spontaneous voiding and decreased the volume of residual urine (Roshani et al. 2010; Tadayyon et al. 2012; Ückert et al. 2020). In this study, the alternative activation of this cGMP signalling pathway via NPs was investigated in more detail.

The activation of the cGMP signalling pathway via NPs, especially CNP, is interesting since CNP was found in high concentrations in the male reproductive tract. On one hand, previous studies measured high concentrations of CNP in porcine and cattle seminal plasma (Chrisman et al. 1993; Codognoto et al. 2020), and on the other hand, the expression of CNP in reproductive organs was demonstrated. The highest amount was even detected in porcine and human prostate (Nielsen et al. 2008; Nielsen et al. 2009). The exact reason and function behind the high amounts of CNP in reproductive organs is still unclear.

The relative expression of the cGMP pathway components, such as *GCs*, *sGCβ1*, *PKG I*, *PDEs*, *NPRC*, determined by qPCR showed that all components are expressed in the prostate of BPH patients, but also in a prostatic SMCs (HPrSMCs), a cell line derived from a young healthy male. Clear evidence of cGMP pathway components in HPrSMCs indicates that the relaxing pathway is expressed in SMCs of the human prostate and may be a potential target in the treatment of BPH. Interestingly, in 27 of 29 BPH patients, the local relative expression of *GC-B*, the receptor for CNP, was higher than that of *GC-A* and *sGCβ1*. In addition to the receptors, the transcript for CNP was also measured, indicating local production of this NP and supporting previous studies and the same hypotheses of Nielsen et al 2009. that CNP is produced locally in prostatic SMCs. The expression measurements in HPrSMCs support these results and indicate that the signalling pathway is predominantly expressed in SMCs since *GC-B* was always expressed at higher levels than *GC-A* and *sGCβ1* in HPrSMCs. This relatively high expression of the CNP/GC-B signalling pathway in the human prostate, especially in HPrSMCs, could inspire the

development of new therapeutic options for BPH. Various studies have shown that CNP levels can be increased by various factors. These factors include TGF-β, platelet-derived growth factor BB (PDGF-BB) and basic fibroblast growth factor (bFGF) (Sellitti et al. 2011). In cultured human-derived aortic SMCs these factors have been shown to increase CNP levels (Sellitti et al. 2011). As the positive effect of these factors on CNP production has been demonstrated in human aortic SMCs, it is conceivable that these effects could also be applied to prostatic SMCs. However, this needs to be investigated in future studies.

Activation of the cGMP pathway by synthetic NPs or NP analogues is used in the treatment of achondroplasia using the synthetic CNP analogue, Vosoritide. Such an application of NPs or analogues could also be used in BPH, and the activation of the cGMP signalling pathway should be considered.

Manipulation of the cGMP signalling pathway in BPH treatment with PDE5 inhibitors showed no serious side effects, such as ejaculation dysfunction (Miernik and Gratzke 2020). Kun et al. suggested that a therapeutic approach via the CNP/GC-B pathway may also be suitable for erectile dysfunction. This not only shows that CNP offers different therapeutic approaches in male reproductive organs, but also that side effects such as erectile dysfunction would not be expected in the treatment BPH (Kun et al. 2008). The cGMP pathway is already used in BPH via PDE5 inhibitors. Previous treatments with α-blockers often lead to side effects, such as erectile dysfunction, because NA-induced contractions are inhibited during emission and expulsion. A recent study by our group showed that treatment of prostates with a PDE5 inhibitor did not cause these side effects and that NA-induced contractions were not suppressed (Seidensticker et al. 2022). This would make the cGMP pathway a better alternative to current BPH treatments.

In addition to the expression studies, correlation studies between the genes showed that *GC-B* correlates positively with the expression of *PKG I* which encodes the cGMP-binding protein. This could indicate a positive feedback loop of the cGMP signalling pathway. This positive correlation was not only found in the human prostate of BPH patients, but also in HPrSMCs. The expression of *PKG I* was correlated with the local hormone levels of E2, suggesting a hormonal regulation of this signalling pathway by E2. A previous study by our group showed the hormonal influence of T on the expression of GC, GC-A, GC-B, and sGC in rat prostate (Müller et al. 2011).

Furthermore, components that downregulate the cGMP signalling pathway were also investigated, including PDEs, *PDE5* and *PDE9*, *NEP*, and *NPRC*. All these components were found to be expressed in the prostate of BPH patients as well as in HPrSMCs. Interestingly, *PDE9* had a very high relative expression in the human prostate, but not in HPrSMCs. In the human prostate, the expression of *PDE9* was even significantly higher than that of *PDE5*, but the expression of *PDE9* was highly variable between patients. The human prostate consists of different epithelial and stromal components, which

differ in their density. In BPH an increase in the stromal component occurs and the ratio between glandular and stromal areas changes (Bartsch et al. 1979). The observation of PDE9 expression suggests, on the one hand, that PDE9 is likely to be increasingly expressed in cell types other than SMCs in the prostate and, on the other hand, that PDE9 could be used as a target in BPH therapy to positively influence cGMP signalling in epithelial cells. The study by Nagasaki et al. strengthens this hypothesis, as they found by immunological staining that PDE9 is expressed in the human lower urinary tract. They demonstrated its expression in the urothelium of the bladder, prostatic urethra, and prostatic glandular epithelium (Nagasaki et al. 2012). Although PDE9 expression was not detected in SMCs at high amounts, selective PDE9 inhibitors have been shown to affected SMCs. For instance, PDE9 inhibitors have a relaxing effect on various SMCs, such as the corpus cavernosum and bovine trachea (Da Silva and Souza 2019; Tajima et al. 2018). In addition, PDE9 was detected in other organs, such as the brain, and appears to be associated with neurodegenerative diseases. The use of the BAY-73-6691 inhibitor, as an selective PDE9 inhibitor, has shown to improve learning, memory, and basal synaptic transmission and is evaluated in studies to treat Alzheimer's disease (Singh and Patra 2014). Further detailed studies on the role and function of PDE9 especially in the epithelium of the prostate or lower urinary tract of men are needed to identify new applications of PDE9 inhibitors.

In addition to HPrSMCs, other SMCs were examined for comparison. SMCs from human aorta (HAoSMCs) were selected for this study. It is well known and demonstrated in many studies that the cGMP signalling pathway is expressed and plays an important role in the aorta and other tissues of the cardiovascular system. The most important role of NPs in this system is mediated by GC-A, which regulates blood pressure and volume (Potter et al. 2006).

In cultivation, HAoSMCS and HPrSMCs showed a high relative expression of the CNP receptor *GC-B*, which was higher than that of *GC-A*. Moreover, *GC-B* expression was higher than that of *sGCβ1* in these cells. Unfortunately, there was no human tissue for comparison with the HAoSMCs, as there was between the human prostate and HPrSMCs. Although no direct comparison between expression in the human prostate and HPrSMCs was possible, because of the different expression level of the housekeeping gene, the expression profiles of both were compared. Both entities had a similar expression profile, whereby *GC-B* was higher expressed than *GC-A* and *sGCβ1*, and *GC-B* correlated positively with *PKG I*.

Expression of cGMP pathway components could be compared between HPrSMCs and HAoSMCs, as the expression of *ACTB* was at the same level. Direct comparison showed that all cGMP pathway components were expressed at significantly higher levels in HPrSMCs. In both cell lines, *GC-B* showed the highest relative expression, followed by *PKG I*. When looking at the expression of the *CNP* transcript, it was 3-fold higher expressed in HPrSMCs than in HAoSMCs. This further supports the

assumption of local production and the specific role of CNP in male reproductive organs. However, the greatest difference in expression was observed in *PDE9*. In HPrSMCs, *PDE9* was 51-fold higher expressed than HAoSMCs. This difference may indicate an important role of *PDE9* in the prostate. Even though HPrSMCs express less *PDE9* than other prostate cell types, they are still higher expressed than HAoSMCs. Therefore, it would be interesting to investigate the expression profile of PDE9 in other SMCS from different tissue types in more detail. This could reveal some new functions. Functional experiments in male reproductive organs with PDE9 inhibitors, such as BAY-73-6691, could provide further insights, as they have already showed to relax SMCs in the study by Tajima et al. in bovine trachea (Tajima et al. 2018).

6.3 Effects of natriuretic peptides on cGMP production and cells

For studies on the function of NPs in SMCs, the primary cell lines HPrSMCs and HAoSMCs were used. Specific cGMP ELISA experiments showed that in both HPrSMCs and HAoSMCs, treatment with the NPs ANP and CNP led to significant cGMP production. In both HPrSMCs and HAoSMCs, treatment with the lowest concentration of 0.1 nM CNP resulted in significant cGMP production above the basal levels. For ANP, a significant increase in cGMP production was observed only at a higher concentration of 10 nM. This is consistent with the qPCR results from both cell lines, as the CNP receptor *GC-B* was significantly higher expressed than the ANP receptor *GC-A*. Therefore, higher expression of *GC-B* obviously resulted in a significant cGMP production at lower concentrations of CNP. A previous study by our research group showed that treatment with ANP and CNP led to cGMP production in the epididymis. In this male reproductive organ, treatment with CNP stimulated higher cGMP production than ANP treatment (Müller et al. 2011). Experiments in this study demonstrated that the CNP/GC-B pathway also acts in prostate SMCs via cGMP and that the downstream signalling pathway is likely mediated via cGMP-binding PKG I (Müller et al. 2011). These findings support the assumption that the CNP/GC-B signalling pathway could represent a new therapeutic target for patients with BPH. The activation of this pathway is possible via NPs or their analogues. Such a CNP analogue was investigated in further experiments to demonstrate the long-term effects of NPs.

For this purpose, the synthetic chimeric peptide Vasonatrin (VNP) was used. Due to the ring structure and N-terminus of CNP with the additional C-terminus of ANP, Vasonatrin binds to both GC-A and GC-B with a higher affinity for GC-B (Jiang et al. 2014). To demonstrate the effect of CNP and VNP on cell growth, HPrSMCs were treated with NPs for three days, and the cells were counted. Significantly fewer cells were present after treatment with NPs compared to untreated HPrSMCs. Previous studies on CNP have demonstrated both antiproliferative and proliferative effects. The proliferative effect of CNP on growth plate chondrocytes is targeted for the treatment of achondroplasia (Savarirayan et al. 2019).

In this context, Vosoritide, a CNP analogue, is used to stimulate the growth of plate chondrocytes (Savarirayan et al. 2019; Savarirayan et al. 2020). However, in other studies, CNP has been shown to have an antiproliferative effect on vascular SMCs. Early after the discovery of CNP, Furuja et al. 1991 discovered its antiproliferative effect on cultured rat vascular SMCs. In the study of Furuya et al. 1991, it was suggested that CNP has an effect on the cell cycle and Doi et al. 1997 confirmed this finding. Overexpression of CNP led to increased production of cGMP, which in turn led to arrest in the G1 phase (Furuya et al. 1991; Doi et al. 1997). Further studies have confirmed the antiproliferative effect of CNP in bovine aortic SMCs, cardiomyocytes, and rodent cardiac fibroblasts (Porter et al. 1992; Horio et al. 2003; Tokudome et al. 2004).

Lu et al. 2004 were also able to demonstrate an antiproliferative effect for VNP using vascular SMCs from internal mammary artery and saphenous vein. Since the effect of VNP could be mimicked by 8-bromo-cGMP, it was shown that the cGMP signalling pathway is responsible for reduced cell proliferation (Lu et al. 2004).

To determine whether the antiproliferative effect is mediated via the second messenger cGMP and the cGMP-dependent PKG I, the literature points out further studies performed on different cell types.. In primary vascular aortic SMCs, it was demonstrated that the cGMP signalling pathway via PKG I regulates Ca^{2+} concentration and thus calcineurin activity (Li and Sun 2005). Li and Sun 2005 showed that PKG I influenced the cell cycle via downstream signals, leading to reduced cell proliferation; however, cell viability was not affected (Li and Sun 2005). Ren et al. 2014 demonstrated the antiproliferative effect of the cGMP signalling pathway in human renal carcinoma cells. Furthermore, they showed that the signalling pathway is related to PDE5, and that downregulation of PDE5 expression inhibits cell proliferation and stimulates apoptosis. This effect could also be mimicked by 8-bromo cGMP, which was blocked by a PKG I inhibitor (KT5823) (Ren et al. 2014). Using ovine fetal pulmonary vascular SMCs, Negash et al. found that PKG I not only mediates cell proliferation, but also controls cell adhesion and migration. Under hypoxic conditions in ovine fetal pulmonary vascular SMCs, PKG I was downregulated in these cells, resulting in increased cell adhesion and migration (Negash et al. 2009).

This and previous studies on CNP and VNP on cell proliferation suggest that although it depends on the cell type, the peptides may have an antiproliferative effect on prostatic SMCs. This implies that the cGMP signalling pathway via PKG I targets both the characteristic symptoms of BPH. With a therapeutic approach via the cGMP pathway, increased muscle tone and uncontrolled growth can be targeted.

In addition to cell proliferation, gene expression was examined in HPrSMCs treated with CNP or VNP. It was found that the components of the cGMP signalling pathway, such as *GC-A*, *GC-B*, and *PKG I*, were downregulated after 3 days of treatment compared to those in untreated HPrSMCs. However,

inhibitory components, such as *NPRC*, *PDE5*, and *PDE9A1* were also downregulated after treatment with NPs. It seems that there is a self-regulatory effect, and the signalling pathway is downregulated when the cells are exposed to the NPs as activators of the signalling pathway for a longer period of time. The sensitivity of the cGMP signalling pathway must be considered for the potential use of NPs in the prostate. Short-term treatment with NPs led to relaxation of SMCs, but prolonged exposure of SMCs to NPs on SMCs showed a negative effect on the expression of pathway components.

To demonstrate the relaxing effect of NPs on prostate tissue, *ex vivo* experiments were performed using the rat ventral prostate.

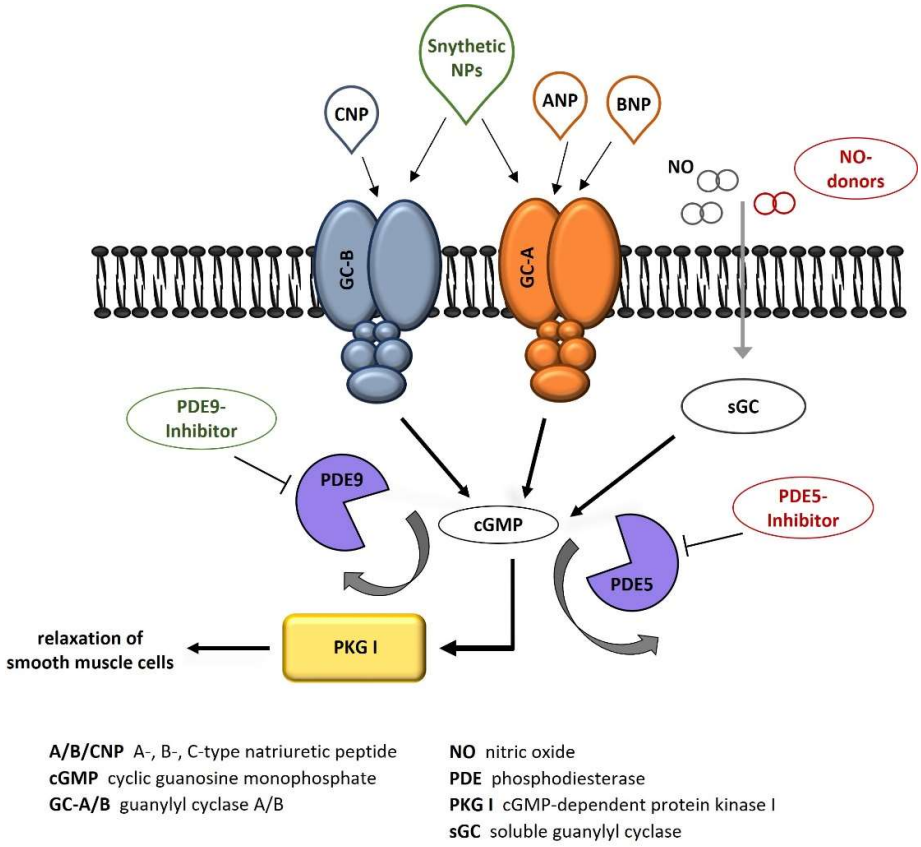

Figure 28 | Possible and already used targets in the cGMP signalling pathway.
The production of the second messenger cyclic guanylyl monophosphate (cGMP) can be activated by nitric oxide (NO), that binds to the soluble guanylyl cyclase (sGC), or natriuretic peptides (A-, B- or C-NP). ANP and BNP bind guanylyl cyclase A (GC A), whereby CNP only interacts with GC B. The activation of the cGMP dependent protein kinase I (PKG I) by cGMP leads through a signalling cascade to relaxation of smooth muscle cells. B. The level of cGMP synthesized by GCs is regulated by phosphodiesterases (PDEs), that hydrolyze cGMP in an inactive form. Targets already used in the treatment of BPH include the use of PDE5 inhibitors. New approaches could be to also use PDE9 inhibitors or to activate the pathway in other ways. The activation could be achieved by NO donors or by synthetic and modified natriuretic peptides.

6.4 The rat as a good model for *ex vivo* live imaging experiments

To demonstrate the relaxing effect of the NPs CNP and VNP, the rat prostate was chosen as a model for the *ex vivo* experiments. The rat prostate as an animal model was already used in previous studies by our research group, to demonstrate the relaxing effect of NP on the rat epididymis (Mietens et al. 2014). Additionally, the CLARITY method was used to demonstrate colocalization and expression of SMA as a marker for smooth muscle cells and PDE5 in the rat prostate (Kügler et al. 2018).

6.4.1 Gene expression of cGMP signalling pathway components in the rat prostate gland

The expression of cGMP pathway components was investigated in the rat prostate. Expression studies showed that the rat ventral prostate, human prostate, and human prostatic SMCs had similar, if not almost the same, expression profiles. *Gc-b* was higher expressed in the rat prostate than *Gc-a* or *Sgcβ1* in each sample. Thus, this made the rat prostate a suitable model for further functional studies of NPs in the prostate. Similarly to the human prostate, *Pde9a1* was the most highly expressed gene and showed higher expression compared to *Pde5*. However, the whole prostate tissue is composed of different cell types; therefore, the high expression of *Pde9a1* probably originates from the epithelial portion. As observed in HPrSMCs, *PDE9A1* expression was lower in the SMCs. Although PDE9 is not highly expressed in prostatic SMCs (Zhang et al. 2020), this enzyme may have specific effects on prostatic SMCs because it exhibits a relaxing effect on SMCs in other organs (corpus cavernosum and bovine trachea) (Da Silva and Souza 2019; Tajima et al. 2018).

For further functional experiments on rat prostate, a deliberate decision was made not to use the rat BPH model, which was created by adding T. In this BPH model, castrated rats were administered T, which led to significant prostate growth (Li et al. 2018). However, this T-induced BPH model is questionable as it shows some inconsistencies and does not reflect the conditions seen in humans. In humans, the opposite is observed, with a decrease in serum T levels with concomitant prostate growth (Roehrborn 2008). Moreover, Zhang et al. discussed the advantages and disadvantages of the hormone-induced rat BPH model, often showing an increase in epithelial components, but some studies also showed an increase in stromal components (Zhang et al. 2020).

Besides the hormonal influences, with a decrease in T with age in older men, inflammation is thought to play a major role in the development of BPH. Zhang et al. developed a rat BPH model whereby they induced inflammation by autoimmune disease leading to the development of BPH in rats (Zhang et al. 2020). However, because the origin of BPH in humans is not clear, and an animal model is limited in reflecting another species, healthy adult rats were used in this study. Therefore, live imaging experiments have focused on showing the relaxing effect of NPs on SMCs in the prostate.

6.4.2 Effects of natriuretic peptides on the contractility of rat prostate glands

For preparation of tissue and live imaging, methods established by our working group were used (for details see Methods 4.3 (Mietens et al. 2014). The prostate tissue was treated with either 1 µM or 100 nM NPs after spontaneous contractions were recorded as a reference score. Vitality control was performed by adding NA and a single strong and persistent contraction of the prostate was observed. The recordings were analysed twice at each of the two different time points, for details please refer to Methods 4.3 and Fig. 26. Two different time points were investigated to determine when the NPs started to act on the prostate and in what time frame the relaxation effect lasted.

For CNP, the exact function in male reproductive organs has not yet been clarified. High concentrations of CNP were found in porcine and cattle seminal plasma and high amounts of CNP were also detected in tissues such as the prostate (Chrisman et al. 1993; Nielsen et al. 2008; Nielsen et al. 2009; Codognoto et al. 2020). However, functional studies showed a relaxing effect of CNP on some male reproductive organs. In a previous study by our group, the relaxing effect of NPs in the epididymis was compared using the live imaging method. Although both NPs led to relaxation, ANP had a stronger effect on the epididymis than CNP did (Mietens et al. 2014). CNP have also been shown to relax SMCs in the penile arteries and corpus cavernosum via its GC-B receptor (Küthe et al. 2003; Kun et al. 2008). In the present study, CNP and VNP showed a relaxing effect on SMCs in the prostate. Thus, activation of the cGMP signalling pathway also led to relaxation in the prostate and offers a therapeutic approach for BPH.

In this study, live imaging methods were used for recording, and a newly developed method was used to evaluate and image contractions. Previous evaluation methods capture only one point of the tissue and analyse simple movements, as found in most regions of the epididymis (Mietens et al. 2014). The new evaluation was based on the wiggle-index code (Denecke et al. 2015; Preston et al. 2015; Preston et al. 2016) (https://doi.org/10.26180/13653614), which was further modified by Cameron Nowell (Monash University) and Dr. Beatrix Bester from our research group (Stadler et al. 2021). This allows the capture of the complex and multidirectional movement characteristics of the prostate glands. The investigated tissue is converted into multiple individual pixels, and thus data points, which provide a much more accurate analysis and a movement score, can be derived (details see Methods 4.3).

For *ex vivo* experiments, additionally to CNP, the synthetic chimeric peptide VNP was investigated, which has a high binding affinity for both GC-A and GC-B. Experiments demonstrated that CNP and VNP has a short relaxing effect at a concentration of 1 µM. Further experiments with a lower dose of 100 nM of CNP or VNP showed that CNP led to short-term relaxation, but the effect decreased over time. In comparison, experiments with VNP showed a relaxing effect on prostate glands. The ability and high affinity of VNP to bind to both GC receptors was demonstrated in these experiments, as it led to relaxation both at a higher concentration of 1 µM and also had a short- and long-term relaxing effect

at only 100 nM. The studies indicate that activation of the CNP/GC-B signalling pathway would be suitable as a therapeutic approach for the treatment of BPH. The local production of CNP shown here, which Nielsen also suggested with his measurement of high CNP concentrations (Nielsen et al. 2008), could be considered a therapeutic target. The *ex vivo* study presented here provides initial evidence that synthetic NPs such as Vasonatrin may be of interest for the treatment of BPH and further studies on human prostate should be carried out. Recently, the synthetic NP Vosoritde is used to treat achondroplasia and shows no serious side effects. In this therapeutic approach, the function of CNP in endochondral ossification is to stimulate bone growth in children. The growth and differentiation of chondrocytes are initiated by activating the cGMP signalling pathway via GC-B (Rintz et al. 2022). Thus, therapeutic approaches using peptides may offer new possibilities.

In addition to activation, the cGMP pathway can be used to therapeutically manipulate other components. Recently, PDE5 inhibitors are used to prevent the degradation of intracellular cGMP. Treatment with PDE5 inhibitors showed fewer major side effects than α1-blockers or 5-α-reductase, and no impact on libido or ejaculatory dysfunction (Miernik and Gratzke 2020).

In addition to increased muscle tone, the prostates of patients with BPH show uncontrolled proliferation. To treat uncontrolled prostate proliferation, 5-α-reductase inhibitors have been used to inhibit the enzymes responsible for the conversion of DHT from T. With this treatment, it has been observed that apoptosis is induced in the epithelial part of the prostate (Miernik and Gratzke 2020).

To reduce proliferation of prostatic SMCs, cGMP is also of interest. The antiproliferative effect of the cGMP signalling pathway via PKG I has been shown in a few studies in SMCs, but not in prostatic SMCs (Li and Sun 2005; Negash et al. 2009). In this study, experiments on the growth of HPrSMCs after treatment with CNP or VNP provided the first indication that cell growth in prostatic SMCs can also be inhibited via the cGMP signalling pathway.

It was shown that the activation of the cGMP signalling pathway by NPs not only led to relaxation of prostate glands, but also inhibited the proliferation of HPrSMCs.

Summary

Benign prostatic hyperplasia (BPH) is the most common disease in men, with 40 % of men aged 40 years suffering from BPH. The incidence continues to rise and 70-80 % of men aged 80 years have BPH. The disease develops in the transition zone of the prostate, and both the epithelial and stromal parts are involved. There is uncontrolled growth and proliferation of cells, whereby the stromal part with it smooth muscle cells (SMCs) is more affected. Due to the anatomical specificity of the prostate with its outer capsule, growth takes place inward and prostate tissue presses on the urethra. This leads to lower urinary tract symptoms (LUTS).

Current treatment options with α1-adreneroreceptor antagonists or 5-α-reductase inhibitor aim to reduce the muscle tone and to inhibit cell proliferation. However, these treatments have side effects and a massive impact on patients' lives due to libido loss and ejaculatory disorders. Novel treatment options with phosphodiesterase (PDE)-5 inhibitors influence the cGMP signalling pathway, which leads to the relaxation of SMCs. Here, none of the side effects observed with α1-adreneroreceptor antagonists or 5-α-reductase inhibitors were seen. Thus, the cGMP pathway represents a target for the development of new therapeutic options for BPH. This pathway was further investigated because a high concentration of the natriuretic peptide CNP, which activates the pathway via guanylyl cyclase-B (GC-B), was found in the prostate and seminal plasma. In this study, a more detailed investigation of CNP/GC-B was aimed at revealing new therapeutic applications of the cGMP signalling pathway.

The expression of key components of the cGMP signalling pathway was measured in the human prostate, with a significantly higher expression of the CNP receptor GC-B than the other GCs (GC-A and sGC) and local expression of the natriuretic peptide CNP. This indicates that the CNP/GC-B signalling pathway may play a more important role than ANP/GC-A or nitric oxide/soluble GC in the human prostate. In this study, stronger activation of the cGMP signalling pathway in prostatic SMCs (HPrSMCs) via CNP (compared with ANP) was demonstrated using a specific cGMP ELISA. This cGMP signalling pathway could be specifically activated by NPs or their analogues in the prostate to treat BPH. As the cGMP signalling pathway not only led to relaxation in SMCs, but also had an antiproliferative effect, this was also investigated. Both CNP and the synthetic peptide VNP led to significantly reduced growth of HPrSMCs.

Since previous studies of our group showed, a hormonal correlation between cGMP pathway components and testosterone in the rat prostate, the local concentration of testosterone (T) and estradiol (E2) in the prostate of BPH patients was investigated. Measurements showed that T was more concentrated than E2 in the human prostate, and the concentrations of T and E2 correlated positively. Since one of the causes of BPH is considered to be the decrease in serum T levels and concomitant hormonal changes between serum levels of T and E2 in males, this ratio in the prostate was considered.

These changes in the T/E2 ratio are probably not reflected in the prostate, since the enzyme aromatase converts T to E2 and the ratio is therefore constant.

An *ex vivo* rat model was used for functional experiments. Expression analyses revealed a similar expression profile among the three entities examined in this study. Among them, GC-B was expressed at significantly higher levels than the other GCs (GC-A and sGC); therefore, the rat prostate was considered suitable for demonstrating the effect of NPs on tissues. For the analysis, an extended code was used that evaluates the entire tissue. The tissue is converted into individual pixels, and thus, data points that allow a more precise analysis. The resulting results were converted into a movement score and allowed an accurate representation of the movement in the tissue. Experiments showed that CNP and VNP resulted in significant relaxation of rat prostate glands.

The results of this thesis suggest that in addition to used PDE5 inhibitors, there are further possibilities to use the cGMP pathway in the treatment of BPH. Manipulation of this pathway shows fewer side effects in practice with PDE5 inhibitors, which severely affect the patient's life. Thus, additional activation of the cGMP signalling pathway via NPs or analogues should be considered for treatment of BPH. This signalling pathway not only leads to prostate relaxation, but also inhibits the proliferation of HPrSMCs. By targeting the CNP/GC-B signalling pathway, both characteristics of BPH could be addressed.

Zusammenfassung

Die gutartige Prostatahyperplasie (BPH) ist die häufigste Erkrankung bei Männern, wobei 40 % der Männer im Alter von 40 Jahren daran leiden. Die Inzidenz steigt weiter an, und 70-80 % der Männer im Alter von 80 Jahren haben BPH. Die Krankheit entwickelt sich in der Übergangszone der Prostata, wobei sowohl die epithelialen als auch die stromalen Anteile betroffen sind. Es kommt zu unkontrolliertem Wachstum und Proliferation der Zellen, wobei der stromale Anteil und die glatten Muskelzellen (SMCs) stärker involviert sind. Aufgrund der anatomischen Besonderheit der Prostata mit ihrer äußeren Kapsel findet das Wachstum nach innen statt und das Prostatagewebe drückt auf die Harnröhre. Dies führt zu Symptomen des unteren Harntrakts.

Die derzeitigen Behandlungsmöglichkeiten mit α1-Adreneroreceptor Antagonisten oder 5-α-Reduktase Inhibitoren zielen darauf ab, den Muskeltonus zu verringern und die Zellproliferation zu hemmen. Diese Behandlungen haben jedoch Nebenwirkungen und beeinträchtigen das Leben der Patienten aufgrund von Libidoverlust und Ejakulationsstörungen massiv. Neuere Behandlungsmöglichkeiten mit Phosphodiesterase-(PDE) 5-Inhibitoren beeinflussen den cGMP-Signalweg, der zur Entspannung der SMCs führt. Hier wurden keine der Nebenwirkungen beobachtet, die bei α1- Adrenorezeptor Antagonisten oder 5-α-Reduktase-Hemmern auftreten. Somit stellt der cGMP-Signalweg ein potenzielles Ziel für die Entwicklung neuer therapeutischer Optionen für BPH dar. Dieser Weg wurde weiter untersucht, da in der Prostata und im Seminalplasma eine hohe Konzentration des natriuretischen Peptids CNP gefunden wurde, das diesen Weg über die Guanylylcyclase-B (GC-B) aktiviert. In dieser Arbeit sollte der CNP/GC-B näher untersucht werden und neue therapeutische Nutzung des cGMP Signalweges aufgezeigt werden.

Die Expression von Schlüsselkomponenten des cGMP-Signalwegs wurde in der menschlichen Prostata gemessen, wobei die Expression des CNP-Rezeptors GC-B deutlich höher war als die der anderen GCs (GC-A und sGC) und die lokale Expression des natriuretischen Peptids CNP. Dies zeigt, dass der CNP/GC-B Signalweg eine wichtigere Rolle als der ANP/GC-A oder Stickstoffmonoxid/lösliche GC in der humanen Prostata spielen könnte. In dieser Arbeit wurde die stärkere Aktivierung des cGMP Signalweges in prostatischen SMCs (HPrSMCs) über CNP (im Vergleich zu ANP) anhand von spezifischen cGMP ELISA nachgewiesen. Dieser cGMP Signalweg könnte durch NPs oder deren Analoga gezielt in der Prostata aktiviert werden um BPH zu behandeln. Seit kurzem wird der cGMP Signalweg als Ziel für die BPH Behandlung genutzt und die dabei verwendeten PDE5-Inhibitoren zeigen weniger schwerwiegende Nebenwirkungen.

Da der cGMP Signalweg nicht nur zur Relaxation in SMCs führt, sondern auch einen antiproliferativen Effekt besitzt, wurde dieser ebenfalls untersucht. Es zeigte sich, dass sowohl CNP als auch das

synthetische Peptid VNP, welches ein Analog zu CNP darstellt zu einem deutlich verringerten Wachstum von HPrSMCs führt.

Da frühere Studien unserer Gruppe einen hormonellen Zusammenhang zwischen Komponenten des cGMP-Signalwegs und Testosteron in der Rattenprostata zeigten, wurde die lokale Konzentration von Testosteron (T) und Estradiol (E2) in der Prostata von Patienten mit BPH untersucht. Die Messungen zeigten, dass Testosteron höher konzentriert war als Estradiol in der humanen Prostata und zudem korrelierten die Konzentrationen von Testosteron und Estradiol positiv. Da als eine der Ursachen für BPH das sinkende Testosteronserumlevel und damit einhergehend die hormonelle Veränderung zwischen den Serumlevel T und E2 beim Mann betrachtet wird, wurde auch dieses Verhältnis in der Prostata betrachtet. Diese Veränderungen im Verhältnis von T/E2 spiegeln sich wahrscheinlich nicht in der Prostata wieder, da das dortige Enzym Aromatase T in E2 umwandelt und das Verhältnis daher gleichbleibend ist.

Für funktionelle Experimente wurde ein Ex-vivo-Rattenmodell verwendet. Expressionsanalysen ergaben ein ähnliches Expressionsprofil bei den drei in dieser Studie untersuchten Entitäten. Dabei war GC-B signifikant höhere exprimiert als die andere GCs (GC-A und sGC) und wurde daher wurde die Rattenprostata als geeignet betrachtet um die Wirkung der NPs auf Gewebe aufzuzeigen. Für die Analyse wurde ein erweiterter Code verwendet, der das gesamte Gewebe auswertet. Dabei wird das Gewebe in einzelne Pixel und damit Datenpunkte umgewandelt welche eine viel genauere Analyse erlauben. Die resultierenden Ergebnisse werden in einem sogenannten “movement score” umgerechnet und erlauben eine genaue Darstellung der Bewegung im Gewebe. Die Experimente zeigten, dass CNP und VNP zu einer signifikanten Relaxation der Prostatadrüsen führten.

Die Ergebnisse dieser Thesis deuten darauf hin, dass neben den bereits verwendeten PDE5-Inhibitoren, es weitere Möglichkeiten gibt den cGMP Signalweg bei der Behandlung von BPH zu nutzen. Die Manipulation dieses Signalweges zeigt in der Praxis mit PDE5-Inhibitoren weniger Nebenwirkungen, welches das Patientenleben schwerwiegend beeinträchtigen. So könnte eine zusätzliche Aktivierung des cGMP-Signalweges über NPs oder Analoga eingesetzt werden. Dieser Signalweg führt nicht nur zur Entspannung der Prostata, sondern hemmt auch die Proliferation der HPrSMCs. Durch die Nutzung des CNP/GC-B-Signalweges könnten beide Merkmale der BPH gezielt angegangen werden.

References

Abbey SE, Potter LR (2003) Lysophosphatidic acid inhibits C-type natriuretic peptide activation of guanylyl cyclase-B. Endocrinology 144: 240–246. doi: 10.1210/en.2002-220702

Adams JY, Leav I, Lau K-M, Ho S-M, Pflueger SMV (2002) Expression of estrogen receptor beta in the fetal, neonatal, and prepubertal human prostate. Prostate 52: 69–81. doi: 10.1002/pros.10103

Alheid U, Frölich JC, Förstermann U (1987) Endothelium-derived relaxing factor from cultured human endothelial cells inhibits aggregation of human platelets. Thromb Res 47: 561–571. doi: 10.1016/0049-3848(87)90361-6

Alves EF, Freitas Ribeiro BLM de, Costa WS, Gallo CBM, Sampaio FJB (2018) Histological and quantitative analyzes of the stromal and acinar components of normal human prostate zones. Prostate 78: 289–293. doi: 10.1002/pros.23472

Alwaal A, Breyer BN, Lue TF (2015) Normal male sexual function: emphasis on orgasm and ejaculation. Fertil Steril 104: 1051–1060. doi: 10.1016/j.fertnstert.2015.08.033

Aumüller G, Aust G, Conrad A, Engele J, Kirsch J, Maio G, Mayerhofer A, Mense S, Reißig D, Salvetter J, Schmidt W, Schmitz F, Schulte E, Spanel-Borowski K, Wennemuth G, Wolff W, Wurzinger LJ, Zilch H-G (2020) Duale Reihe Anatomie. Georg Thieme Verlag. Stuttgart

Balk SP, Ko Y-J, Bubley GJ (2003) Biology of prostate-specific antigen. J Clin Oncol 21: 383–391. doi: 10.1200/JCO.2003.02.083

Bartsch G, Müller HR, Oberholzer M, Rohr HP (1979) Light microscopic stereological analysis of the normal human prostate and of benign prostatic hyperplasia. J Urol 122: 487–491. doi: 10.1016/s0022-5347(17)56476-9

Behrends JC, Bischofberger J, Deutzmann R, Ehmke H, Frings S, Grissmer S, Hoth M, Kurtz A, Leipziger J, Müller F, Pedain C, Rettig J, Wagner C, Wischmeyer E (2021) Duale Reihe Physiologie. Georg Thieme Verlag KG. Stuttgart

Bennett BD, Bennett GL, Vitangcol RV, Jewett JR, Burnier J, Henzel W, Lowe DG (1991) Extracellular domain-IgG fusion proteins for three human natriuretic peptide receptors. Hormone pharmacology and application to solid phase screening of synthetic peptide antisera. J Biol Chem 266: 23060–23067

Berry SJ, Coffey DS, Walsh PC, Ewing LL (1984) The development of human benign prostatic hyperplasia with age. J Urol 132: 474–479. doi: 10.1016/s0022-5347(17)49698-4

Bold AJ de, Borenstein HB, Veress AT, Sonnenberg H (1981) A rapid and potent natriuretic response to intravenous injection of atrial myocardial extract in rats. Life Sci 28: 89–94. doi: 10.1016/0024-3205(81)90370-2

Bold AJ de, Bruneau BG, Kuroski de Bold ML (1996) Mechanical and neuroendocrine regulation of the endocrine heart. Cardiovasc Res 31: 7–18

Bold AJ de, Ma KK, Zhang Y, Bold ML de, Bensimon M, Khoshbaten A (2001) The physiological and pathophysiological modulation of the endocrine function of the heart. Can J Physiol Pharmacol 79: 705–714

Bosland MC, Tuomari DL, Elwell MR, Shirai T., Ward JM, McConnell RF (1998) Proliferative lesions of the prostate and other accessory sex glands in male rats. Guides for Toxicologic Pathology, STP/ARP/AFIP. Washington, DC

Braeckman J, Denis L (2017) Management of BPH then 2000 and now 2016 - From BPH to BPO. Asian J Urol 4: 138–147. doi: 10.1016/j.ajur.2017.02.002

Brieva J, Wanner A (2001) Adrenergic airway vascular smooth muscle responsiveness in healthy and asthmatic subjects. J Appl Physiol (1985) 90: 665–669. doi: 10.1152/jappl.2001.90.2.665

Budworth J, Meillerais S, Charles I, Powell K (1999) Tissue distribution of the human soluble guanylate cyclases. Biochem Biophys Res Commun 263: 696–701. doi: 10.1006/bbrc.1999.1444

References

Buskin A, Singh P, Lorenz O, Robson C, Strand DW, Heer R (2021) A Review of Prostate Organogenesis and a Role for iPSC-Derived Prostate Organoids to Study Prostate Development and Disease. Int J Mol Sci 22. doi: 10.3390/ijms222313097

Calderone A, Thaik CM, Takahashi N, Chang DL, Colucci WS (1998) Nitric oxide, atrial natriuretic peptide, and cyclic GMP inhibit the growth-promoting effects of norepinephrine in cardiac myocytes and fibroblasts. J Clin Invest 101: 812–818. doi: 10.1172/JCI119883

Canda AE, Turna B, Cinar GM, Nazli O (2007) Physiology and pharmacology of the human ureter: basis for current and future treatments. Urol Int 78: 289–298. doi: 10.1159/000100830

Cargill RI, Lipworth BJ (1995) Pulmonary vasorelaxant activity of atrial natriuretic peptide and brain natriuretic peptide in humans. Thorax 50: 183–185. doi: 10.1136/thx.50.2.183

Carson C, Rittmaster R (2003) The role of dihydrotestosterone in benign prostatic hyperplasia. Urology 61: 2–7. doi: 10.1016/s0090-4295(03)00045-1

Carvajal JA, Germain AM, Huidobro-Toro JP, Weiner CP (2000) Molecular mechanism of cGMP-mediated smooth muscle relaxation. J Cell Physiol 184: 409–420. doi: 10.1002/1097-4652(200009)184:3<409::AID-JCP16>3.0.CO;2-K

Chakrabarty B, Lee S, Exintaris B (2019) Generation and Regulation of Spontaneous Contractions in the Prostate. Adv Exp Med Biol 1124: 195–215. doi: 10.1007/978-981-13-5895-1_8

Chrisman TD, Schulz S, Potter LR, Garbers DL (1993) Seminal plasma factors that cause large elevations in cellular cyclic GMP are C-type natriuretic peptides. J Biol Chem 268: 3698–3703

Christ GJ, Andersson K-E (2007) Rho-kinase and effects of Rho-kinase inhibition on the lower urinary tract. Neurourol Urodyn 26: 948–954. doi: 10.1002/nau.20475

Chusho H, Tamura N, Ogawa Y, Yasoda A, Suda M, Miyazawa T, Nakamura K, Nakao K, Kurihara T, Komatsu Y, Itoh H, Tanaka K, Saito Y, Katsuki M (2001) Dwarfism and early death in mice lacking C-type natriuretic peptide. Proc Natl Acad Sci U S A 98: 4016–4021. doi: 10.1073/pnas.071389098

Clemmons DR, Maile LA (2005) Interaction between insulin-like growth factor-I receptor and alphaVbeta3 integrin linked signaling pathways: cellular responses to changes in multiple signaling inputs. Mol Endocrinol 19: 1–11. doi: 10.1210/me.2004-0376

Codognoto VM, Yamada PH, Schmith RA, Rydygier de Ruediger F, Paula Freitas-Dell'Aqua C de, Souza FF de, Brochine S, do Carmo LM, Vieira AF, Oba E (2020) Cross comparison of seminal plasma proteins from cattle and buffalo (Bubalus bubalis). Reprod Domest Anim 55: 81–92. doi: 10.1111/rda.13589

Costello LC, Franklin RB (2009) Prostatic fluid electrolyte composition for the screening of prostate cancer: a potential solution to a major problem. Prostate Cancer Prostatic Dis 12: 17–24. doi: 10.1038/pcan.2008.19

Cunha GR, Vezina CM, Isaacson D, Ricke WA, Timms BG, Cao M, Franco O, Baskin LS (2018) Development of the human prostate. Differentiation 103: 24–45. doi: 10.1016/j.diff.2018.08.005

Da Silva MHA, Souza DB de (2019) Current evidence for the involvement of sex steroid receptors and sex hormones in benign prostatic hyperplasia. Res Rep Urol 11: 1–8. doi: 10.2147/RRU.S155609

Davies KP (2015) Development and therapeutic applications of nitric oxide releasing materials to treat erectile dysfunction. Future Sci OA 1. doi: 10.4155/fso.15.53

Denecke S, Nowell CJ, Fournier-Level A, Perry T, Batterham P (2015) The Wiggle Index: An Open Source Bioassay to Assess Sub-Lethal Insecticide Response in Drosophila melanogaster. PLoS One 10: e0145051. doi: 10.1371/journal.pone.0145051

Derbyshire ER, Marletta MA (2012) Structure and regulation of soluble guanylate cyclase. Annu Rev Biochem 81: 533–559. doi: 10.1146/annurev-biochem-050410-100030

Devine CE, Simpson FO, Bertaud WS (1971) Surface features of smooth muscle cells from the mesenteric artery and vas deferens. J Cell Sci 8: 427–443. doi: 10.1242/jcs.8.2.427

Devlin CM, Simms MS, Maitland NJ (2021) Benign prostatic hyperplasia - what do we know? BJU Int 127: 389–399. doi: 10.1111/bju.15229

References

Dimmeler S, Zeiher AM (1999) Nitric oxide-an endothelial cell survival factor. Cell Death Differ 6: 964–968. doi: 10.1038/sj.cdd.4400581

Doi K, Itoh H, Ikeda T, Hosoda K, Ogawa Y, Igaki T, Yamashita J, Chun TH, Inoue M, Masatsugu K, Matsuda K, Ohmori K, Nakao K (1997) Adenovirus-mediated gene transfer of C-type natriuretic peptide causes G1 growth inhibition of cultured vascular smooth muscle cells. Biochem Biophys Res Commun 239: 889–894. doi: 10.1006/bbrc.1997.7576

Drewett JG, Fendly BM, Garbers DL, Lowe DG (1995) Natriuretic peptide receptor-B (guanylyl cyclase-B) mediates C-type natriuretic peptide relaxation of precontracted rat aorta. Journal of Biological Chemistry 270: 4668–4674. doi: 10.1074/jbc.270.9.4668

Dupuis M, Houdeau E, Mhaouty-Kodja S (2008) Increased potency of alpha 1-adrenergic receptors to induce inositol phosphates production correlates with the up-regulation of alpha 1d/Gh alpha/phospholipase C delta 1 signaling pathway in term rat myometrium. Reproduction 135: 55–62. doi: 10.1530/REP-07-0332

Ellem SJ, Risbridger GP (2009) The dual, opposing roles of estrogen in the prostate. Ann N Y Acad Sci 1155: 174–186. doi: 10.1111/j.1749-6632.2009.04360.x

El-Wakeel LM, Fouad FA, Saleem MD, Saber-Khalaf M (2020) Efficacy and tolerability of sildenafil/l-arginine combination relative to sildenafil alone in patients with organic erectile dysfunction. Andrology 8: 143–147. doi: 10.1111/andr.12671

Fehsel K, Jalowy A, Qi S, Burkart V, Hartmann B, Kolb H (1993) Islet cell DNA is a target of inflammatory attack by nitric oxide. Diabetes 42: 496–500. doi: 10.2337/diab.42.3.496

Fisher DA, Smith JF, Pillar JS, St Denis SH, Cheng JB (1998) Isolation and characterization of PDE9A, a novel human cGMP-specific phosphodiesterase. Journal of Biological Chemistry 273: 15559–15564. doi: 10.1074/jbc.273.25.15559

Förstermann U, Mülsch A, Böhme E, Busse R (1986) Stimulation of soluble guanylate cyclase by an acetylcholine-induced endothelium-derived factor from rabbit and canine arteries. Circ Res 58: 531–538. doi: 10.1161/01.res.58.4.531

Förstermann U, Sessa WC (2012) Nitric oxide synthases: regulation and function. Eur Heart J 33: 829-37, 837a-837d. doi: 10.1093/eurheartj/ehr304

Franko A, Kovarova M, Feil S, Feil R, Wagner R, Heni M, Königsrainer A, Ruoß M, Nüssler AK, Weigert C, Häring H-U, Lutz SZ, Peter A (2018) cGMP-dependent protein kinase I (cGKI) modulates human hepatic stellate cell activation. Metabolism 88: 22–30. doi: 10.1016/j.metabol.2018.09.001

Fuller F, Porter JG, Arfsten AE, Miller J, Schilling JW, Scarborough RM, Lewicki JA, Schenk DB (1988) Atrial natriuretic peptide clearance receptor. Complete sequence and functional expression of cDNA clones. Journal of Biological Chemistry 263: 9395–9401

Furchgott RF, Zawadzki JV (1980) The obligatory role of endothelial cells in the relaxation of arterial smooth muscle by acetylcholine. Nature 288: 373–376. doi: 10.1038/288373a0

Furuya M, Yoshida M, Hayashi Y, Ohnuma N, Minamino N, Kangawa K, Matsuo H (1991) C-type natriuretic peptide is a growth inhibitor of rat vascular smooth muscle cells. Biochem Biophys Res Commun 177: 927–931. doi: 10.1016/0006-291x(91)90627-j

Garg UC, Hassid A (1989) Nitric oxide-generating vasodilators and 8-bromo-cyclic guanosine monophosphate inhibit mitogenesis and proliferation of cultured rat vascular smooth muscle cells. J Clin Invest 83: 1774–1777. doi: 10.1172/JCI114081

Ginja M, Pires MJ, Gonzalo-Orden JM, Seixas F, Correia-Cardoso M, Ferreira R, Fardilha M, Oliveira PA, Faustino-Rocha AI (2019) Anatomy and Imaging of Rat Prostate: Practical Monitoring in Experimental Cancer-Induced Protocols. Diagnostics (Basel) 9. doi: 10.3390/diagnostics9030068

Giuliano F, Clément P (2005) Physiology of ejaculation: emphasis on serotonergic control. Eur Urol 48: 408–417. doi: 10.1016/j.eururo.2005.05.017

Hafen BB, Burns B (2024) StatPearls. Physiology, Smooth Muscle. Treasure Island (FL)

Hafen BB, Shook M, Burns B (2024) StatPearls. Anatomy, Smooth Muscle. Treasure Island (FL)

Hammond GL, Kontturi M, Vihko P, Vihko R (1978) Serum steroids in normal males and patients with prostatic diseases. Clin Endocrinol (Oxf) 9: 113–121. doi: 10.1111/j.1365-2265.1978.tb02189.x

Hanley PJ (2023) Elusive physiological role of prostatic acid phosphatase (PAP): generation of choline for sperm motility via auto-and paracrine cholinergic signaling. Front Physiol 14: 1327769. doi: 10.3389/fphys.2023.1327769

Hauger RL, Saelzler UG, Pagadala MS, Panizzon MS (2022) The role of testosterone, the androgen receptor, and hypothalamic-pituitary-gonadal axis in depression in ageing Men. Rev Endocr Metab Disord 23: 1259–1273. doi: 10.1007/s11154-022-09767-0

Hayashi N, Sugimura Y, Kawamura J, Donjacour AA, Cunha GR (1991) Morphological and functional heterogeneity in the rat prostatic gland. Biol Reprod 45: 308–321. doi: 10.1095/biolreprod45.2.308

Hiramatsu M, Maehara I, Ozaki M, Harada N, Orikasa S, Sasano H (1997) Aromatase in hyperplasia and carcinoma of the human prostate. Prostate 31: 118–124. doi: 10.1002/(sici)1097-0045(19970501)31:2<118::aid-pros7>3.0.co;2-j

Hoffmann B, Höveler R, Hasan SH, Failing K (1992) Ovarian and pituitary function in dogs after hysterectomy. J Reprod Fertil 96: 837–845. doi: 10.1530/jrf.0.0960837

Hoffmann B, Rostalski A, Mutembei HM, Goericke-Pesch S (2010) Testicular steroid hormone secretion in the boar and expression of testicular and epididymal steroid sulphatase and estrogen sulphotransferase activity. Exp Clin Endocrinol Diabetes 118: 274–280. doi: 10.1055/s-0029-1231082

Horio T, Tokudome T, Maki T, Yoshihara F, Suga S-I, Nishikimi T, Kojima M, Kawano Y, Kangawa K (2003) Gene expression, secretion, and autocrine action of C-type natriuretic peptide in cultured adult rat cardiac fibroblasts. Endocrinology 144: 2279–2284. doi: 10.1210/en.2003-0128

Hutch JA, Rambo OS (1970) A study of the anatomy of the prostate, prostatic urethra and the urinary sphincter system. J Urol 104: 443–452. doi: 10.1016/s0022-5347(17)61756-7

Ignarro LJ, Harbison RG, Wood KS, Kadowitz PJ (1986) Activation of purified soluble guanylate cyclase by endothelium-derived relaxing factor from intrapulmonary artery and vein: stimulation by acetylcholine, bradykinin and arachidonic acid. J Pharmacol Exp Ther 237: 893–900

Imperato-McGinley J, Sanchez RS, Spencer JR, Yee B, Vaughan ED (1992) Comparison of the effects of the 5 alpha-reductase inhibitor finasteride and the antiandrogen flutamide on prostate and genital differentiation: dose-response studies. Endocrinology 131: 1149–1156. doi: 10.1210/endo.131.3.1324152

Jesik CJ, Holland JM, Lee C (1982) An anatomic and histologic study of the rat prostate. Prostate 3: 81–97. doi: 10.1002/pros.2990030111

Jiang YS, Lei JY, Chen Y, Jin J (2014) Vasonatrin peptide stimulates both of the natriuretic peptide receptors, NPRA and NPRB. Biochem Biophys Res Commun 446: 1276–1280. doi: 10.1016/j.bbrc.2014.03.110

Kenny AJ, Bourne A, Ingram J (1993) Hydrolysis of human and pig brain natriuretic peptides, urodilatin, C-type natriuretic peptide and some C-receptor ligands by endopeptidase-24.11. Biochem J 291 (Pt 1): 83–88. doi: 10.1042/bj2910083

Kim IY, Zelner DJ, Sensibar JA, Ahn HJ, Park L, Kim JH, Lee C (1996) Modulation of sensitivity to transforming growth factor-beta 1 (TGF-beta 1) and the level of type II TGF-beta receptor in LNCaP cells by dihydrotestosterone. Exp Cell Res 222: 103–110. doi: 10.1006/excr.1996.0013

Kim N, Azadzoi KM, Goldstein I, Saenz de Tejada I (1991) A nitric oxide-like factor mediates nonadrenergic-noncholinergic neurogenic relaxation of penile corpus cavernosum smooth muscle. J Clin Invest 88: 112–118. doi: 10.1172/JCI115266

Kim SZ, Kim SH, Park JK, Koh GY, Cho KW (1998) Presence and biological activity of C-type natriuretic peptide-dependent guanylate cyclase-coupled receptor in the penile corpus cavernosum. J Urol 159: 1741–1746. doi: 10.1097/00005392-199805000-00104

Kirsch J, May CA, Lorke DE, Winkelmann A, Schwab W, Herrmann G, Funk R (2017) Taschenlehrbuch Anatomie, 2nd edn. Georg Thieme Verlag. Stuttgart, New York

Kishimoto I, Rossi K, Garbers DL (2001) A genetic model provides evidence that the receptor for atrial natriuretic peptide (guanylyl cyclase-A) inhibits cardiac ventricular myocyte hypertrophy. Proc Natl Acad Sci U S A 98: 2703–2706. doi: 10.1073/pnas.051625598

Komalavilas P, Lincoln TM (1994) Phosphorylation of the inositol 1,4,5-trisphosphate receptor by cyclic GMP-dependent protein kinase. J Biol Chem 269: 8701–8707

Kong HY, Byun J (2013) Emerging roles of human prostatic Acid phosphatase. Biomol Ther (Seoul) 21: 10–20. doi: 10.4062/biomolther.2012.095

Kubes P, Suzuki M, Granger DN (1991) Nitric oxide: an endogenous modulator of leukocyte adhesion. Proc Natl Acad Sci U S A 88: 4651–4655. doi: 10.1073/pnas.88.11.4651

Kügler R, Mietens A, Seidensticker M, Tasch S, Wagenlehner FM, Kaschtanow A, Tjahjono Y, Tomczyk CU, Beyer D, Risbridger GP, Exintaris B, Ellem SJ, Middendorff R (2018) Novel imaging of the prostate reveals spontaneous gland contraction and excretory duct quiescence together with different drug effects. FASEB J 32: 1130–1138. doi: 10.1096/fj.201700430R

Kuhn M (2004) Molecular physiology of natriuretic peptide signalling. Basic Res Cardiol 99: 76–82. doi: 10.1007/s00395-004-0460-0

Kuhn M (2016) Molecular Physiology of Membrane Guanylyl Cyclase Receptors. Physiol Rev 96: 751–804. doi: 10.1152/physrev.00022.2015

Kun A, Kiraly I, Pataricza J, Marton Z, Krassoi I, Varro A, Simonsen U, Papp JG, Pajor L (2008) C-type natriuretic peptide hyperpolarizes and relaxes human penile resistance arteries. J Sex Med 5: 1114–1125. doi: 10.1111/j.1743-6109.2008.00775.x

Kurtz A, Della Bruna R, Pfeilschifter J, Taugner R, Bauer C (1986) Atrial natriuretic peptide inhibits renin release from juxtaglomerular cells by a cGMP-mediated process. Proc Natl Acad Sci U S A 83: 4769–4773. doi: 10.1073/pnas.83.13.4769

Küthe A, Reinecke M, Uckert S, Becker A, David I, Heitland A, Stief CG, Forssmann W-G, Mägert H-J (2003) Expression of guanylyl cyclase B in the human corpus cavernosum penis and the possible involvement of its ligand C-type natriuretic polypeptide in the induction of penile erection. J Urol 169: 1918–1922. doi: 10.1097/01.ju.0000055602.35858.8f

Kuwahara K (2021) The natriuretic peptide system in heart failure: Diagnostic and therapeutic implications. Pharmacol Ther 227: 107863. doi: 10.1016/j.pharmthera.2021.107863

La Vignera S, Condorelli RA, Russo GI, Morgia G, Calogero AE (2016) Endocrine control of benign prostatic hyperplasia. Andrology 4: 404–411. doi: 10.1111/andr.12186

Lam M, Shigemasa Y, Exintaris B, Lang RJ, Hashitani H (2011) Spontaneous Ca2+ signaling of interstitial cells in the guinea pig prostate. J Urol 186: 2478–2486. doi: 10.1016/j.juro.2011.07.082

Lanfear DE (2010) Genetic variation in the natriuretic peptide system and heart failure. Heart Fail Rev 15: 219–228. doi: 10.1007/s10741-008-9113-y

Lang RJ, Nguyen D-TT, Matsuyama H, Takewaki T, Exintaris B (2006) Characterization of spontaneous depolarizations in smooth muscle cells of the Guinea pig prostate. J Urol 175: 370–380. doi: 10.1016/S0022-5347(05)00003-0

Lee SN, Chakrabarty B, Wittmer B, Papargiris M, Ryan A, Frydenberg M, Lawrentschuk N, Middendorff R, Risbridger GP, Ellem SJ, Exintaris B (2017) Age Related Differences in Responsiveness to Sildenafil and Tamsulosin are due to Myogenic Smooth Muscle Tone in the Human Prostate. Sci Rep 7: 10150. doi: 10.1038/s41598-017-07861-x

Lepor H, Tang R, Meretyk S, Shapiro E (1993a) Alpha 1 adrenoceptor subtypes in the human prostate. J Urol 149: 640–642. doi: 10.1016/s0022-5347(17)36170-0

Lepor H, Tang R, Shapiro E (1993b) The alpha-adrenoceptor subtype mediating the tension of human prostatic smooth muscle. Prostate 22: 301–307. doi: 10.1002/pros.2990220404

Li J, Tian Y, Guo S, Gu H, Yuan Q, Xie X (2018) Testosterone-induced benign prostatic hyperplasia rat and dog as facile models to assess drugs targeting lower urinary tract symptoms. PLoS One 13: e0191469. doi: 10.1371/journal.pone.0191469

Li S, Sun N (2005) Regulation of intracellular Ca2+ and calcineurin by NO/PKG in proliferation of vascular smooth muscle cells. Acta Pharmacol Sin 26: 323–328. doi: 10.1111/j.1745-7254.2005.00049.x

Lopez MJ, Garbers DL, Kuhn M (1997) The guanylyl cyclase-deficient mouse defines differential pathways of natriuretic peptide signaling. Journal of Biological Chemistry 272: 23064–23068. doi: 10.1074/jbc.272.37.23064

Lu SY, Zhu MZ, Wang DS, Chen SY, Zhang WD, Dong H, Yu J, Guo HT (2004) Inhibition of the proliferation of smooth muscle cells from human coronary bypass vessels by vasonatrin peptide. Physiol Res 53: 387–393

Lu S-Y, Wang D-S, Zhu M-Z, Zhang Q-H, Hu Y-Z, Pei J-M (2005) Inhibition of hypoxia-induced proliferation and collagen synthesis by vasonatrin peptide in cultured rat pulmonary artery smooth muscle cells. Life Sci 77: 28–38. doi: 10.1016/j.lfs.2004.11.026

MacDonald JA, Walsh MP (2018) Regulation of Smooth Muscle Myosin Light Chain Phosphatase by Multisite Phosphorylation of the Myosin Targeting Subunit, MYPT1. Cardiovasc Hematol Disord Drug Targets 18: 4–13. doi: 10.2174/1871529X18666180326120638

Madersbacher S, Sampson N, Culig Z (2019) Pathophysiology of Benign Prostatic Hyperplasia and Benign Prostatic Enlargement: A Mini-Review. Gerontology 65: 458–464. doi: 10.1159/000496289

Mahapokai W, van Sluijs FJ, Schalken JA (2000) Models for studying benign prostatic hyperplasia. Prostate Cancer Prostatic Dis 3: 28–33. doi: 10.1038/sj.pcan.4500391

Matsukawa N, Grzesik WJ, Takahashi N, Pandey KN, Pang S, Yamauchi M, Smithies O (1999) The natriuretic peptide clearance receptor locally modulates the physiological effects of the natriuretic peptide system. Proc Natl Acad Sci U S A 96: 7403–7408. doi: 10.1073/pnas.96.13.7403

Matzkin H, Soloway MS (1992) Immunohistochemical evidence of the existence and localization of aromatase in human prostatic tissues. Prostate 21: 309–314. doi: 10.1002/pros.2990210407

Maurice DH, Ke H, Ahmad F, Wang Y, Chung J, Manganiello VC (2014) Advances in targeting cyclic nucleotide phosphodiesterases. Nat Rev Drug Discov 13: 290–314. doi: 10.1038/nrd4228

McDougal DH, Gamlin PD (2015) Autonomic control of the eye. Compr Physiol 5: 439–473. doi: 10.1002/cphy.c140014

McNeal JE (1981) The zonal anatomy of the prostate. Prostate 2: 35–49. doi: 10.1002/pros.2990020105

McNeal JE (1988) Normal histology of the prostate. Am J Surg Pathol 12: 619–633. doi: 10.1097/00000478-198808000-00003

McPherson SJ, Hussain S, Balanathan P, Hedwards SL, Niranjan B, Grant M, Chandrasiri UP, Toivanen R, Wang Y, Taylor RA, Risbridger GP (2010) Estrogen receptor-beta activated apoptosis in benign hyperplasia and cancer of the prostate is androgen independent and TNFalpha mediated. Proc Natl Acad Sci U S A 107: 3123–3128. doi: 10.1073/pnas.0905524107

Mei C, Kang Y, Zhang C, He C, Liao A, Huang D (2021) C-Type Natriuretic Peptide Plays an Anti-Inflammatory Role in Rat Epididymitis Induced by UPEC. Front Cell Infect Microbiol 11: 711842. doi: 10.3389/fcimb.2021.711842

Mendes CR, Dilarri G, Forsan CF, Sapata VdMR, Lopes PRM, Moraes PB de, Montagnolli RN, Ferreira H, Bidoia ED (2022) Antibacterial action and target mechanisms of zinc oxide nanoparticles against bacterial pathogens. Sci Rep 12: 2658. doi: 10.1038/s41598-022-06657-y

Middendorff R, Müller D, Mewe M, Mukhopadhyay AK, Holstein AF, Davidoff MS (2002) The tunica albuginea of the human testis is characterized by complex contraction and relaxation activities regulated by cyclic GMP. J Clin Endocrinol Metab 87: 3486–3499. doi: 10.1210/jcem.87.7.8696

Miernik A, Gratzke C (2020) Current Treatment for Benign Prostatic Hyperplasia. Dtsch Arztebl Int 117: 843–854. doi: 10.3238/arztebl.2020.0843

Miernik A, Roehrborn CG (2022) Benign Prostatic Hyperplasia Treatment On Its Way to Precision Medicine: Dream or Reality? Eur Urol Focus 8: 363–364. doi: 10.1016/j.euf.2022.03.023

Mietens A, Tasch S, Stammler A, Konrad L, Feuerstacke C, Middendorff R (2014) Time-lapse imaging as a tool to investigate contractility of the epididymal duct--effects of cGMP signaling. PLoS One 9: e92603. doi: 10.1371/journal.pone.0092603

Misono KS, Grammer RT, Fukumi H, Inagami T (1984) Rat atrial natriuretic factor: isolation, structure and biological activities of four major peptides. Biochem Biophys Res Commun 123: 444–451. doi: 10.1016/0006-291x(84)90250-x

Morgentaler A, Traish AM (2009) Shifting the paradigm of testosterone and prostate cancer: the saturation model and the limits of androgen-dependent growth. Eur Urol 55: 310–320. doi: 10.1016/j.eururo.2008.09.024

Müller D, Mukhopadhyay AK, Davidoff MS, Middendorff R (2011) Cyclic GMP signaling in rat urinary bladder, prostate, and epididymis: tissue-specific changes with aging and in response to Leydig cell depletion. Reproduction 142: 333–343. doi: 10.1530/REP-10-0517

Müller D, Mukhopadhyay AK, Speth RC, Guidone G, Potthast R, Potter LR, Middendorff R (2004) Spatiotemporal regulation of the two atrial natriuretic peptide receptors in testis. Endocrinology 145: 1392–1401. doi: 10.1210/en.2003-0706

Müller D, Schulze C, Baumeister H, Buck F, Richter D (1992) Rat insulin-degrading enzyme: cleavage pattern of the natriuretic peptide hormones ANP, BNP, and CNP revealed by HPLC and mass spectrometry. Biochemistry 31: 11138–11143. doi: 10.1021/bi00160a026

Muncey W, Sellke N, Kim T, Mishra K, Thirumavalavan N, Loeb A (2021) Alternative Treatment for Erectile Dysfunction: a Growing Arsenal in Men's Health. Curr Urol Rep 22: 11. doi: 10.1007/s11934-020-01023-9

Murthy KS, Makhlouf GM (1998) cGMP-mediated Ca2+ release from IP3-insensitive Ca2+ stores in smooth muscle. Am J Physiol 274: C1199-205. doi: 10.1152/ajpcell.1998.274.5.C1199

Nagasaki S, Nakano Y, Masuda M, Ono K, Miki Y, Shibahara Y, Sasano H (2012) Phosphodiesterase type 9 (PDE9) in the human lower urinary tract: an immunohistochemical study. BJU Int 109: 934–940. doi: 10.1111/j.1464-410X.2011.10429.x

Nakaki T, Nakayama M, Kato R (1990) Inhibition by nitric oxide and nitric oxide-producing vasodilators of DNA synthesis in vascular smooth muscle cells. Eur J Pharmacol 189: 347–353. doi: 10.1016/0922-4106(90)90031-r

Nathan CF, Hibbs JB (1991) Role of nitric oxide synthesis in macrophage antimicrobial activity. Curr Opin Immunol 3: 65–70. doi: 10.1016/0952-7915(91)90079-g

Negash S, Narasimhan SR, Zhou W, Liu J, Wei FL, Tian J, Raj JU (2009) Role of cGMP-dependent protein kinase in regulation of pulmonary vascular smooth muscle cell adhesion and migration: effect of hypoxia. Am J Physiol Heart Circ Physiol 297: H304-12. doi: 10.1152/ajpheart.00077.2008

Nguyen D-TT, Dey A, Lang RJ, Ventura S, Exintaris B (2011) Contractility and pacemaker cells in the prostate gland. J Urol 185: 347–351. doi: 10.1016/j.juro.2010.09.036

Nickel JC, Roehrborn CG, O'Leary MP, Bostwick DG, Somerville MC, Rittmaster RS (2008) The relationship between prostate inflammation and lower urinary tract symptoms: examination of baseline data from the REDUCE trial. Eur Urol 54: 1379–1384. doi: 10.1016/j.eururo.2007.11.026

Nielsen SJ, Gøtze JP, Jensen HL, Rehfeld JF (2008) ProCNP and CNP are expressed primarily in male genital organs. Regul Pept 146: 204–212. doi: 10.1016/j.regpep.2007.09.022

Nielsen SJ, Iversen P, Rehfeld JF, Jensen HL, Goetze JP (2009) C-type natriuretic peptide in prostate cancer. APMIS 117: 60–67. doi: 10.1111/j.1600-0463.2008.00016.x

Niu Y, Xu Y, Zhang J, Bai J, Yang H, Ma T (2001) Proliferation and differentiation of prostatic stromal cells. BJU Int 87: 386–393. doi: 10.1046/j.1464-410x.2001.00103.x

Nunokawa Y, Tanaka S (1992) Interferon-gamma inhibits proliferation of rat vascular smooth muscle cells by nitric oxide generation. Biochem Biophys Res Commun 188: 409–415. doi: 10.1016/0006-291x(92)92400-r

Ogawa Y, Itoh H, Tamura N, Suga S, Yoshimasa T, Uehira M, Matsuda S, Shiono S, Nishimoto H, Nakao K (1994) Molecular cloning of the complementary DNA and gene that encode mouse brain natriuretic peptide and generation of transgenic mice that overexpress the brain natriuretic peptide gene. J Clin Invest 93: 1911–1921. doi: 10.1172/JCI117182

Oliver PM, Fox JE, Kim R, Rockman HA, Kim HS, Reddick RL, Pandey KN, Milgram SL, Smithies O, Maeda N (1997) Hypertension, cardiac hypertrophy, and sudden death in mice lacking natriuretic peptide receptor A. Proc Natl Acad Sci U S A 94: 14730–14735. doi: 10.1073/pnas.94.26.14730

Pape H-C, Kurtz A, Silbernagl S (2019) Physiologie. Georg Thieme Verlag. Stuttgart

Pask A (2016) The Reproductive System. Adv Exp Med Biol 886: 1–12. doi: 10.1007/978-94-017-7417-8_1

Porter JG, Catalano R, McEnroe G, Lewicki JA, Protter AA (1992) C-type natriuretic peptide inhibits growth factor-dependent DNA synthesis in smooth muscle cells. Am J Physiol 263: C1001-6. doi: 10.1152/ajpcell.1992.263.5.C1001

Potter LR (2005) Domain analysis of human transmembrane guanylyl cyclase receptors: implications for regulation. Front Biosci 10: 1205–1220. doi: 10.2741/1613

Potter LR (2011) Guanylyl cyclase structure, function and regulation. Cell Signal 23: 1921–1926. doi: 10.1016/j.cellsig.2011.09.001

Potter LR, Abbey-Hosch S, Dickey DM (2006) Natriuretic peptides, their receptors, and cyclic guanosine monophosphate-dependent signaling functions. Endocr Rev 27: 47–72. doi: 10.1210/er.2005-0014

Potter LR, Yoder AR, Flora DR, Antos LK, Dickey DM (2009) Natriuretic peptides: their structures, receptors, physiologic functions and therapeutic applications. Handb Exp Pharmacol: 341–366. doi: 10.1007/978-3-540-68964-5_15

Preston S, Jabbar A, Nowell C, Joachim A, Ruttkowski B, Baell J, Cardno T, Korhonen PK, Piedrafita D, Ansell BRE, Jex AR, Hofmann A, Gasser RB (2015) Low cost whole-organism screening of compounds for anthelmintic activity. Int J Parasitol 45: 333–343. doi: 10.1016/j.ijpara.2015.01.007

Preston S, Jabbar A, Nowell C, Joachim A, Ruttkowski B, Cardno T, Hofmann A, Gasser RB (2016) Practical and low cost whole-organism motility assay: A step-by-step protocol. Mol Cell Probes 30: 13–17. doi: 10.1016/j.mcp.2015.08.005

Prins GS, Korach KS (2008) The role of estrogens and estrogen receptors in normal prostate growth and disease. Steroids 73: 233–244. doi: 10.1016/j.steroids.2007.10.013

Prins GS, Lindgren M (2015) Accessory Sex Glands in the Male. In: Knobil and Neill's Physiology of Reproduction. Elsevier

Radomski MW, Palmer RM, Moncada S (1987) The anti-aggregating properties of vascular endothelium: interactions between prostacyclin and nitric oxide. Br J Pharmacol 92: 639–646. doi: 10.1111/j.1476-5381.1987.tb11367.x

Rajfer J, Aronson WJ, Bush PA, Dorey FJ, Ignarro LJ (1992) Nitric oxide as a mediator of relaxation of the corpus cavernosum in response to nonadrenergic, noncholinergic neurotransmission. N Engl J Med 326: 90–94. doi: 10.1056/NEJM199201093260203

Ren Y, Zheng J, Yao X, Weng G, Wu L (2014) Essential role of the cGMP/PKG signaling pathway in regulating the proliferation and survival of human renal carcinoma cells. Int J Mol Med 34: 1430–1438. doi: 10.3892/ijmm.2014.1925

Rentero C, Monfort A, Puigdomènech P (2003) Identification and distribution of different mRNA variants produced by differential splicing in the human phosphodiesterase 9A gene. Biochem Biophys Res Commun 301: 686–692. doi: 10.1016/s0006-291x(03)00021-4

RICHARDSON KC (1962) The fine structure of autonomic nerve endings in smooth muscle of the rat vas deferens. J Anat 96: 427–442

Rintz E, Węgrzyn G, Fujii T, Tomatsu S (2022) Molecular Mechanism of Induction of Bone Growth by the C-Type Natriuretic Peptide. Int J Mol Sci 23. doi: 10.3390/ijms23115916

Roberts RO, Jacobson DJ, Rhodes T, Klee GG, Leiber MM, Jacobsen SJ (2004) Serum sex hormones and measures of benign prostatic hyperplasia. Prostate 61: 124–131. doi: 10.1002/pros.20080

Roecken FE, Nothelfer H.-B., Hoffmann B. (1995) Testosteronkonzentrationen im peripheren Plasma sowie morphologische Hodenbefunde von Rüden mit einer Perinealhernie. Kleintierpraxis 1995: 261–267

Roehrborn CG (2008) Pathology of benign prostatic hyperplasia. Int J Impot Res 20 Suppl 3: S11-8. doi: 10.1038/ijir.2008.55

Roshani A, Khosropanah I, Salehi M, Kamran AN (2010) Effects of isosorbide dinitrate on the urinary flow rate in patients with benign prostatic hyperplasia. Urol J 7: 183–187

Ryl A, Rotter I, Slojewski M, Dolegowska B, Grabowska M, Baranowska-Bosiacka I, Laszczynska M (2015) Hormone concentration, metabolic disorders and immunoexpression of androgen and estrogen-alpha receptors in men with benign prostatic hyperplasia and testosterone deficiency syndrome. Folia Histochem Cytobiol 53: 227–235. doi: 10.5603/fhc.a2015.0026

Sanbe A, Tanaka Y, Fujiwara Y, Tsumura H, Yamauchi J, Cotecchia S, Koike K, Tsujimoto G, Tanoue A (2007) Alpha1-adrenoceptors are required for normal male sexual function. Br J Pharmacol 152: 332–340. doi: 10.1038/sj.bjp.0707366

Savarirayan R, Irving M, Bacino CA, Bostwick B, Charrow J, Cormier-Daire V, Le Quan Sang K-H, Dickson P, Harmatz P, Phillips J, Owen N, Cherukuri A, Jayaram K, Jeha GS, Larimore K, Chan M-L, Huntsman Labed A, Day J, Hoover-Fong J (2019) C-Type Natriuretic Peptide Analogue Therapy in Children with Achondroplasia. N Engl J Med 381: 25–35. doi: 10.1056/NEJMoa1813446

Savarirayan R, Tofts L, Irving M, Wilcox W, Bacino CA, Hoover-Fong J, Ullot Font R, Harmatz P, Rutsch F, Bober MB, Polgreen LE, Ginebreda I, Mohnike K, Charrow J, Hoernschemeyer D, Ozono K, Alanay Y, Arundel P, Kagami S, Yasui N, White KK, Saal HM, Leiva-Gea A, Luna-González F, Mochizuki H, Basel D, Porco DM, Jayaram K, Fisheleva E, Huntsman-Labed A, Day J (2020) Once-daily, subcutaneous vosoritide therapy in children with achondroplasia: a randomised, double-blind, phase 3, placebo-controlled, multicentre trial. Lancet 396: 684–692. doi: 10.1016/S0140-6736(20)31541-5

Schermuly RT, Stasch J-P, Pullamsetti SS, Middendorff R, Müller D, Schlüter K-D, Dingendorf A, Hackemack S, Kolosionek E, Kaulen C, Dumitrascu R, Weissmann N, Mittendorf J, Klepetko W, Seeger W, Ghofrani HA, Grimminger F (2008) Expression and function of soluble guanylate cyclase in pulmonary arterial hypertension. Eur Respir J 32: 881–891. doi: 10.1183/09031936.00114407

Sebastianelli A, Spatafora P, Morselli S, Vignozzi L, Serni S, McVary KT, Kaplan S, Gravas S, Chapple C, Gacci M (2020) Tadalafil Alone or in Combination with Tamsulosin for the Management for LUTS/BPH and ED. Curr Urol Rep 21: 56. doi: 10.1007/s11934-020-01009-7

Seidensticker M, Tasch S, Mietens A, Exintaris B, Middendorff R (2022) Treatment of benign prostatic hyperplasia and abnormal ejaculation: live imaging reveals tamsulosin - but not tadalafil - induced dysfunction of prostate, seminal vesicles and epididymis. Reproduction 164: 291–301. doi: 10.1530/REP-22-0197

Sellitti DF, Koles N, Mendonça MC (2011) Regulation of C-type natriuretic peptide expression. Peptides 32: 1964–1971. doi: 10.1016/j.peptides.2011.07.013

Selman SH (2011) The McNeal prostate: a review. Urology 78: 1224–1228. doi: 10.1016/j.urology.2011.07.1395

Shapiro E, Huang H, Masch RJ, McFadden DE, Wilson EL, Wu X-R (2005) Immunolocalization of estrogen receptor alpha and beta in human fetal prostate. J Urol 174: 2051–2053. doi: 10.1097/01.ju.0000176472.90432.5b

Shesely EG, Maeda N, Kim HS, Desai KM, Krege JH, Laubach VE, Sherman PA, Sessa WC, Smithies O (1996) Elevated blood pressures in mice lacking endothelial nitric oxide synthase. Proc Natl Acad Sci U S A 93: 13176–13181. doi: 10.1073/pnas.93.23.13176

Shi Z, Fu F, Yu L, Xing W, Su F, Liang X, Tie R, Ji L, Zhu M, Yu J, Zhang H (2015) Vasonatrin peptide attenuates myocardial ischemia-reperfusion injury in diabetic rats and underlying mechanisms. Am J Physiol Heart Circ Physiol 308: H281-90. doi: 10.1152/ajpheart.00666.2014

Siiteri PK, Wilson JD (1970) Dihydrotestosterone in prostatic hypertrophy. I. The formation and content of dihydrotestosterone in the hypertrophic prostate of man. J Clin Invest 49: 1737–1745. doi: 10.1172/JCI106391

Simpson ER, Mahendroo MS, Means GD, Kilgore MW, Hinshelwood MM, Graham-Lorence S, Amarneh B, Ito Y, Fisher CR, Michael MD (1994) Aromatase cytochrome P450, the enzyme responsible for estrogen biosynthesis. Endocr Rev 15: 342–355. doi: 10.1210/edrv-15-3-342

Singh N, Patra S (2014) Phosphodiesterase 9: insights from protein structure and role in therapeutics. Life Sci 106: 1–11. doi: 10.1016/j.lfs.2014.04.007

Song L, Shen W, Zhang H, Wang Q, Wang Y, Zhou Z (2016) Differential expression of androgen, estrogen, and progesterone receptors in benign prostatic hyperplasia. Bosn J Basic Med Sci 16: 201–208. doi: 10.17305/bjbms.2016.1209

Sreenivasulu K, Nandeesha H, Dorairajan LN, Rajappa M, Vinayagam V (2017) Elevated insulin and reduced insulin like growth factor binding protein-3/prostate specific antigen ratio with increase in prostate size in Benign Prostatic Hyperplasia. Clin Chim Acta 469: 37–41. doi: 10.1016/j.cca.2017.03.012

Stadler B, Nowell CJ, Whittaker MR, Arnhold S, Pilatz A, Wagenlehner FM, Exintaris B, Middendorff R (2021) Physiological and pharmacological impact of oxytocin on epididymal propulsion during the ejaculatory process in rodents and men. FASEB J 35: e21639. doi: 10.1096/fj.202100435R

Steiner GE, Newman ME, Paikl D, Stix U, Memaran-Dagda N, Lee C, Marberger MJ (2003) Expression and function of pro-inflammatory interleukin IL-17 and IL-17 receptor in normal, benign hyperplastic, and malignant prostate. Prostate 56: 171–182. doi: 10.1002/pros.10238

Steiner MS, Couch RC, Raghow S, Stauffer D (1999) The chimpanzee as a model of human benign prostatic hyperplasia. J Urol 162: 1454–1461

Steinert JR, Chernova T, Forsythe ID (2010) Nitric oxide signaling in brain function, dysfunction, and dementia. Neuroscientist 16: 435–452. doi: 10.1177/1073858410366481

Steinhelper ME, Cochrane KL, Field LJ (1990) Hypotension in transgenic mice expressing atrial natriuretic factor fusion genes. Hypertension 16: 301–307. doi: 10.1161/01.hyp.16.3.301

Stephenson SL, Kenny AJ (1987) The hydrolysis of alpha-human atrial natriuretic peptide by pig kidney microvillar membranes is initiated by endopeptidase-24.11. Biochem J 243: 183–187. doi: 10.1042/bj2430183

Sudoh T, Kangawa K, Minamino N, Matsuo H (1988) A new natriuretic peptide in porcine brain. Nature 332: 78–81. doi: 10.1038/332078a0

Sudoh T, Minamino N, Kangawa K, Matsuo H (1990) C-type natriuretic peptide (CNP): a new member of natriuretic peptide family identified in porcine brain. Biochem Biophys Res Commun 168: 863–870. doi: 10.1016/0006-291x(90)92401-k

Suga S, Nakao K, Hosoda K, Mukoyama M, Ogawa Y, Shirakami G, Arai H, Saito Y, Kambayashi Y, Inouye K (1992) Receptor selectivity of natriuretic peptide family, atrial natriuretic peptide, brain natriuretic peptide, and C-type natriuretic peptide. Endocrinology 130: 229–239. doi: 10.1210/endo.130.1.1309330

Tadayyon F, Izadpanahi M, Aali S, Mazdak H, Khorrami M-H (2012) The effect of sublingual isosorbide dinitrate on acute urinary retention due to benign prostatic hyperplasia. Saudi J Kidney Dis Transpl 23: 782–785. doi: 10.4103/1319-2442.98160

Tajima T, Shinoda T, Urakawa N, Shimizu K, Kaneda T (2018) Phosphodiesterase 9 (PDE9) regulates bovine tracheal smooth muscle relaxation. J Vet Med Sci 80: 499–502. doi: 10.1292/jvms.18-0011

Tamura N, Doolittle LK, Hammer RE, Shelton JM, Richardson JA, Garbers DL (2004) Critical roles of the guanylyl cyclase B receptor in endochondral ossification and development of female reproductive organs. Proc Natl Acad Sci U S A 101: 17300–17305. doi: 10.1073/pnas.0407894101

Tamura N, Ogawa Y, Chusho H, Nakamura K, Nakao K, Suda M, Kasahara M, Hashimoto R, Katsuura G, Mukoyama M, Itoh H, Saito Y, Tanaka I, Otani H, Katsuki M (2000) Cardiac fibrosis in mice lacking brain natriuretic peptide. Proc Natl Acad Sci U S A 97: 4239–4244. doi: 10.1073/pnas.070371497

Togashi H, Sakuma I, Yoshioka M, Kobayashi T, Yasuda H, Kitabatake A, Saito H, Gross SS, Levi R (1992) A central nervous system action of nitric oxide in blood pressure regulation. J Pharmacol Exp Ther 262: 343–347

Tokudome T, Horio T, Soeki T, Mori K, Kishimoto I, Suga S-I, Yoshihara F, Kawano Y, Kohno M, Kangawa K (2004) Inhibitory effect of C-type natriuretic peptide (CNP) on cultured cardiac myocyte hypertrophy: interference between CNP and endothelin-1 signaling pathways. Endocrinology 145: 2131–2140. doi: 10.1210/en.2003-1260

Tsurusaki T, Aoki D, Kanetake H, Inoue S, Muramatsu M, Hishikawa Y, Koji T (2003) Zone-dependent expression of estrogen receptors alpha and beta in human benign prostatic hyperplasia. J Clin Endocrinol Metab 88: 1333–1340. doi: 10.1210/jc.2002-021015

Uckert S, Oelke M, Stief CG, Andersson K-E, Jonas U, Hedlund P (2006) Immunohistochemical distribution of cAMP- and cGMP-phosphodiesterase (PDE) isoenzymes in the human prostate. Eur Urol 49: 740–745. doi: 10.1016/j.eururo.2005.12.050

Ückert S, Kedia GT, Tsikas D, Simon A, Bannowsky A, Kuczyk MA (2020) Emerging drugs to target lower urinary tract symptomatology (LUTS)/benign prostatic hyperplasia (BPH): focus on the prostate. World J Urol 38: 1423–1435. doi: 10.1007/s00345-019-02933-1

Ulfig N, Brand-Saberi B (2017) Kurzlehrbuch Embryologie, 3rd edn. Georg Thieme Verlag. Stuttgart, New York

van den Akker F (2001) Structural insights into the ligand binding domains of membrane bound guanylyl cyclases and natriuretic peptide receptors. J Mol Biol 311: 923–937. doi: 10.1006/jmbi.2001.4922

van der Staay FJ, Rutten K, Bärfacker L, Devry J, Erb C, Heckroth H, Karthaus D, Tersteegen A, van Kampen M, Blokland A, Prickaerts J, Reymann KG, Schröder UH, Hendrix M (2008) The novel selective PDE9 inhibitor BAY 73-6691 improves learning and memory in rodents. Neuropharmacology 55: 908–918. doi: 10.1016/j.neuropharm.2008.07.005

van Velde RL de, Risley PL (1963) The Origin and Development of Smooth Muscle and Contractility in the Ductus Epididymidis of the Rat. Development 11: 369–382. doi: 10.1242/dev.11.2.369

Vanneste Y, Michel A, Dimaline R, Najdovski T, Deschodt-Lanckman M (1988) Hydrolysis of alpha-human atrial natriuretic peptide in vitro by human kidney membranes and purified endopeptidase-24.11. Evidence for a novel cleavage site. Biochem J 254: 531–537. doi: 10.1042/bj2540531

Vickman RE, Franco OE, Moline DC, Vander Griend DJ, Thumbikat P, Hayward SW (2020) The role of the androgen receptor in prostate development and benign prostatic hyperplasia: A review. Asian J Urol 7: 191–202. doi: 10.1016/j.ajur.2019.10.003

Vihko P, Kontturi M, Korhonen LK (1978) Purification of human prostatic acid phosphatase by affinity chromatography and isoelectric focusing. Part I. Clin Chem 24: 466–470

Virtanen I, Kallajoki M, Närvänen O, Paranko J, Thornell LE, Miettinen M, Lehto VP (1986) Peritubular myoid cells of human and rat testis are smooth muscle cells that contain desmin-type intermediate filaments. Anat Rec 215: 10–20. doi: 10.1002/ar.1092150103

Vuolteenaho O, Ala-Kopsala M, Ruskoaho H (2005) BNP as a biomarker in heart disease. Adv Clin Chem 40: 1–36

Watanabe Y, Nakajima K, Shimamori Y, Fujimoto Y (1997) Comparison of the hydrolysis of the three types of natriuretic peptides by human kidney neutral endopeptidase 24.11. Biochem Mol Med 61: 47–51. doi: 10.1006/bmme.1997.2584

Webb RC (2003) Smooth muscle contraction and relaxation. Adv Physiol Educ 27: 201–206. doi: 10.1152/advan.00025.2003

Wei CM, Kim CH, Khraibi AA, Miller VM, Burnett JC (1994) Atrial natriuretic peptide and C-type natriuretic peptide in spontaneously hypertensive rats and their vasorelaxing actions in vitro. Hypertension 23: 903–907. doi: 10.1161/01.hyp.23.6.903

Wei CM, Kim CH, Miller VM, Burnett JC (1993) Vasonatrin peptide: a unique synthetic natriuretic and vasorelaxing peptide. J Clin Invest 92: 2048–2052. doi: 10.1172/JCI116800

Wilson JD, Roehrborn C (1999) Long-term consequences of castration in men: lessons from the Skoptzy and the eunuchs of the Chinese and Ottoman courts. J Clin Endocrinol Metab 84: 4324–4331. doi: 10.1210/jcem.84.12.6206

Wink DA, Kasprzak KS, Maragos CM, Elespuru RK, Misra M, Dunams TM, Cebula TA, Koch WH, Andrews AW, Allen JS (1991) DNA deaminating ability and genotoxicity of nitric oxide and its progenitors. Science 254: 1001–1003. doi: 10.1126/science.1948068

Xia H, Chen Y, Wu K-J, Zhao H, Xiong C-L, Huang D-H (2016) Role of C-type natriuretic peptide in the function of normal human sperm. Asian J Androl 18: 80–84. doi: 10.4103/1008-682X.150254

Yeung VT, Ho SK, Nicholls MG, Cockram CS (1996) Binding of CNP-22 and CNP-53 to cultured mouse astrocytes and effects on cyclic GMP. Peptides 17: 101–106. doi: 10.1016/0196-9781(95)02099-3

Yu J, Zhu M, Fu Z, Zhu X, Zhao Y, Chen B (2010) Vasorelaxing action of vasonatrin peptide is associated with activation of large-conductance Ca(2+)-activated potassium channels in vascular smooth muscle cells. Physiol Res 59: 187–194. doi: 10.33549/physiolres.931746

Yuen PS, Potter LR, Garbers DL (1990) A new form of guanylyl cyclase is preferentially expressed in rat kidney. Biochemistry 29: 10872–10878. doi: 10.1021/bi00501a002

Zelivianski S, Comeau D, Lin MF (1998) Cloning and analysis of the promoter activity of the human prostatic acid phosphatase gene. Biochem Biophys Res Commun 245: 108–112. doi: 10.1006/bbrc.1998.8386

Zenzmaier C, Sampson N, Pernkopf D, Plas E, Untergasser G, Berger P (2010) Attenuated proliferation and trans-differentiation of prostatic stromal cells indicate suitability of phosphodiesterase type 5 inhibitors for prevention and treatment of benign prostatic hyperplasia. Endocrinology 151: 3975–3984. doi: 10.1210/en.2009-1411

Zhang M, Luo C, Cui K, Xiong T, Chen Z (2020) Chronic inflammation promotes proliferation in the prostatic stroma in rats with experimental autoimmune prostatitis: study for a novel method of inducing benign prostatic hyperplasia in a rat model. World J Urol 38: 2933–2943. doi: 10.1007/s00345-020-03090-6

Zhang P, Hu W-L, Cheng B, Zeng Y-J, Wang X-H, Liu T-Z, Zhang W-B (2016) Which play a more important role in the development of large-sized prostates (≥80 ml), androgen receptors or oestrogen receptors? A comparative study. Int Urol Nephrol 48: 325–333. doi: 10.1007/s11255-015-1181-z

Zhao J, Dong X, Hu X, Long Z, Wang L, Liu Q, Sun B, Wang Q, Wu Q, Li L (2016) Zinc levels in seminal plasma and their correlation with male infertility: A systematic review and meta-analysis. Sci Rep 6: 22386. doi: 10.1038/srep22386

Zhou L, Zhu D-Y (2009) Neuronal nitric oxide synthase: structure, subcellular localization, regulation, and clinical implications. Nitric Oxide 20: 223–230. doi: 10.1016/j.niox.2009.03.001

Zhu X, Zhai K, Mi Y, Ji G (2017) Expression and function of phosphodiesterases (PDEs) in the rat urinary bladder. BMC Urol 17: 54. doi: 10.1186/s12894-017-0244-0

List of Posters

„The correlation between the expression of cGMP signalling pathway components and hormone levels; its significance in BPH“ Kuchta M.A., Seidensticker M., Gronau A., Wagenlehner F., Schuler G., Middendorff R. (12th Annual GGL Conference 2019)

„The correlation between the expression of cGMP signalling pathway components and hormone levels; its significance in BPH“ Kuchta M.A., Seidensticker M., Gronau A., Wagenlehner F., Schuler G., Middendorff R. (Molecular Andrology 2019)

“Benigne Prostatahyperplasie und PDE-Inhibitoren – neue Therapieoptionen durch Untersuchung des Zusammenhanges zwischen cGMP/PDE-Signalwegen und den Hormonspiegeln” Kuchta M.A., Seidensticker M., Gronau A., Wagenlehner F., Schuler G., Middendorff R. (8th DVR Congress 2019)

“C-type natriuretic peptide and analogues are potential drugs for BPH treatment” Kuchta M.A., Exintaris B., Middendorff R. (13th Annual GGL Conference 2020 – digital)

“Natriuretic peptides as a future alternative for Tamsulosin in BPH treatment?” Kuchta M.A., Wagenlehner F., Middendorff R.(12th International, 11th European and 32nd German Congress of Andrology 2020 – digital)

“Natriuretic peptides affect prostatic smooth muscle cells and are potential drugs for BPH” Kuchta M.A., Rager C., Wagenlehner F., Middendorff R. (14th Annual GGL Conference 2021 – digital)

“Natriuretische Peptide beeinflussen die prostatischen glatten Muskelzellen und können potentielle Therapieoptionen für BPH sein ohne negativen Einfluss auf die Ejakulation” Kuchta M.A., Rager C., Wagenlehner F., Middendorff R. (9th DVR Congress 2021 – digital)

Acknowledgement

First, I would like to thank Prof. Dr. Ralf Middendorff for giving me the opportunity to work in his Signal Transduction group. Thank you for the exciting topic and warm welcome to the working group. I was able to develop so much in these years, not only academically but also personally. Thank you for supporting me with all my ideas, and for all your help and knowledge.

I would also like to thank Prof. Dr. Nikola-Michael Prpic-Schäper, who took me as an external doctoral student!

A big and special “thank you” goes to my supervisors at Monash University, Melbourne. Although it was only a short time, it was unforgettable. Thank you Dr. Betty Exintaris and Dr. Mikey Whittaker for always time for me, for your support and commitment.

Thank you to the Signal Transduction group and the great welcome. I have made friends for life during this time. Sabine Tasch, the working group would not be what it is without you! Thank you for always being there and for being the best help. Many thanks also to Andrea Mietens for her ideas that always bring me forward. I would like to take this opportunity to thank Bea, Dany, Chrissy, and Alina for our unforgettable time in the lab.

Special thanks also go to the IRTG for enabling the extraordinary exchange between JLU and Monash University. Thank you for the experience of being a member and being able to participate in all great seminars and events.

Thank you to GGL for offering great opportunities to improve my skills. I enjoyed participating in different courses and am grateful for this possibility!

We would like to thank all our collaborators who provided us with human and rat tissues.

Ein besonderes Dankeschön an meine Freunde und Familie. Danke an meine Eltern, Großeltern und Patentante für ihre Unterstützung.